REFERENCE ONLY

UNIVERSITY OF LONDON THESIS

Degree PhD Year 2005 Name of Author CINQUIN, O.

Clocks, gradients, and molecular networks: mathematical models for morphogenesis

Olivier Cinquin

University College London

Submitted for PhD in Modeling of biological complexity

September 2005

ProQuest LLC
789 East Eisenhower Parkway
P.O. Box 1346
Ann Arbor, MI 48106-1346

Abstract

The acquisition of a spatial structure during embryo development involves the differentiation of cells, often according to positional information. The complexity of the molecular networks regulating differentiation and of the mechanisms generating positional information makes it necessary to study them by means of mathematical modeling. Vertebrate embryos also acquire a segmented structure during somitogenesis; this requires spatial and temporal variations in gene expression, which mathematical modeling can also help understand.

A molecular mechanism for the somitogenesis clock is proposed, which accounts for inter-cellular synchronisation, and is based on positive feedback, even though it is compatible with all experimental data interpreted as showing that the clock is based on negative feedback. Experiments proposed to test this model involve real-time clock reporters, as well as inducible systems to induce spatially-controlled perturbations.

Theoretical and experimental results have led to conflicting ideas as to how useful positional information can be established. In particular, it has been pointed out that some models of extracellular diffusion of morphogen exhibit inadequate traveling waves of receptor saturation. Two alternative (but not mutually exclusive) models are proposed, which are based on recent experimental results highlighting the roles of extracellular glycoproteins and morphogen oligomerization.

The readout of positional information is translated to a discrete set of gene expression patterns. Intriguingly, it has been observed in numerous contexts that genes regulating differentiation are initially co-expressed in progenitors despite their antagonism. We characterise conditions under which three classes of generic "master regulatory networks" can behave as a "multi-switch", directing differentiation in an all-or-none fashion to a specific cell-type chosen among more than two possible outcomes. bHLH dimerisation networks can

readily display coexistence of many antagonistic factors when competition is low. Decision-making can be forced by a transient increase in competition, which could correspond to some unexplained experimental observations related to Id proteins.

Contents

List of Tables

List of Figures

Acknowledgements

This PhD was made possible by an AstraZeneca studentship awarded to CoMPLEX, obtained by the Director Anne Warner, and by support from Claudio Stern, who allowed me to carry out experiments despite their risky aspect, and funded them through an EU Framework 6 Network of Excellence 'Cells into Organs' LSHM-CT-2003-504468 grant, as well as other MRC, BBSRC and NIH grants. I am grateful to him for his supervision, and for suggesting improvements to this manuscript, and to Jacques Demongeot for introducing me to the subject of mathematical biology.

I am also grateful to David Whitmore and Kathy Tamai for numerous discussions and sharing of lab equipment and facilities, to Karl Swann for help and advice with luciferase imaging, to Michael White for a discussion about luciferase lifetimes, to Sabina Passamonti for a discussion about bilitranslocase, to Matthieu Lacolle for discussions about optics, to Masa Tada and Ari Fassati for sharing reagents, to Jonathan Ashmore for energetically providing help at various points, to Mary Rahman, Daniel Cintiar, and Sharon Boast for technical assistance, to the Chemistry Department for lending glassware, to Shamshad Cockcroft and Sadaf Shadan for sharing a piece of liver, to Stephen Price for the use of his electroporator, to the many labs who provided plasmid constructs indispensable in the course of this work, and to Stern lab members who all gave me help at some point.

I am indebted to Amanda Albazerchi for her early involvement in the lightswitch experiments, help with embryology, and for countless pieces of advice, to

Jacques Demongeot and Karen Page for their respective contributions to Chapters 6 and 8, to Michel Kerszberg for suggesting the title of this thesis, and to Christian Bottomley, Dan Brewer, and Dave Dale for biweekly entertainment.

Chapter 1

Introduction

1.1 Somitogenesis

Somites are transient, segmental structures in vertebrate and cephalochordate embryos, derived from paraxial mesoderm (Saga & Takeda, 2001). They are formed on both sides by budding off anteriorly, at regular intervals (30 minutes in zebrafish, 90 minutes in chick, 2 hours in mouse), from the presomitic mesoderm (PSM). Mesoderm segmentation and the polarity of the resulting somites play an essential role in the patterning of other structures, such as nerves, vertebrae, muscles and blood vessels (Keynes & Stern, 1988, Saga & Takeda, 2001). The polarity of somites is an essential aspect of their development, and possibly of their maintenance (Stern & Keynes, 1987, Nomura-Kitabayashi et al., 2002). It arises by a very complex process which will not be detailed here, but in which the "clock" described below might play a fundamental role.

Cells ingress from the primitive streak into the most posterior part of the PSM, and continue proliferating while in the PSM; in the chick, Primmett et al. (1989) identified regions of high mitotic activity near the caudal end (cells undergoing mitosis there have one descendant which does not contribute to PSM, Stern et al., 1988), in the middle of the PSM, and at its rostral end. There is little cell movement in the PSM (Stern et al., 1988, Selleck & Stern,

1991, Selleck & Stern, 1992, Psychoyos & Stern, 1996), but sufficient for cells to cross boundaries of presumptive somites (Stern et al., 1988, Kulesa & Fraser, 2002).

While cells undergo relatively little migration in the PSM, they do undergo a movement relative to the whole of the PSM, as its anterior end regresses posteriorly as new somites are formed, and its posterior end also progresses posteriorly, as a result of cell proliferation and ingression.

1.1.1 Oscillatory gene expression

The species considered here are chicken and mouse, which were the focus of the study, and zebrafish, as much data has been derived from it. Some oscillatory gene expression has been shown in Xenopus (Li et al., 2003), but much less is known about that model.

A number of genes have been identified whose expression oscillates in the PSM, and are collectively referred to as the "somitogenesis clock". The ones which are mentioned in this section are those which oscillate with the same periodicity as that of somitogenesis. All of those identified so far but one are related to the ubiquitous membrane receptor Notch, which is cleaved upon binding of one of its ligands, Delta or Serrate (reviewed by Mumm & Kopan, 2000; see however Ladi et al., 2005, for a recently-documented exception to this rule). This cleavage releases an intra-cellular domain, which can activate gene transcription in association with other proteins. Among these targets are members of the Hes and Hey/Herp families (reviewed by Iso et al., 2003), which have been shown to be transcriptional repressors (Hes6 being an exception). Genes of these families whose expression in the PSM is cyclic are c-hairy1 (Palmeirim et al., 1997), c-hairy2 (chick)/ Hes1 (mouse; Jouve et al., 2000), Hes7 (Bessho et al., 2001b), her1 and her7 (zebrafish; Holley et al., 2000, Oates & Ho, 2002), and Hey2 (chick and mouse; Leimeister et al., 2000).

Oscillatory expression has been shown in chick and mouse for Lunatic fringe

(Forsberg et al., 1998, McGrew et al., 1998), which modifies Notch to make it more sensitive to activation by Delta (Blair, 2000), which is the Notch ligand expressed in the PSM; zebrafish Lunatic fringe does not show similar oscillatory expression (Prince et al., 2001), but the Notch ligand DeltaC does (Jiang et al., 2000; it has also been very recently proposed that expression of the mouse ligand Dll1 oscillates as well, Maruhashi et al., 2005).

Notch-related genes exhibit waves of expression which sweep from the posterior to the anterior end of the PSM. Axin2, a Wnt pathway gene, also shows oscillatory expression in mouse PSM (Aulehla et al., 2003), but with a different pattern. Disruption of Notch-related oscillations alters the pattern of Axin2 oscillatory expression, but does not completely suppress the oscillations; it has been proposed that disruption of Axin2 oscillations suppresses Notch-related oscillations, but that does not seem to be completely clear from the figures presented by Aulehla et al. (2003). At the time of writing, the details of the relationship between Notch-pathway and Axin2 oscillations had not been elucidated.

1.1.2 Wavefront

FGF8 mRNA and protein form a concentration gradient in the PSM, decreasing from the posterior end to the anterior end (Sawada et al., 2001, Dubrulle et al., 2001, Dubrulle & Pourquié, 2004); signaling occurs through the MAPK/ERK pathway (Sawada et al., 2001, Delfini et al., 2005). The implantation of FGF8 or FGF inhibitor SU5402 beads affects the size of somites, as does retinoic acid deficiency (Maden et al., 2000). The mechanisms by which this occurs are however unclear; it is particularly intriguing that FGF8 and SU5402 beads have asymmetrical effects anterior and posterior to their implementation site (Dubrulle et al., 2001). It has been proposed that lowered FGF signaling increases maturity of cells in the PSM as well as their ability to respond to the clock by segmenting. Since the PSM, considered as a dynamical population

of cells, is under constant movement in the posterior direction, but seems to be at a steady state as regards gene expression and cell behaviour, regions with a constant level of FGF signalling presumably also travel posteriorly. The term "wavefront" refers to the region where FGF signalling is at the *putative* critical level where segmentation is induced; this wavefront presumably travels posteriorly, at the same average speed as the PSM when the size of the PSM is constant.

1.1.3 Clock and wavefront

The clock and wavefront model was initially proposed by Cooke & Zeeman (1976), based on experimental data from *Xenopus*, with the concern of explaining the regulation of somite number, which was argued to vary very little between individuals of a same species, and to be unaffected in mutant embryos of smaller size (this view was however contradicted by Primmett et al., 1988). The progression of a wavefront (proposed to be a cell-intrinsic "timing gradient", or a physical wave involving "propagatory interactions between cells") was supposed to be alternatively inhibited and accelerated by an oscillator, so that cells destined to segment together would be reached by the wavefront, and undergo a change in adhesiveness properties, within a short time-frame.

Two hidden and anonymous, but major variations have been brought to the original clock and wavefront model. The model presented by Dubrulle et al. (2001), according to which the FGF8 concentration forms a determination wavefront, brings those two major variations together, because it implicitly assumes that clock and wavefront are independent, even though data presented by the authors does show that the grafting of FGF8 beads affects the oscillatory pattern in the PSM (but that was not investigated in detail), and because it assumes that the oscillator specifies cells to become boundary cells if they are reached at a specific phase of their oscillation, somite compaction happening subsequently. Compaction being a phenomenon subsequent to boundary

formation is compatible with data from zebrafish mutants (Henry et al., 2000).

Dale & Pourquie (2000) proposed another clock and wavefront model with only one major variation from the original model, in which cells have a "positional information" value which increases with time and endows competence to segment above a threshold value; the oscillator, when it reaches a specific phase, provokes segmentation of cells which are competent to do so.

Contrary to what is stated in the numerous reviews on somitogenesis, it is totally unclear how FGF signalling and the clock interact to regulate segmentation. The various clock and wavefront models detailed above do not account for asymmetrical effects of grafted FGF beads, the coupling that there seems to be between clock and wavefront, the periodic effects of heat shocks (Primmett et al., 1988; the cell-cycle model for somitogenesis, Primmett et al., 1989, Collier et al., 2000, is unique in being able to account for them), or various inductive effects related to the segmentation process (Sato et al., 2002, Sato & Takahashi, 2005). The experiments described below (section 1.1.7) would have allowed to investigate some aspects of the relationship between clock and FGF wavefront.

1.1.4 Coupling of the oscillations

Early experiments on the clock showed that oscillatory expression could go on after sectioning of the PSM and separate incubation (Palmeirim et al., 1997, McGrew et al., 1998, Forsberg et al., 1998); this has been confirmed for most genes of the clock, and more recently investigated in more detail, by cutting the PSM into more than two pieces (Maroto et al., 2005). This was first interpreted as suggesting that the clock was cell-autonomous; there are however a number of reasons to expect some form of coupling, which are detailed in Chapter 2 (in the specific case of zebrafish, it had already been suggested that there was some coupling, Jiang et al., 2000). The model in Chapter 2 shows that it is possible to reconcile both the autonomous and non-autonomous aspects.

Maroto et al. (2005) show summarily that dissociation of PSM cells leads to a disruption of the oscillations, but that is not proof that cellular cross-talk is taking place *in vivo*, as the disruption of the oscillations could just as well be an artifact due to the dissociation (in the case of Xenopus neurogenesis, the dissociation of animal cap cells, long thought to result in the dilution of neurogenesis inhibitors, has been shown to activate the FGF pathway, leading to neurogenesis, Kuroda et al., 2005; FGF is the very same signalling pathway which has been shown by the same group to interact with the somitogenesis clock). The experiments described in section 1.1.7 were designed to address the question of coupling.

The role of retinoic acid signalling in the setup or maintenance of oscillation synchrony between the left and right sides of the PSM has been reported by a number of groups (Vermot & Pourquié, 2005, Vermot et al., 2005, Kawakami et al., 2005, Saúde et al., 2005). However, no details are available as regards the molecular mechanism by which that happens, and that data is not of direct relevance to the model in Chapter 2.

1.1.5 Hes autorepression

It has been shown that Hes1 can undergo oscillatory expression in a variety of cell types (Hirata et al., 2002). Since Hes1 can downregulate its own expression (Takebayashi et al., 1994), it was proposed that self-repression (in combination with a cofactor) mediates oscillatory expression. Hes1 is not necessary for somitogenesis, as Hes1 mutants do not have any somitogenesis phenotype (Ishibashi et al., 1995; neither do Hes1/Hes5 double mutants, Ohtsuka et al., 1999). On the other hand, Hes7 mutation does disrupt somitogenesis (Bessho et al., 2001b, Hirata et al., 2004). It has thus been proposed that delayed self-repression of Hes7 is responsible for its oscillatory expression (Hirata et al., 2004; see also Bessho et al., 2003). This however overlooks the fact that Hes7 has been shown not to repress transcription from its own promoter, in a model system involving

cultured cells (Bessho et al., 2001a). It thus seems rather unlikely that Hes7 provides oscillatory expression by single-handedly repressing itself; of course it could be that Hes7 can repress its own expression in combination with other factors, present in the PSM but not in cultured cells, or that Hes7 is part of a negative feedback loop involving other factors (which would explain why Hes7 disruption leads to upregulation of its own promoter in the PSM, Bessho et al., 2003). It is noteworthy that stabilization of Hes7 leading to a disruption of oscillations (Hirata et al., 2004) does not in the least prove a direct autorepression mechanism for the generation of the somitogenesis oscillations (it could just as well be that it is the average level of Hes7 repression which matters to maintain the oscillations).

Her1/Her7 direct autorepression has also been proposed to be the mechanism generating the oscillations in zebrafish PSM, taking into account the delays stemming from mRNA and protein production (Lewis, 2003). A basic prediction one would make from such a model is that disruption of her1 or her7 results in the upregulation of their promoter activity; however, if one carefully distinguishes morpholino-stabilised mRNA from nascent transcripts, the opposite is true for her1 and her7 morphants (Gajewski et al., 2003). Other unresolved problems with the model proposed by Lewis (2003) are that it was not attempted to have the model reproduce the oscillatory pattern in the PSM (the posterior-anterior waves of expression), and that its synchronization properties were studied only for a pair of cells.

1.1.6 Models for the oscillations

Many mathematical models have been proposed for somitogenesis in general (Cooke & Zeeman, 1976, Meinhardt, 1986, Collier et al., 2000, Schnell & Maini, 2000, Kerszberg & Wolpert, 2000, Kaern et al., 2000, Jaeger & Goodwin, 2001), but only two address directly the molecular mechanism of the oscillations (Cinquin, 2003, Lewis, 2003). It is interesting to note that models have been pro-

posed for Lunatic fringe-Notch mediated oscillations (Cinquin, 2003, Dale et al., 2003), and for her/hes-mediated oscillations (Lewis, 2003, Bessho et al., 2001b), but that the two mechanisms for the generation of oscillations are hardly ever studied together, which only goes to show just how little is understood about the somitogenesis clock.

Because the experimental system available was chick, and Lunatic fringe-Notch interactions are much better characterized than hairy and Hey genes, it was decided to focus on the Lunatic fringe-Notch feedback loop. A molecular model for the oscillations is proposed in Chapter 2, which resolves the problem of inter-cellular coupling mentioned above. This model is based on a positive feedback loop, unlike that of Dale et al. (2003), which proposes a negative feedback loop for the same system; the experimental data from which a negative feedback loop is inferred is however only indirect, and it is shown in Chapter 2 that that data is actually more compatible with a positive feedback model. Very recently, is has been shown that Notch signalling is upregulated in the PSM of Lunatic fringe mutants (Morimoto et al., 2005; intriguingly, the same antibody seems to give staining patterns different from those reported by Huppert et al., 2005). This has been interpreted as supporting the hypothesis that Lunatic fringe inhibits Notch signalling, but disruption of Lunatic fringe activity in the model presented in Chapter 2 also leads to a level of Notch signalling above baseline levels (manuscript in preparation). This is due to the fact that Lunatic fringe activity can lead to a depletion of the Notch pool, by transforming it to the sensitized form which is supposed to have a shorter half-life.

Chapter 2 therefore shows how mathematical modeling of the mechanism of the clock can help understand its mechanism from a biological point of view.

1.1.7 Experiments

The model detailed in Chapter 2, as well as the problems with the clock and wavefront models mentioned above, made it interesting to test predictions ex-

perimentally. The most obvious prediction to be made from the model in Chapter 2 is that a perturbation of the clock created locally in the PSM will propagate to the rest of the PSM; another is that ectopic upregulation of Lunatic fringe will lead to upregulation of Notch signalling, *at least transiently.* Misexpression of clock-related genes in the anterior-most PSM would have addressed whether the timing of segmentation can be altered by the segmentation clock, how the size of a somite is determined, and what the effects of clock gene misexpression on somite polarity are.

However, no convenient experimental techniques were available to create perturbations in gene expression with sufficient spatial precision. Many systems of inducible expression have been designed, the most common ones being based on tetracycline-responsive proteins (Gossen & Bujard, 1992), temperature-responsive promoters (Chou & Perrimon, 1992), and hormone-responsive proteins (Wang et al., 1994). But few misexpression systems provide the experimentalist with tight spatial control; one is based on heat shocks (Halfon et al., 1997), which makes it unsuitable because heat shocks disrupt somitogenesis by an undetermined mechanism in chicks (Primmett et al., 1988), frogs (Elsdale et al., 1976), and zebrafish (Roy et al., 1999). Others are based on the photo-release of caged compounds (see Shigeri et al., 2001, Ando et al., 2001 for reviews), but do not provide the flexibility of the system described in Chapter 3, which would have allowed to turn gene expression both on and off, with a control of intensities, without having recourse to chemical modification of DNA, RNA, or proteins.

The plant phytochrome PhyB has been previously used to create a light-switch in yeast cells, in a double-hybrid assay which required purification of chromophore from algae extracts Shimizu-Sato et al. (2002). Although spatial control of induction was not attempted by the authors, it was expected that that would only require a tightly-focused light source. Chapter 3 describes an attempt to adapt the system to animal cells, and to enhance it with endogenous

biosynthesis of the chromophore (which hasn not been reported before in animal cells). There was however insufficient time to develop the system to a point where it would work well enough to be used.

In order to read out the effects of the perturbations of clock genes, it was attempted to design a real-time, *in vivo* clock reporter, as described in Chapter 4. This reporter was based on electroporation in chick embryos of a luciferase reporter construct; the reporter construct seemed however to interfere with somitogenesis, and there was insufficient time to resolve that problem.

1.2 Establishment of morphogen gradients

It is considered of great interest to study the process by which cells come to differentiate, both to understand embryo formation, and for possible medical applications. Embryos have a reproducible spatial structure, which stems partly from localized differences in cellular behaviour; somitogenesis is a complex process by which spatial structure is created.

Another way spatial structure can be created is by means of positional information, as proposed by Wolpert (1969, 1996); according to this idea, the localized production of a chemical substance, termed morphogen, leads to a spatial variation in its concentration, which can regulate which type cells differentiate to. It has since been shown that this concept seems to be valid in different instances of development, and in particular for the Drosophila wing disc (Cadigan, 2002). However, a conceptual problem with positional information was pointed out by Kerszberg & Wolpert (1998): for models in which a morphogen diffuses freely in the extracellular matrix, and in which the concentration is read out by membrane receptors, the gradient of bound receptor which is formed tends to be far from linear, meaning that cells differentiating in the regions where it is flat should be exquisitely sensitive to morphogen concentrations, which is probably not realistic. It has been shown that this

problem can be alleviated by hypothesizing a mechanism of ligand-receptor complex degradation and slow association constants (Lander et al., 2002), the possibility of signaling for internalized complexes (Lander et al., 2002), similar to the ligand-triggered, but ligand-free, receptor dimers of Kerszberg & Wolpert (1998), or self-enhanced ligand degradation (Eldar et al., 2003). In Chapter 5, we propose two other simple mechanisms for suitably-shaped morphogen gradients to arise, one based on morphogen oligomerization, and one based on the role of extracellular glycoproteins. The model involving extracellular glycoproteins also has the advantage of providing potential explanations for some of the aspects of the experimental system it is based on.

1.3 High-dimensional switches

Chapters 2, 3, 4, and 5 deal, directly or indirectly, with ways in which positional information can be set up. Models for highly non-linear readouts of that information have been proposed (McCarrey & Riggs, 1986, Kerszberg & Changeux, 1994, Kerszberg, 1996; see Kerszberg, 1999, for a review). The next logical question to address is how positional information can be integrated with other sources of information (such as developmental history) to drive differentiation to specific outcomes. Differentiation is a process during which one cell-type is chosen and all others excluded, in an all-or-none fashion; it is generally driven by a set of key transcription factors. Transcription factors driving cells to assume different fates are often observed to antagonize one another's activity or expression, but they are also often coexpressed, either early on in development or in multipotent cells. Chapter 6 models sets of regulatory networks, identifying those which are capable both of coexpression of antagonistic elements, at a low level (corresponding to cells in early development, or multipotent ones), and of exclusive expression of a specific element; the way the system moves from a state of coexpression to a state of exclusive expression is related to

experimental observations. This study suggests a role for Id proteins which had not been foreseen, highlighting the use of mathematical modeling in conceptualizing experimental data. Chapter 8 extends significantly the range of the networks to which the results in Chapter 6 apply, allowing one to determine not only how the number of coexpressed elements can be regulated, but also how specific elements can be directed to be up- or down-regulated; this is linked to the way the properties of the elements can be affected by intercellular signalling.

These results provide specific examples of how mathematical modeling can be used to aid the understanding of embryo development.

Chapter 2

Is the somitogenesis clock really cell-autonomous? A coupled-oscillator model of segmentation

This chapter is a reproduction of an article whose reference is Is the somitogenesis clock really cell-autonomous? A coupled-oscillator model of segmentation, Cinquin O., J. Theor. Biol. 222(4), pp459-468 (2003)

Abstract

A striking pattern of oscillatory gene expression, related to the segmentation process (somitogenesis), has been identified in chick, mouse, and zebrafish embryos. Somitogenesis displays great autonomy, and it is generally assumed in the literature that somitogenesis-related oscillations are cell-autonomous in chick and mouse. We point out in this article that there would be many biological reasons to expect some mechanism of coupling between cellular oscillators, and we present a model with such coupling, but which also has autonomous

properties. Previous experiments can be re-interpreted in light of this model, showing that it is possible to reconcile both autonomous and non-autonomous aspects. We also show that experimental data, previously interpreted as supporting a purely negative-feedback model for the mechanism of the oscillations, is in fact more compatible with this new model, which relies essentially on positive feedback.

2.1 Introduction

Somites are transient, segmental structures in vertebrate and cephalochordate embryos, derived from paraxial mesoderm (Saga & Takeda, 2001). They are formed on both sides by budding off anteriorly, at regular intervals (90 min in the chick, 2 hours in the mouse), from the presomitic mesoderm (PSM). Mesoderm segmentation and the polarity of the resulting somites play an essential role in the patterning of other structures, such as nerves, vertebrae, muscles and blood vessels (Keynes & Stern, 1988, Saga & Takeda, 2001).

A molecular "segmentation clock", or "somitogenesis clock", was recently identified by Palmeirim et al. (1997), and involves oscillations in both mRNA and protein levels of *c-hairy1*, a chick homologue of a gene first identified in Drosophila. *c-hairy1* expression is not synchronous throughout the PSM: a wave, originating from a large region of posterior PSM, spreads anteriorly while shrinking, and stabilises at the anterior border of the PSM (see below for a more detailed description). A new somite is formed every time a wave reaches the border.

Subsequently, other cycling genes were identified: *c-hairy2* (chick) / *HES1* (mammals) cycles in both chick and mouse PSM (Jouve et al., 2000), and *Lunatic fringe* (*L-fng*), an important regulator of the Notch pathway (Blair, 2000), involved in boundary-formation in insect development, cycles in the chick (McGrew et al., 1998) and mouse (Forsberg et al., 1998) (but not zebrafish, Prince

et al., 2001). A Notch ligand, DeltaC, was also identified as cycling in zebrafish PSM (Jiang et al., 2000). The period of oscillation is 90 minutes for the chick, 2 hours for the mouse, and 20-30 minutes for the zebrafish (Stickney et al., 2000). In the chick, PSM cells experience about 2 cell-cycles (Primmett et al., 1989) and 12 clock-pulses before being incorporated into a somite (Palmeirim et al., 1997).

The oscillatory expression pattern has been classified with 3 stages; in the first stage, cells in the caudal half of the PSM (youngest cells) express the genes in synchrony (or at least with much smaller phase-lags than in the rest of the PSM). In the second stage, the expression pattern moves rostrally and narrows; this narrowing was supposed by Palmeirim et al. (1997) and others (Kaern et al., 2000, Jaeger & Goodwin, 2001, Jaeger & Goodwin, 2002) to stem from a progressive increase of the clock period, but it has also been proposed that it results from shorter synthesis bursts (Cooke, 1998). In the third stage, expression becomes stabilised in one half of a prospective somite, and this somite forms shortly thereafter. Cells undergo a relative movement at constant speed in the PSM, and they oscillate about 8 times while moving from the posterior end to the middle of the PSM. When cells reach the middle of the PSM, the intensity of the oscillations in *c-hairy1* increases sharply (O. Pourquié, personal communication). For other genes such as *c-hairy2*, the intensity of oscillations is on the contrary down-regulated. *L-fng* and *c-hairy1* expression patterns are synchronous in most of the PSM, and diverge when they reach the boundary of the forming somite (McGrew et al., 1998); a stripe of *L-fng* expression stabilises in the anterior part of the forming somite in the chick, but not in the mouse.

Normal functioning of the clock seems to be essential for segmentation, as its disruption by mutations affecting the Notch pathway (Barrantes et al., 1999, Jouve et al., 2000, Jiang et al., 2000, Dunwoodie et al., 2002), or enforcement of a non-zero baseline of *l-fng* expression (Serth et al., 2003, Dale et al., 2003),

result in severe segmentation defects. Different models provide a link between clock oscillations and actual somite segmentation, but our purpose here is to address the mechanism for the oscillations, rather than the way they are read out. Somitogenesis is a process which shows great autonomy; for example, PSM explanted from an embryo still undergoes partial segmentation (even though the process requires ectoderm to go all the way, the segmental pattern is observable, Packard et al., 1993; Lash & Ostrovsky, 1986). Based on one type of experiment, the segmentation clock is generally assumed to be cell-autonomous in chick and mice (see section 2.3.2). However, there is also evidence that there could be some intercellular coupling in segmentation-clock oscillations (see section 2.2.1), as first suggested by Jiang et al., 2000, in the case of the zebrafish. The two aspects seem difficult to reconcile. In the following, we propose however a model for segmentation-clock oscillations which allows for coupling, but can also behave as if oscillations were cell-autonomous, providing a new possible explanation for experiments previously interpreted as ruling out intercellular coupling. The model could easily be extended to account for the very first segmentation clock oscillations in the primitive streak, which occur at a much earlier stage of embryonic development than PSM segmentation (Jouve et al., 2002), and which remain unexplained by current models. Oscillations in the proposed model partially rely on a positive feedback mechanism, but the model is compatible with experimental data which has been interpreted as supporting a negative-feedback mechanism, and is also compatible with experimental data which contradicts a purely negative-feedback model.

2.2 Lunatic fringe secretion model

Many experiments suggest that the somitogenesis clock is not cell-autonomous (see below), but some experiments have been interpreted as ruling out the existence of coupling (see section 2.3.2). The Lunatic fringe secretion model was

formulated to resolve this contradiction, within the framework of current experimental data. The model addresses the way segmentation-clock oscillations are generated and synchronised between cells, in the primitive streak as well as in the PSM. It does not address the relationship between the oscillations, physical somite segmentation, and polarity-establishment, but it is compatible with all major current models, which involve either the existence of a critical threshold maturity (original clock and wavefront model, Cooke & Zeeman, 1976), the spread of a signal (cell-cycle model, Primmett et al., 1989), or an FGF8 wavefront (Dubrulle et al., 2001).

2.2.1 Motivation for the model: intercellular coupling

There seems to be some evidence that PSM clock-gene oscillations are not totally cell-autonomous:

- Primitive-streak precursors of the lateral and medial parts of the same somite do not have the same anterio-posterior position in the primitive streak (Selleck & Stern, 1991, Psychoyos & Stern, 1996, Eloy-Trinquet & Nicolas, 2002), and the expression of their somitogenesis-clock genes does not oscillate in synchrony (Jouve et al., 2002). However, synchrony seems to be achieved quickly upon ingression into the PSM. While other complicated mechanisms could be at play, synchronisation of physically close cells seems to be the simplest explanation.

- Somites are not "developmental compartments": groups of PSM cells with a restricted spatial extent shortly after ingression can have descendants which span many somites (Kulesa & Fraser, 2002), and a single cell, labeled shortly before it is incorporated into a somite, can have descendants in two adjacent somites (Stern et al., 1988). It would be a complicated model, if oscillations are totally cell-autonomous, for daughter cells to inherit different phases after cell division, and to "sort out"

at segmentation time.

- Inversion of the anteroposterior polarity of presumptive somites in the caudal PSM does not result in segmentation or polarity defects (Dubrulle et al., 2001); segmentation models relying on the somitogenesis clock require re-synchronisation of the inverted tissue with surrounding PSM for this to be possible.

- Analysis of zebrafish mutants in the segmentation-clock genes has led Jiang et al. (2000) to conclude that the role of Notch signalling is to synchronise the segmentation clock between neighbouring cells.

- One would expect stochastic effects to have a measurable impact on the individual cellular oscillators, which could not be overcome if oscillations were cell-autonomous. Randomness in transcriptional regulation was discussed by Kepler & Elston (2001); phenotypic effects of varying biochemical parameters were shown by Ozbudak et al. (2002). Intercellular synchronisation was argued by Cooke (1998) to be necessary for the somitogenesis clock pattern to be so refined.

2.2.2 Biological grounding of the model

The Lunatic fringe secretion model is based on experimental data showing the crucial importance of Notch in somite segmentation, on the regulation of *L-fng* in the PSM, which shows that *L-fng* is a target of Notch activity (Cole et al., 2002, Morales et al., 2002, Barrantes et al., 1999, Dale et al., 2003), on the action of L-fng on Notch (Blair, 2000), and on the fact that Notch receptor and ligand expression levels seem to be constant in the chick and mouse PSM (Barrantes et al., 1999, Forsberg et al., 1998). It is fundamentally different from previous models of lateral inhibition mediated by Notch signalling (Collier et al., 1996), in that ligand levels are constant, and Notch signalling is periodically active in

all cells. It is also very different from the clock and induction model (Schnell & Maini, 2000), in which there is no explicit molecular mechanism, Lunatic fringe is seen as a passive output, and oscillations are cell autonomous (the ratchet mechanism at the heart of that model is made very unlikely by experimental results discussed in section 2.3.4, which show that a non-zero baseline of Lunatic fringe disrupts oscillations).

The model accounts for coupling between cellular oscillators by secretion of L-fng, which has not been documented in the PSM, but has been in other experimental contexts (Wu et al., 1996). Notch signalling is very versatile and not fully understood, and cleavage of ligands could be involved in signalling (Artavanis-Tsakonas et al., 1999), providing another potential source of coupling; this could require oscillation of Delta levels, as has been observed in zebrafish (Jiang et al., 2000), but would not necessarily be incompatible with Delta levels being constant on a large scale, as in the chick and mouse.

The secreted factor could be different (and involve a more complex mechanism downstream of the clock) without the results presented in this section being necessarily compromised. It is also conceivable that inter-cellular communication could be mediated by gap-junctions (which do exist between PSM cells, Blackshaw & Warner, 1976); in this specific case, the structure of the model could remain the same, but the equations would probably need to be significantly modified to take into account the strong differences between ionic currents and enzyme kinetics.

2.2.3 Details of the model

In the following, proteins and their concentrations are denoted in the same way.

- Two forms of the Notch receptor are considered, a regular one (n), and another one (n^s), which has been greatly sensitised to Delta signalling by L-fng (l). L-fng makes Notch more sensitive to Delta signalling and less

sensitive to Serrate signalling, which could make the outcome of L-fng modification of Notch uncertain if both ligands were expressed, but Serrate has been shown not to be expressed in the chick embryo up to the first somite stage (Caprioli et al., 2002). Notch is supposed to be translated at a constant rate (in the PSM, no oscillations in Notch mRNA have been shown). Because there is no evidence for oscillations in the levels of Notch-binding proteins in the mouse or the chick, Notch signalling is taken to be proportional to the quantities of Notch protein, with a weighting factor on unsensitised Notch to account for its lower efficiency. This approximates the time for Notch cleavage, for intra-cellular fragment migration to the nucleus, and for degradation of the transcriptionally-active intra-cellular fragment, as being small compared to the period of the somitogenesis clock, so that the intensity of signalling is at a quasi-equilibrium for both sensitised and unsensitised Notch.

- Cell-cell coupling is accounted for by the action of secreted L-fng on neighbouring cells. To keep the model simple, diffusion is not explicitly considered, being replaced by a weighting factor on L-fng from neighbours (if L-fng is indeed secreted, it can probably not travel over distances covering more than a few cells). The strength of coupling is discussed in more detail in section 2.2.4.

- Notch drives the transcription of *L-fng*, with a cooperativity which has been chosen to be 3 (a minimum cooperativity is required for oscillations; 3 is not the minimum, as oscillations are also observed for example with a cooperativity coefficient of 2.7). Notch-dependent expression of *L-fng* is intricate, but two binding-sites for CBF1, which directly mediates Notch signalling, have been identified in the *L-fng* regulatory region (Morales et al., 2002); what's more, experimental data suggests that other such binding sites could be present (Morales et al., 2002). There is thus a

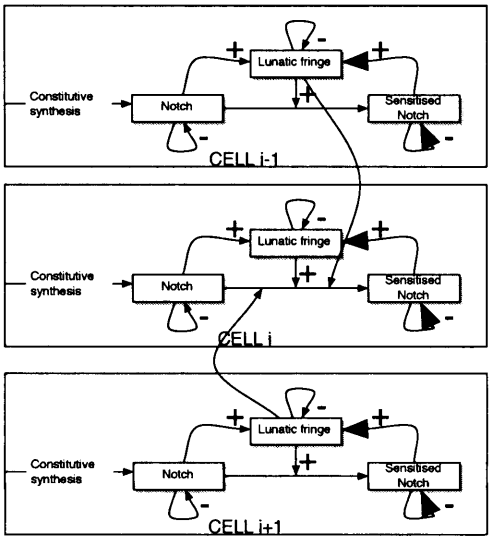

Figure 2.1: Interaction graph of the Lunatic fringe secretion model. For clarity, the influence of cell i on cells i-1 and i+1 is not shown.

basis for cooperative action of Notch on the *L-fng* gene.

- All three proteins undergo exponential decay. This corresponds to degradation which is either spontaneous or mediated by proteases functioning far from saturation.

The graph of the interactions between the components of the model is shown in Figure 2.1. Corresponding equations are given in section 2.6.

Although the general mathematical description of the model is given in two dimensions, only a linear chain of coupled cells will be considered in the following. Results for simulations in 2 dimensions could be in agreement with the experimentally-observed chevron of clock-gene expression (Freitas et al., 2001, Jouve et al., 2002), if one supposes that oscillations are initiated in a laterally-restricted posterior region, and that lateral coupling is weaker then longitudinal coupling. One reason for the lateral coupling to be weaker than the longitudinal coupling (in or close to the primitive streak, not in the PSM), could be that only a proportion of cells are competent to oscillate; if the lateral density of such cells is lower than the longitudinal density, weaker coupling

could be a crude approximation of the decreased efficiency of lateral diffusion of L-fng from one cell to another (since competent cells are more distant laterally than longitudinally). This will be addressed in a later study.

2.2.4 Initial phase and PSM flow

Cells stay only transiently in the PSM. This can be safely ignored when considering cell-autonomous oscillations, but a coupled system can be influenced by conditions at its boundaries, which depend on how newly-ingressed cells and freshly-segmented cells behave.

One important question is that of the initial phase of cells which ingress into the PSM. In the cell-autonomous model, that initial phase must be a complex function of time (the clock and trail model of Kerszberg & Wolpert, 2000, also requires an oscillating initial phase). In the Lunatic fringe secretion model, it may be constant. Since the problem of synchronising newly-ingressed cells with posterior PSM is easier if these cells ingress with an oscillating initial phase (data not shown), simulations presented below were carried out with these cells taking on a fixed initial phase when they ingress.

Oscillations in anterior-most cells were stopped on arrival of an expression wave, with a crude, artificial algorithm (the Lunatic fringe secretion model does not seek to address the mechanism by which cells segment). Cells which had segmented were considered not to influence other cells any more, and their oscillatory phase was blocked.

One important aspect of somitogenesis clock oscillations is that the posterior half of the PSM should keep oscillating in near-synchrony (and that the region of synchrony should not extend anteriorly, beyond the middle of the PSM). To reproduce this, it had to be assumed that coupling was stronger in the posterior half of the PSM. This could be an indirect effect of different cell densities in the anterior and posterior halves of the PSM. Alternatively, it could be that FGF8 has the effect of making coupling stronger (FGF8 has been shown to be

expressed much more intensely in posterior PSM than in caudal PSM, Dubrulle et al., 2001); this would also explain why the caudal-like domain of clock-gene expression can be extended anteriorly by grafts of FGF8 beads, as shown in Figure 4L by Dubrulle et al. (2001). Stronger coupling in posterior PSM could explain why this region is labile with respect to its segmentation programme, while anterior PSM is not. The effects of FGF8-beads grafts could also be explained by effects on the coupling strength, which will be addressed in a later study.

Simulations were performed with coupling being three times stronger in the caudal PSM than in the rostral PSM, the coupling strength being a continuous but sharp function of the relative position in the PSM (see Appendix 2.6 for details). The coupling strength needs not be a continuous function, but this was deemed more biologically realistic.

2.3 Simulation of the model

2.3.1 Reproduction of the somitogenesis clock pattern

The pattern of oscillatory gene expression, as first described by (Palmeirim et al., 1997), can be readily reproduced with the Lunatic fringe secretion model: the posterior half of the PSM can oscillate in near-synchrony, with each wave of expression travelling anteriorly (see Figures 2.2 to 2.4, and Movie 1). It is not straightforward to model the shrinkage of the wave of expression as it travels; rather, a small domain of roughly constant size travels anteriorly from the region of near-synchrony.

Note the difference in intensities of Lunatic fringe expression between the anterior and posterior parts of the PSM, which is compatible with experimental data, and does not require a specific mechanism as in the cell-autonomous case.

The way the system works seems to be the following: the coupling in the model seems to reduce the oscillation period, as L-fng provided by neighbours

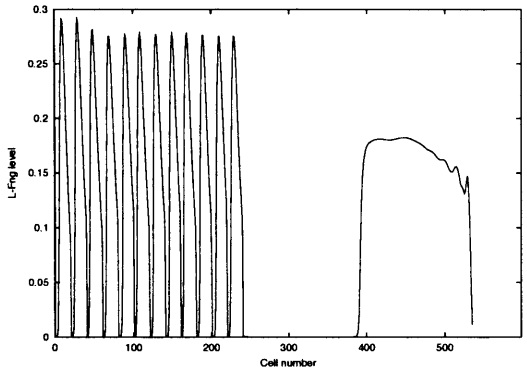

Figure 2.2: Phase 1 in the Lunatic fringe secretion model: a wave of expression initiates in the posterior half of the PSM. Abscissae correspond to cell number in the PSM (anterior is to the left, posterior to the right), and ordinates to L-fringe expression levels (in arbitrary units). At the anterior end, 12 somites have already formed, and their oscillation phase is frozen.

prompts earlier firing (secreted L-fng acts both cell-autonomously and on neighbouring cells, and it is thus possible for an isolated cell to show oscillating expression of clock genes). The stronger coupling in the posterior PSM has two effects. Firstly, its cells tend to fire earlier than those in the anterior PSM (with the right initial conditions). Secondly, cells in the posterior PSM fire more in synchrony than those in the anterior PSM. A wave originated in the posterior PSM travels to the anterior PSM, but more slowly, because of the reduced coupling. It is crucial that L-fng is involved in a positive feedback circuit (with Notch signalling), so that a cell which is firing recruits its neighbours.

2.3.2 Discontinuities in the PSM

Experiments which have been interpreted as proving that somitogenesis clock oscillations are cell-autonomous consist in cutting the PSM transversally, and observing that oscillations continue in both halves for up to two cycles (Palmeirim et al., 1997, McGrew et al., 1998, Forsberg et al., 1998). Within the frame-

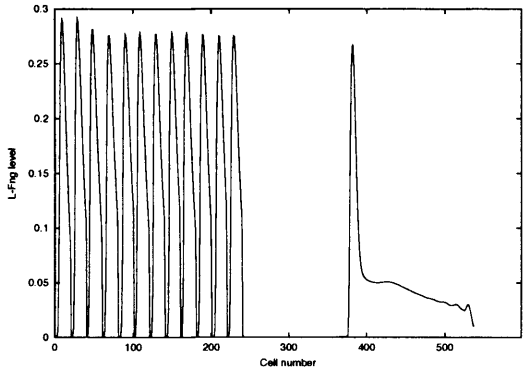

Figure 2.3: Phase 2 in the Lunatic fringe secretion model: the wave of expression now has a much more restricted extent and is travelling anteriorly. Abscissae correspond to cell number in the PSM (anterior is to the left, posterior to the right), and ordinates to L-fringe expression levels (in arbitrary units).

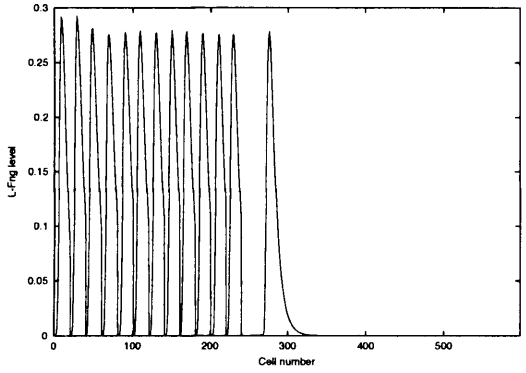

Figure 2.4: Phase 3 in the Lunatic fringe secretion model: the wave of expression reaches the anterior border of the PSM. Abscissae correspond to cell number in the PSM (anterior is to the left, posterior to the right), and ordinates to L-fringe expression levels (in arbitrary units).

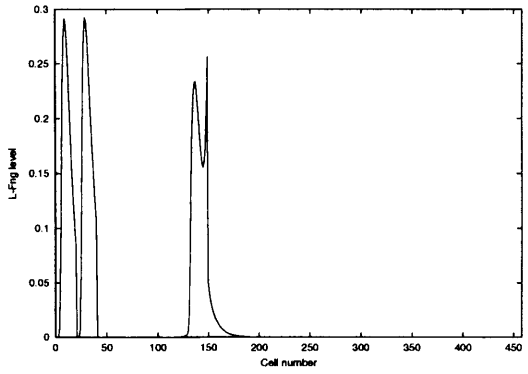

Figure 2.5: 2 cycles after the introduction of the coupling boundary at cell 150, the disruption of the pattern is minimal. An anomaly is only observed at times when the wave of expression reaches the coupling boundary. Abscissae correspond to cell number in the PSM (anterior is to the left, posterior to the right), and ordinates to L-fringe expression levels (in arbitrary units).

work of the Lunatic fringe secretion model, these experiments can be modelled as introducing at some time a coupling boundary in the chain of oscillators, across which oscillators do not influence each other. Simulations have been performed (see Movie 2), which show that the oscillatory pattern is essentially unaffected for many cycles after the introduction of the boundary (see Figure 2.5 for a snapshot 4 cycles after the introduction of the boundary). The disruption becomes larger with time, but current experimental data does not allow verification of whether this actually happens, as tissues were fixed after at most two cycles of oscillation.

2.3.3 Stochastic perturbations

Similar random perturbations were applied during simulations of the Lunatic fringe secretion model, and of the model given by J. Lewis as supplemental data to the article by Palmeirim et al. (1997), which considers cell-autonomous oscillations (see Appendix 2.9 for simulation details). Results are shown in

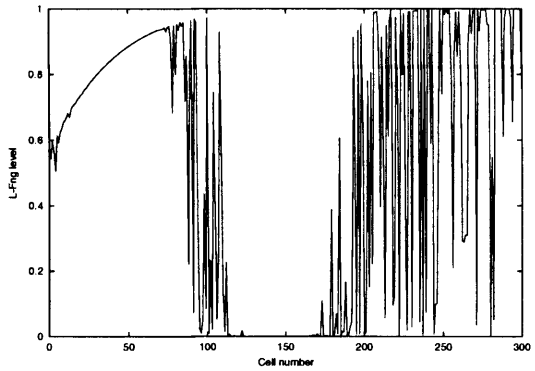

Figure 2.6: Simulation of the cell-autonomous model proposed by Palmeirim et al. (1997), with random perturbations in the phase of each cell. A pattern in unsegmented PSM is barely discernable. Abscissae correspond to cell number in the PSM (anterior is to the left, posterior to the right), and ordinates to L-Fringe expression levels (in arbitrary units). The model was originally proposed for c-hairy1 oscillations, but L-Fringe oscillates with the same pattern.

Figures 2.6 to 2.8 (see Movies 3 and 4 for a complete time-animation). With the Lunatic fringe secretion model, the overall pattern is totally preserved; some variations of expression intensity can be observed in the caudal PSM, but the different phases of oscillation can still be sharply distinguished (Figures 2.7 and 2.8). In the case of the cell-autonomous model (Figure 2.6), stripes of expression corresponding to already-segmented somites are discernable, but levels of Lunatic fringe are extremely heterogeneous in unsegmented PSM.

The model is also robust against parameter variations, as discussed in section 2.7.

2.3.4 Effect of *L-fng* misexpression

It has been observed by Dale et al. (2003) that constitutive misexpression of *L-fng* in the PSM blocks the somitogenesis clock, and suppresses the expression of endogenous *L-fng*. This has been interpreted by the authors as supporting the

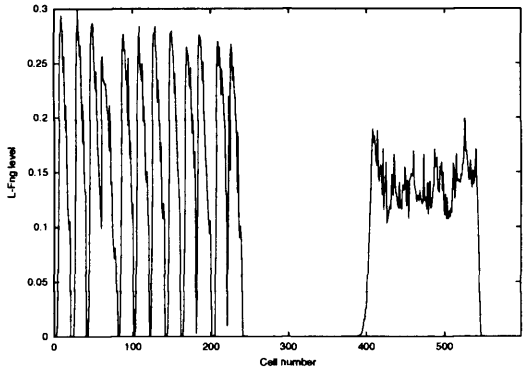

Figure 2.7: Phase 1 in the Lunatic fringe secretion model, with random perturbations: the pattern is still very similar to that shown in Figure 2.2. Abscissae correspond to cell number in the PSM (anterior is to the left, posterior to the right), and ordinates to L-fringe expression levels (in arbitrary units).

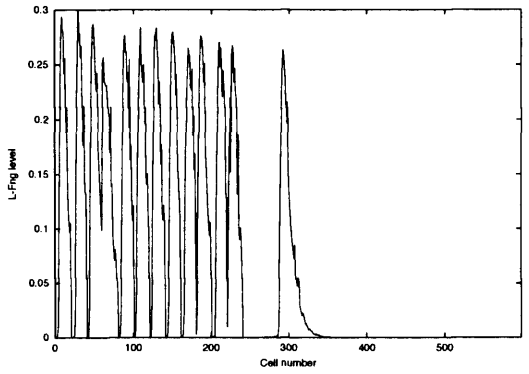

Figure 2.8: Phase 2 in the Lunatic fringe secretion model, with random perturbations: the pattern is still very similar to that shown in Figure 2.3. Abscissae correspond to cell number in the PSM (anterior is to the left, posterior to the right), and ordinates to L-fringe expression levels (in arbitrary units).

existence of a negative feedback circuit between L-fng and Notch signalling: Notch signalling would activate L-fng transcription, and L-fng would down-regulate Notch-signalling; this circuit would be the core of the somitogenesis clock. However, while it has been demonstrated that *L-fng* transcription is indeed activated by Notch signalling (Cole et al., 2002, Morales et al., 2002, confirmed by other means by Dale et al., 2003), L-fng-induced down-regulation of Delta-mediated Notch signalling is contrary to present biological evidence, which shows L-fng-catalysed glycosylation to make the Notch receptor *more* sensitive to activation by Delta (Blair, 2000) (of the two Notch ligands Delta and Serrate, only Delta is expressed in the chick up to the first somite stage, Caprioli et al., 2002).

What is more, suppression of endogenous *L-fng* expression by misexpression of *L-fng* does not imply that the oscillations rely exclusively on a negative-feedback circuit. In the L-fng secretion model, for a single cell there are 4 feedback circuits between the 3 variables, one of which (between L-fng and sensitised Notch) is positive and essential for the oscillations. If the model is modified to account for misexpression of *L-fng*, and if the misexpression strength is above a threshold, oscillations are stopped and *L-fng* is endogenously expressed at a dramatically lower intensity (data not shown). The intuitive reason for this is that continuous *L-fng* expression depletes the pool of un-sensitised Notch; in the model, sensitised Notch has a shorter half-life than Notch, and even though it is continuously produced if *L-fng* is continuously expressed, its concentration is much lower than its peak concentration when it is produced in bursts.

The L-fng secretion model is thus compatible with the data reported by Dale et al. (2003), as well as with the data on sensitisation of Notch by L-fng.

In contrast to Dale et al. (2003), Serth et al. (2003) reported that misexpression of L-fng in mouse PSM does not suppress endogenous oscillations, but disrupts their pattern. A major difference between the method employed by

the two groups is that Dale et al. (2003) electroporated plasmids carrying *l-fng* under the control of a strong, constitutive promoter, while Serth et al. (2003) created transgenic mice with *l-fng* under the control of a portion of the *delta* promoter. It is thus quite possible that a stronger level of misexpression was achieved by Dale et al. (2003). The L-fng secretion model can reconcile both results, because suppression of endogenous oscillations is only achieved above a threshold level of misexpression, comparable to the amplitude of endogenous oscillations; what is more, the amplitude of the endogenous oscillations is reduced by misexpression, as reported by Serth et al. (2003) (however, it was not possible to reproduce the disappearance of oscillations specifically in the anterior PSM).

2.4 Conclusion

The Lunatic fringe secretion model can account for the oscillatory gene expression pattern exhibited by the PSM of chick and mouse embryos. It is dependent on local coupling between cells, which allows it for example to not require new cells to ingress into the PSM with an oscillatory initial phase, and to be more resistant to random perturbations. However, oscillations also have an autonomous character, in that the introduction of a coupling boundary at a specific position of the PSM does not significantly affect the oscillatory pattern. Such a behaviour is in agreement with experiments which were previously interpreted as ruling out the existence of coupling between cellular oscillators.

This shows that coupling between the PSM oscillators is compatible with all current experimental data. What's more, such coupling could explain phenomena which have hitherto remained obscure. The model could benefit from an extension to 2 or 3 dimensions, to earlier embryonic times (and explain the way the phase gradient is set up by the spread of the very first wave), and to a strength of coupling set by FGF8 levels (which could then allow to explain

the anisotropic effect of FGF8-beads grafts described by Dubrulle et al., 2001). This will be addressed in later studies.

Finally, the model, even though it is based on L-fng activation of Notch signalling (in agreement with biological studies of L-fng), is also compatible with data interpreted as supporting L-fng-mediated repression of Notch signalling.

2.5 Note added in proof

After this article went to press, J. Lewis proposed a model for the somitogenesis clock, based on negative feedback and transcriptional delays, inspired by the zebrafish but applicable to chick and mouse (Lewis, 2003). Experiments will be required to distinguish between this model and the Lunatic fringe secretion model, but they could differ in their synchronisation properties, and in their abilities to account for the differences in oscillatory patterns in anterior and posterior PSM.

Acknowledgments

I am very grateful to C. Stern for welcoming me to his lab, for the biological supervision of my work, and critical reading of this manuscript, to K. Page for advice on the mathematical aspects, to O. Pourquié for sharing unpublished information, and to J. Stark and R. Callard for helpful comments. This work was funded by a PhD studentship awarded to CoMPLEX by AstraZeneca. We are grateful to AstraZeneca for their support.

2.6 Equations for the L-fng secretion model

A system defined by a set of the equations below, without coupling to any neighbours, undergoes oscillations for a wide range of parameters. The mecha-

$$\begin{aligned}
\frac{\mathrm{d}l_i}{\mathrm{dt}} &= \alpha_0 \frac{\left(n_i^s + \alpha_3 n_i\right)^3}{\alpha_1 + \left(n_i^s + \alpha_3 n_i\right)^3} - \alpha_2 l_i \\
\frac{\mathrm{d}n_i}{\mathrm{dt}} &= \beta_1 - \gamma_1 n_i \left(l_i + \epsilon_i^l \textstyle\sum_{j \in \vartheta_l(i)} l_j + \epsilon^a \sum_{j \in \vartheta_a(i)} l_j\right) - \beta_2 n_i \\
\frac{\mathrm{d}n_i^s}{\mathrm{dt}} &= \gamma_1 n_i \left(l_i + \epsilon_i^l \textstyle\sum_{j \in \vartheta_l(i)} l_j + \epsilon^a \sum_{j \in \vartheta_a(i)} l_j\right) - \gamma_2 n_i^s
\end{aligned} \tag{2.1}$$

nism seems to rely primarily on the positive feedback circuit, with the system "firing" a burst of sensitised Notch and L-fng once a threshold has been reached in Notch and L-fng.

The equations for cell i (the index denotes the anterio-posterior position in the PSM) are given by equation 2.1, where l_i is the quantity of Lunatic fringe protein in cell i, n_i the quantity of un-sensitised Notch receptor, n_i^s the quantity of sensitised Notch receptor, $\vartheta_a(i)$ the set of axial (longitudinal) neighbours of oscillator i which are considered to influence it, and $\vartheta_l(i)$ the set of lateral neighbours considered to influence it, with ϵ^a and ϵ^l measuring the respective effects of L-fng in proportion to the cell-autonomous effects. In the case of a one-dimensional chain and nearest-neighbour coupling, neighbours of cell i this would be cells $i-1$ and $i+1$, except for the first and last oscillators in the chain. α_3 is expected to be small, and corresponds to weak activation of unsensitised Notch by Delta. The simulations presented below were performed with coupling extending to the 4 nearest neighbours (2 anterior neighbours and 2 posterior neighbours, except for cells close to the borders).

The coupling function used was

$$\epsilon_i^l = \epsilon^l \left(2 + \tanh\left(\frac{-1}{(i/n)^3} + \frac{1}{(1-i/n)^3}\right)\right) \tag{2.2}$$

with n the number of cells in the simulated PSM.

The dynamics of Notch sensitisation are taken to be linear in both enzyme

and substrate as a first simplification. Conditions matching this approximation are saturating un-sensitised Notch or roughly constant levels of un-sensitised Notch.

2.7 Parameters for the L-fng secretion model

Parameters used for simulations are shown in Table 2.1. They were chosen such that the period of the oscillations is about 120 minutes, as in the mouse PSM. Protein concentrations are dimensionless.

The robustness of the model regarding parameter variation was investigated by varying individually each of the parameters in Table 2.1 and equation 2.2, the other parameters and the initial conditions being kept similar (it was too computationaly costly to attempt to find "good" initial conditions for each set of parameters, and the results below thus give a lower bound on robustness). Parameters were deemed satisfactory when a wave spent more than 3 times as much time in the anterior PSM as in the posterior PSM (meaning that oscillations in the posterior PSM are much more synchronous than in the anterior PSM).

The system is least sensitive to parameters governing L-fng (α_0, α_1, α_2, and α_3), the strength of coupling (ϵ^l), and the coupling differential between anterior and posterior PSM (given by equation 2.2), which all can be individually varied 5-fold around the values given in Table 2.1, with the system preserving its behaviour (the oscillation period can be affected). It is slightly more sensitive to the parameters governing the formation of sensitised Notch and its degradation (respectively γ_1 and γ_2), which can be varied 3-fold around the values given in Table 2.1. The most sensitive parameters are those governing Notch synthesis and degradation (respectively β_1 and β_2), which can however be varied by 50%.

The parameters in Table 2.1 correspond to lifetimes of about 3 minutes for L-fng and the sensitised Notch receptor, and of about 64 minutes for the unsen-

sitised Notch receptor. It is normal for the lifetime of the sensitised receptor to be much shorter than that of the sensitised receptor, as it is much more likely to be bound by Delta and cleaved (a process which is not explicitly taken into account by the model). The sensitised receptor is assumed to be about 30 times more efficient at signalling (parameter α_3); thus, if intrinsic stabilities were the same, there should be a 30-fold difference in lifetimes. Since there is only a 20-fold difference, the model assumes that sensitisation makes the receptor more stable than the unsensitised form. Biological data corresponding to these parameters is lacking. The lifetime of L-fng takes into account not only spontaneous or proteolytic degradation, but also diffusion away from the secreting cell, which explains its low value.

Numerical details of the simulations are given in section 2.8.

Parameter	Value
α_0	1.08 min^{-1}
α_1	4.0
α_2	0.217 min^{-1}
α_3	0.03
β_1	0.0217 min^{-1}
β_2	0.0108 min^{-1}
γ_1	15.2 min^{-1}
γ_2	0.217 min^{-1}
ϵ^l	0.3

Table 2.1: Parameters used for simulations.

2.8 Simulation method

Initial conditions were chosen for the system to evolve toward the desired pattern (the Lunatic fringe secretion model currently does not seek to address the

initiation of oscillations). To account for cell-flow in the PSM, new variables were added at regular intervals at the "posterior" extremity, representing new cells entering the PSM, with fixed initial values (corresponding to the state of an isolated oscillator, 1/3rd of its oscillatory period after its L-fng peak). To account for the blocking of the clock once cells had segmented, derivatives in anterior-most cells were set to 0 once they had been reached by an expression wave, and segmented cells were considered not to influence other cells in the PSM anymore.

Integration was performed with the adaptive-stepsize Runge-Kutta algorithm (Press, 1992), which was implemented in a custom Ada program (source available on request). Simulations comprised 300 cells, and were executed on a Macintosh PowerPC running Mac OS 10.2. Graphs were plotted using gnuplot, converted to animated GIFs using gifsicle, and to QuickTime movies with QuickTimePro.

2.9 Random perturbations

The model presented by J. Lewis as supplemental data to the article by Palmeirim et al. (1997) is a phase model, which does not incorporate any molecular mechanism. On the other hand, the Lunatic fringe secretion model is built on a molecular mechanism. It was thus not obvious which perturbation method to use, as the perturbation magnitudes had to be similar for the comparison to be fair. The method chosen consisted in integrating the equations of the two models by small steps (20 per somitogenesis period), and at each step, deciding at random whether each individual oscillator should have its state variables updated or not (the chance of not updating was 20%). The kind of randomness in oscillator behaviour thus modelled corresponds to oscillators "lagging behind" their normal cycle for short periods of time.

Chapter 3

Light-inducible system

I am grateful to Amanda Albazerchi for help with the purification of PCB, as well as early cloning steps in the making of the switch vectors.

This Chapter describes the development of a light-inducible gene expression system, whose purpose is to test the existence of inter-cellular coupling in the somitogenesis clock, which is one of the key features of the model proposed in the previous Chapter. It is impossible with current methods to electroporate the presomitic mesoderm directly, but it is possible to electroporate its precursors. Had the development of the system been successfully completed, precursors of the PSM could have been electroporated with a combination of the clock gene to misexpress and a clock reporter (see next Chapter), the embryo incubated, and misexpression induced later in a well-defined area by shining of a focused beam of light; perturbations in the clock of un-induced cells would have shown the existence of inter-cellular coupling.

3.1 Introduction

A light-inducible system (light-switch) was shown to be functional in yeast by Shimizu-Sato et al. (2002). It is based on *Arabidopsis thaliana*'s phytochrome B (PhyB), a member of a family of photoreceptors regulating de-etiolation

(expansion of the embryonic leaves), shade avoidance, and flowering (reviewed by Schepens et al., 2004). The N-terminus of PhyB (PhyB_NT) can bind the endogenous chromophore phytochromobilin (PΦB) as well as a close cyanobacterial analogue, phycocyanobillin (PCB; Li & Lagarias, 1992). When shone with red light, the chromophore-bound phytochrome adopts a far-red absorbing conformation, and interacts with the Phytochrome-Interacting Factor 3 (PIF3), as assayed by the double-hybrid system; when shone with far-red light, it reverts to its red-absorbing conformation, and stops interacting with PIF3. This has been exploited by Shimizu-Sato et al. (2002) by fusing PhyB_NT to the GAL4 DNA-Binding Domain (GBD) and PIF3 to the GAL4 Activation Domain (GAD), and by driving expression of a LacZ reporter from a GAL4 Upstream Sequence (UAS) enhancer. As neither PCB or PΦB are endogenously present in yeast, the authors incubated the yeast with exogenous PΦB purified from cyanobacterial extracts.

As cultured cells provide a much more convenient setting to assess with precision the properties of an inducible system than a whole embryo, it was attempted to adapt the light-inducible system, as described by Shimizu-Sato et al. (2002), to COS-7 cells (derived by Gluzman, 1981).

Three possible ways to provide the chromophore were envisaged:

1. incubation of the cells in medium supplemented with PCB, purified from cyanobacterial extracts

2. co-transfection of the cells with a vector driving expression of a PCB transporter, to facilitate uptake from the medium

3. co-transfection of the cells with a vector driving expression of enzymes catalyzing PCB synthesis from the endogenously-present heme

(1) did not lead to satisfactory results.

(2) might have been possible with bilitranslocase; bilitranslocase has been identified as importing organic anions structurally-related to PCB into liver

cells (Passamonti & Sottocasa, 1988; see Kamisako et al., 1999, for a review on the subject).

(3) led to the best results (described in more detail below). There were two known avenues to chromophore biosynthesis, one using phycocyanobilin:ferredoxin oxidoreductase (PcyA), and one using PΦB synthase (HY2; see Figure 3.1). Since PcyA misexpression in bacteria had been shown to reconstitute chromophore synthesis (Gambetta & Lagarias, 2001), and PCB was the chromophore used by Shimizu-Sato et al. (2002), it was decided to use that enzyme.

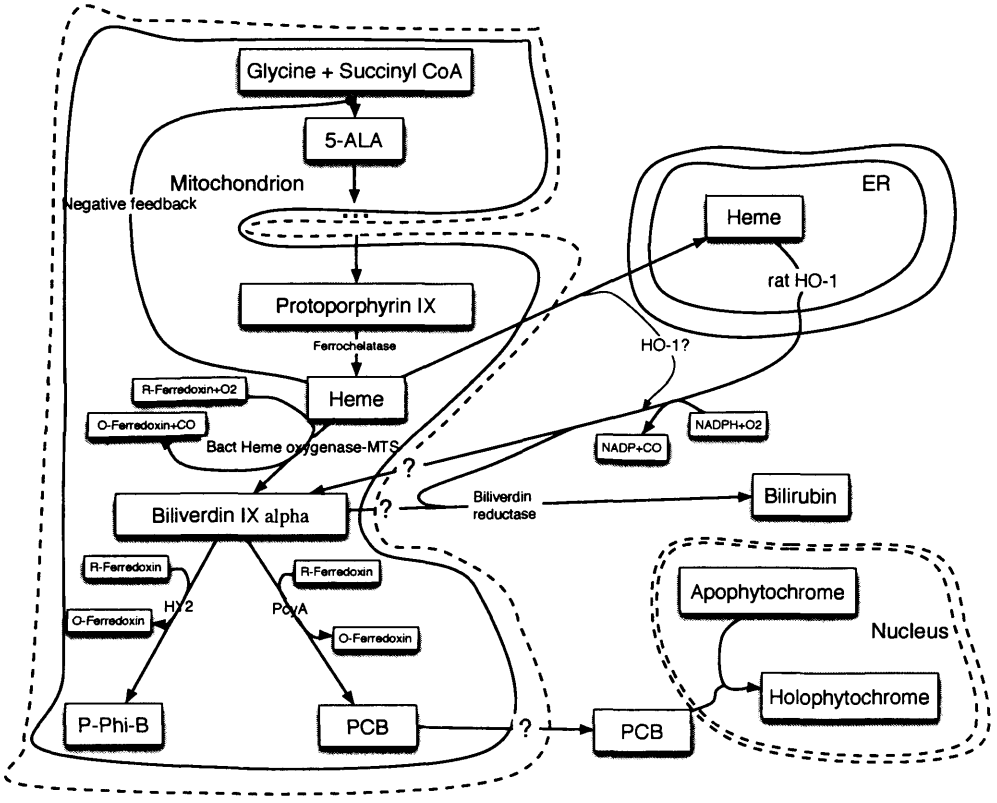

Figure 3.1: Pathway for the biosynthesis of the chromophore. See Frankenberg et al. (2003) for a review of heme biosynthesis.

3.2 Materials and methods

3.2.1 Supplementation with exogenous chromophore

Cells were incubated with PCB at the same concentration as that used by Shimizu-Sato et al. (2002); it had been purified from cyanobacterial according to their protocol, and the preparation was successful as assessed by absorbance spectra, and use of the light-switch in yeast (experiments performed by Kathy Tamai).

3.2.2 Cloning of rat bilitranslocase

The *R. norvegicus* sequence for its mRNA has been reported by Battiston et al. (1998). Intriguingly however, a BLAST search did not produce any hit in the rat or mouse genomes (confirmed by S. Passamonti, personal communication). An RT-PCR on a preparation of rat liver cDNA, with specific forward (ATGTTGATACATAATTGGATCCTGAC) and reverse (TTATTACTCAACCGTGGATCG) primers, based on the sequence reported by (Battiston et al., 1998), did result in the amplification of a single transcript, which was however much too short to be the predicted product (similar results were obtained by S. Passamonti, personal communication). The PCR reaction was performed with Taq in 1.5mM Mg^{2+}-supplemented Promega buffer, with annealing at 55°. Synthesis of the gene would be a possibility, but would carry a very high cost.

3.2.3 Cloning of the switch vectors

The yeast expression vectors used by Shimizu-Sato et al. (2002) were acquired. The open reading frames were re-cloned into vectors adapted to mammalian expression (in particular in terms of mRNA polyadenylation signals; the GAD was also replaced by the VP16 activation domain, which is expected to be 1,200 times more active in vertebrates, Fang et al., 1998). To improve tran-

sient coexpression of the two two-hybrid fusion proteins, along with the chromophore synthesis enzymes, it was decided to have all open reading frames on the same vector (hereafter referred to as "switch vector"). This was achieved in various ways, by combinations of different promoters on the same vector, Encephalomyocarditis virus Internal ribosome Entry Sequences (IRESes; Jang et al., 1989), and fusion with self-cleaving peptides (Szymczak et al., 2004), the latter greatly reducing the size of the vectors and removing the risk of IRES or promoter interference (Adam et al., 1996)

Since apophytochrome - GBD fusions can still bind DNA, it is expected that they might have a dominant-negative effect if they outnumber holophytochrome - GBD fusions (holophytochrome is a stable protein, with a half-life of over 8 hours, references in Eichenberg et al., 1999, but it is not clear what the half-life of apophytochrome is, even if it has been suggested to be less stable, Hennig & Schäfer, 1998). It is therefore probably crucially important that PCB be present in sufficient amounts to bind the majority of the phytochrome (or, equivalently, that the phytochrome be present in sufficiently low amounts). Different promoters driving phytochrome expression were therefore tried: CytoMegaloVirus (CMV) enhancer/promoter, yeast Alcohol DeHydrogenase (ADH; it has been measured to be 100x-fold weaker than the more-common CMV, Lee et al., 1998), and Thymidine Kinase (TK). In some iterations of the switch vector, the GBD-PhyB_NT fusion was expressed from an IRES (a version of which was mutated to provide even lower expression, Rees et al., 1996). PhyB was fused N-terminal to GBD in the system described by Shimizu-Sato et al. (2002), but it proved much more convenient to reconstruct the vector with PhyB fused C-terminal to GBD. Phytochromes are generally fused N-terminal to other proteins, and even though Hennig & Schäfer (1998) successfully recovered phytochrome fused C-terminal to maltose binding protein, they suggest that such fusions can be problematic in the general case. The original vector carried PhyB fused C-terminal to GBD, but the fusion order

was later swapped.

PIF3 was replaced by the first 100 amino acids from PIL2 (also known as PIF6), which were identified by Khanna et al. (2004) as having a 3-fold stronger interaction with the far-red absorbing conformer of PhyB (that data was not available at the time the first constructs were made).

Both bacterial heme oxygenase and pcyA were fused with an N-terminal chicken Mitochondrial Targeting Sequence (MTS; obtained from chicken Mn-superoxide dismutase), shown by confocal observation of an MTS-GFP fusion to be functional in COS-7 cells.

In a variation of the switch vector, bacterial heme oxygenase was replaced by rat ho-1, one of the three mammalian heme oxygenases (first two reviewed by Maines, 1997); ho-1 is the one which is stress-responsive, and which seems to have been most extensively characterized (ho-2 has been proposed to have a more regulatory role, McCoubrey et al., 1997, Galbraith, 1999, and ho-3 has a low catalytic activity, McCoubrey et al., 1997). It is normally targeted to the Endoplasmic Reticulum (ER; although it has recently been shown by Kim et al., 2004, to be also cytosolic in their model), but since biliverdin reductase is cytosolic, biliverdin must be able to diffuse out or be transported.

A summary of the vectors which were tested is presented in Table 3.1.

3.2.4 Reporting of induction

A reporter vector was created comprising a multimerized UAS enhancer, associated to an *hsp70* minimal promoter (as described by Rørth, 1996), driving expression of firefly luciferase from the vector pGL2 (Promega). Another reporter was obtained, comprising a 4-mer UAS enhancer, associated to an adenovirus major late E1B TATA box, driving expression of a *Renilla* luciferase - GFP fusion (Yu & Szalay, 2002). The latter was only used in the first experiments, because *Renilla* luciferase was found to provide a luminescence signal which decayed much more rapidly during IPD imaging (after the addition of

Ref	First transcript	Second transcript
ZX5	ADH:GAD-VP16-PIF3;mutated IRES;GBD-PhyB_NT	CMV:pcyA;mutated IRES;ho1
BG6	ADH:VP16-PIF3;mutated IRES;GBD-PhyB_NT	CMV:pcyA;mutated IRES;ho1
BZ19	ADH:VP16-PIF3;mutated IRES;PhyB_NT-GBD	CMV:pcyA;mutated IRES;ho1
DV2	CMV:VP16-PIF3;mutated IRES;PhyB_NT-GBD	CMV:pcyA;mutated IRES;ho1
DX	ADH:VP16-PIF3;IRES;PhyB_NT-GBD	CMV:pcyA;mutated IRES;ho1
FH5	ADH:VP16-PIF3;IRES;GBD-PhyB_NT	CMV:pcyA;IRES;ho1
FJ5	ADH:VP16-PIF3-SC-PhyB_NT-GBD	CMV:pcyA;IRES;ho1
HG8	ADH:VP16-PIF3-SC-PhyB_NT-GBD	CMV:MTS-pcyA-SC-MTS-ho1
HK1	Beta-actin:neoR ADH:VP16-PIF3-SC-PhyB_NT-GBD	CMV:MTS-pcyA-SC-MTS-ho1
JF3	ADH:VP16-PIL2-SC-neoR-SC-PhyB_NT-GBD	CMV:MTS-pcyA-SC-MTS-ho1
JP3	TK:MTS-pcyA-SC-MTS-ho1;IRES;VP16-PIL2-SC-neoR	-SC-PhyB_NT-GBD
GV	ADH:VP16-PIF3;IRES;PhyB_NT-GBD	CMV:MTS-pcyA-SC-rat ho1
GZ	ADH:VP16-PIF3;mutated IRES;GBD-PhyB_NT	CMV:MTS-pcyA-SC-rat ho1

Table 3.1: Most significant variants of the switch vectors. SC: self-cleaving motif; neoR: neomycin resistance (neomycin phosphotransferase).

coelenterazine to the medium) than the signal from firefly luciferase. Also, the half-life of *Renilla* luciferase was found to have been increased by fusion to GFP (it was measured as being 8.5h by inhibition of protein synthesis with cycloheximide), hampering the assessment of inducibility of the system over a short period of time, as the speed of induction depends heavily on the half-lives of the reporter.

A variant UAS-firefly luciferase reporter was created by introducing an AU-Rich Element (ARE; Chen & Shyu, 1995) in the 3' UTR of the mRNA.

Some of the experiments were carried out with dual-luciferase assays, by cotransfection of a vector driving expression of either firefly or *Renilla* luciferase from a promoter usually considered as constitutive (either the CMV enhancer and promoter, or the Thymidine Kinase (TK) basal promoter). The idea was to normalize the inducibility results by the quantity of cells and/or efficiency of transfection. However, it appeared that both the CMV and TK promoters were up-regulated by the light-treatment of the cells (see below), making them totally inappropriate for that purpose.

3.2.5 Establishment of stable lines

By selection

Switch vectors were designed which carried neomycin resistance as a selection marker, expressed either from its own promoter, or as a fusion to the two-hybrid proteins. Selection was carried out at the lowest neomycin concentration which prevented overgrowth after plating of the electroporated cells (this was found to be $200\mu g/mL$). Once colonies were obtained, they were picked with a yellow tip or trypsinized within cloning rings, and replated in individual wells, or the whole plate was trypsinized and cells replated in individual wells after dilution.

By screening

Lentiviral infection of cells achieves sufficiently high efficiency to warrant direct screening of infected cells, rather than selection. The vector chosen had the advantage of carrying a deletion of the 3' LTR (which results in the deletion of the 5' LTR as well upon integration), alleviating the problem of LTR interference with inducibility and silencing (Yu et al., 1986, Swindle et al., 2004), and insulator elements on both sides, hopefully reducing the basal level expression even further (Ramezani et al., 2003). As the cloning-ring method had been tried previously and had not been successful, the dilution method was used to establish lines (cells were counted, and diluted so that one cell would be expected in the volume pipetted into each well); FACS would have been much more efficient and much more reliable in establishing clonal populations, but a FACS machine was not available.

3.2.6 Induction and assay

Cos-7 cells were cultured in Dulbecco's Modified Eagle's Medium-Glutamax I, supplemented with 10% bovine serum. Switch and reporter vectors were either co-electroporated (10^7 cells/mL, BioRad electroporator settings at 220V for 70 ms, with 4mm BioRad cuvettes and $15\mu g$ DNA), or co-transfected (with Lipofectamine and Plus reagent, Invitrogen, following the manufacturer's protocol). Cells were wrapped up in aluminium foil to avoid both photodamage and unwanted induction, left to recover for 24 or 48 hours, and induction was performed by shining $20\mu W.cm^{-2}$ red light, as measured with a MACAM optical power metre (the light was filtered with a 660nm, 10nm-bandpass filter) for 7 minutes (this exposure was found to give optimal results; reponses did not follow the Bunsen-Roscoe law). Neither the medium (which contained phenol red), nor the plastic lid showed enhanced absorbance in the red as compared to the far-red.

Cells were incubated for 4.5 hours after induction, and assays were performed in one of three ways:

1. Imaging a plate *in vivo*, immediately after addition of 50 nM beetle luciferin (Promega) to the medium, with an Imaging Photon Detector (IPD; Photek, UK, using software and a system design provided by Science Wares, www.sciencewares.com), with a 5x objective.

2. Imaging a 96-well plate *in vivo* (the temperature being maintained at 25°), with a Packard TopCount NXT Microplate Scintillation and Luminescence Counter, which provides photon counts for each well on the plate.

3. Using a photon counter (custom-made by Karl Swann, or from Promega) on a cell lysate (with reagents from the Promega single or double luciferase assay kit); this was the most sensitive (and probably the most reliable) method but photon counters were not always available.

Variations to minimize photodamage

To attempt to reduce photodamage, cells were incubated, prior to induction, overnight with 50μM N-acetyl cysteine, 30μM Trolox, 30mM imidazole, 1mM phenyl-nitrone, 10 minutes with 10mM sodium azide (followed by post-induction washes), or 30 minutes with 20mM imidazole (combinations of those compounds were also tried, as cooperative effects have been shown in antioxidant protection, see Wrona et al., 2004, and references therein).

Deprivation of oxygen prior to induction was attempted, by pre-incubating cells at room temperature in a chamber continuously flushed with pure nitrogen, for periods of time varying from 5 to 20 minutes. It is difficult to know whether oxygen was effectively removed from the medium, as a resazurin solution did not change colour as expected (which is possibly a kinetic problem), and an oxygen electrode was not available.

3.3 Results

3.3.1 Establishment of stable switch lines

The switch vectors, owing to the number of open reading frames they were carrying, were around twice as long as vectors carrying fluorescent markers, electroporated as controls. Short of adding yet another open reading frame with a fluorescent marker (which was not attempted), or designing an mRNA in-situ hybridisation probe, it was impossible to know what the efficiency of electroporation was. IPD imaging of cells after induction showed clusters of activity; it is not clear whether this stems from only cells in those clusters having received both the switch and the reporter vectors, or from heterogeneous responses (which could be related to copy numbers of those vectors).

To have a homogenous cell population, as well as to have a set of different expression levels of the switch proteins, switch vectors were designed which carried a selection marker (neomycin resistance), expressed either from its own promoter, or as a fusion to the two-hybrid proteins.

Very slow growing colonies were obtained (as compared to colonies obtained from cells electroporated with a control vector expressing the neomycin resistance gene under the control of a strong promoter). Despite numerous attempts with three different methods, it proved impossible to obtain viable cells from the small colonies (while that was successful for the control cells).

3.3.2 Establishment of reporter cell-lines

The inducibility of the electroporated UAS-firefly luciferase reporter, as assayed by coelectroporation with a vector driving constitutive expression of a GBD-VP16 fusion with the CMV enhancer and promoter, was around 190-fold 18 hours after electroporation. This is much lower than could have been hoped for. To get better silencing of the uninduced reporter, it was decided to establish reporter cell-lines, with genomic integration of the reporter. The use of

techniques such as transfection or electroporation would have required a promoter driving expression of a selection marker, adjacent to the reporter (unless it was removed after integration, for example with a recombinase), potentially increasing the basal expression level of the reporter. Therefore, genomic integration of the reporter was performed with a lentiviral vector.

Out of about 180 wells plated, only 18 hosted a single, actively-growing colony. Out of these, only 5 showed inducible expression of the luciferase reporter (with induction ratios ranging from 35 to 166, as assayed by transfection with GBD-VP-16, incubation for 18 hours, lysis and photon-counting). The basal expression level of the two lines used for experiments, compared to cells transfected with the same amount of reporter as used in induction experiments, was 50- and 1,000-fold lower.

Thus, although reporter cell-lines were successfully established, and they showed a reduced background expression of the reporter, they did not show a better inducibility than cells co-transfected with a reporter vector.

3.3.3 Proportion of chromophore-bound phytochrome

It would have been extremely helpful, in understanding why only low induction ratios were achieved, to be able to measure what proportion of the phytochrome binds PCB. The fluorescence properties of holophytochrome would have been a great help, as a band of holophytochrome in an SDS-PAGE gel will fluoresce if the gel is supplemented with zinc (Davis et al., 2001). One of the vectors constructed carried a myc-tagged GBD-PhyB_NT fusion. Immunopurification of the fusion was attempted, but proved unsuccessful, possibly because of too low quantities present in the cell extract. The required apparatus was not available to characterize the phytochrome by red/far-red shifting of absorption spectra (difference spectra) of cell extracts, and green fluorescence visualized in vivo did not show any difference between control and switch vector transfected cells. It is thus unclear which quantity of phytochrome is synthesized, and

what proportion is bound to the chromophore.

3.3.4 Supplementation with ALA

The synthesis of Δ-amino-levulinic acid (ALA) is the rate-limiting step of heme biosynthesis, and the negative feedback regulation of heme synthesis is exerted on ALA synthase (Granick & Urata, 1963, Rimington, 1966; see Figure 3.1). It was thus expected that supplementation with ALA would increase the synthesis of PCB, and might alleviate possible detrimental effects of heme breakdown by heme oxygenase.

Pre-incubation with ALA, and induction at the low light intensity described in the induction protocol, was found for some vectors to have a positive effect on the induction ratio. Optimal concentrations were not extensively investigated because of the time-consuming character of the assays, but different vectors seemed to have different optima; in particular, vectors containing rat heme oxygenase seemed to do better with higher concentrations than vectors based on bacterial heme oxygenase.

3.3.5 Investigation of photosensitization

It was noticed that shining ALA-incubated, switch vector electroporated cells, with the intensity and the duration of the standard induction protocol could lead to a dramatic reduction of reporter expression. This effect was later shown not to require any switch vector. More importantly, it was shown that without ALA the switch vectors themselves can cause photosensitization, as assayed by the reduction in expression level of a promoter-less vector containing a luciferase open reading frame (pGL3, Promega). With the higher light-intensity tried, switch-transfected cells showed a 3-fold drop in luciferase expression levels, which can reasonably be assumed to stem from photodamage (an experiment on control-transfected cells was inconclusive and should be repeated).

To have independent readouts of photodamage and induction of expression (which would affect the reporter readout in opposite ways), cotransfection of two luciferases (with different substrates) was performed: one driven by a promoter expected to provide constitutive expression (whose downregulation would have been indicative of cellular damage), and one driven by a UAS (whose upregulation would have been indicative of the system working as intended). However, it turned out that both promoters tested (CMV and TK) can be upregulated by mild light treatment.

3.3.6 Use of antioxidants

To alleviate the photosensitization caused by both ALA and chromophore, induction was performed under low-oxygen conditions, and in the presence of antioxidants. Low oxygen had no detectable effect. Of the antioxidant compounds listed in Materials and Methods, only N-acetyl cysteine and Trolox had a beneficial effect on induction when used with ALA, and a protective effect on constitutively-expressed luciferase; other compounds were found to decrease both luciferase expression and inducibility.

3.3.7 Variations on the illumination protocol

It is not clear whether PCB would be biosynthesized in the active or the inactive conformation. Shining cells with far-red light, and incubating them either overnight or for the same amount of time as for induction assays, did not reduce reporter expression as compared to cells kept in the dark.

Dark reversion of the phytochrome (*i. e.* spontaneous transition from the Pfr form to the Pr form without light stimulation) has been documented in different contexts (see Nagy & Schäfer, 2002, for a general review); reconstituted Arabidopsis PhyB has been shown to undergo only moderate dark reversion (about 25% in an hour, Elich & Chory, 1997), but dark reversion varies with

the systems it is observed in, has been shown to be enhanced by temperature for PhyA (Hennig & Schäfer, 2001), which could be a problem since Cos cells are incubated at 37°, a higher temperature than the one at which either plant or yeast experiments are carried out, and modifications to endogenous phytochromes tend to make them susceptible to dark reversion (Elich & Chory, 1997, Eichenberg et al., 1999). To alleviate possible high dark-reversion rates, continuous overnight incubation in the presence of red-light was attempted, but did not result in enhanced expression of the reporter.

Light intensities much lower than the $20\mu W$ normally used were tested to provide induction, in the hope they might still effectively shift the phytochrome to the active form, while minimizing photodamage, but this did not lead to improved reporter induction.

3.3.8 Best induction results

Table 3.2 shows under which conditions the best induction ratios were obtained. For an unknown reason, Lipofectamine transfection seemed to lead to higher photosensitization of the cells, and to lower induction rates. All the results presented in Table 3.2 were obtained by co-electroporation of switch and reporter vectors. The assay on the Packard well counter was only performed once, and gave better results than assays preformed on lysed cells. This could be because the 96-well white plates hosting the cells (of the format required for imaging) had different optical properties, which affected induction.

3.4 Discussion

3.4.1 Phototoxicity

Phototoxicity seems to be a major issue, but it has proved impossible to investigate to what extent it is responsible for low inducibility. ALA causes

Vector	ALA	AO	Assay	Induction ratio
GX	1x	N-T	P	4.2
GX	4x	-	P	7.4
GV	4x	-	P	6.3
HG	4x	-	P	5.6
FJ	0.3x	-	P	5.4
HG	0	-	P	5.6
FJ	0.3x	-	P	4.6
HG	0	-	L	2.4
FJ	0	-	L	2.6
FJ	1x	N-T	L	3.2
HK	0	-	L	1.8
JF	0	N-T	L	2.5

Table 3.2: Subset of experiments which gave best induction results. AO: antioxidant; N-T: NAC+Trolox; P: Packard; L: lysis. ALA concentration is given as a ratio to 0.5mM

an accumulation of protoporphyrin intermediates, which greatly sensitize cells to phototoxicity (in fact, ALA administration, combined with illumination, is used to treat superficial human cancers, as cancerous cells seem to sensitized much more readily than others, Hasan et al., 2003). The optimum wavelength for ALA-induced photosensitivity has been suggested to be in the red, which is also the range used for activation of the light-switch.

It seems possible that a suitable quantity of holophytochrome is not formed in Cos cells without ALA supplementation and that ALA supplementation causes too much photodamage to see high levels of induction, that Cos cells are more sensitive than yeast to photodamage caused by free or phytochrome-bound chromophore, or that Cos cells expressing the biosynthetic enzymes build up the chromophore to amounts causing higher photodamage than it does at the concentration it is added to the yeast growth medium. The absorption of various chromophores can lead to photosensitization; that did not seem to be the case for phytochrome reconstitution in yeast according to the protocol of Kunkel et al. (1995), but protein synthesis can be inhibited in yeast with phthalocyanine, a dye whose absorption maximum is around the same wavelength as that of PCB (Paardekooper et al., 1995).

The fact that rat ho-1 led to better results than bacterial heme oxygenase, when cells were incubated with ALA, could be due to a variety of reasons, including more efficient removal of protoporphyrins (higher heme oxygenase activity might lead to enhanced clearance of ALA-derived protoporphyrins, depending on what reaction in the pathway is rate-limiting), or different amounts of free chromophore and phytochrome-bound chromophore (which could have different effects on photosensitization). It could be that the bacterial heme oxygenase was not as efficient as native heme-oxygenase. Both bacterial heme oxygenase and pcyA need ferredoxin as a cofactor. Ferredoxins (known as adrenodoxin in vertebrates) are mitochondrial proteins (Grinberg et al., 2000); this is why in the switch vectors PcyA and heme oxygenase were targeted to

the mitochondrion. Conservation of functional interactions between ferredoxins and partners across prokaryotic and eukaryotic sources has been shown, see for example Hlavica et al., 2003, but this interaction could be inefficient.

3.4.2 Possible improvements to the investigation of the cellular responses

- The homogeneity of cell responses is unknown; it could be that some are killed by the shining of light and some survive it, or that all of them sustain a similar amount of damage; the ratio of the two luciferase activities would have been more useful in the first case (a problem with the luciferase assay is that many cells seem to detach from the plate under adverse conditions, although this has not been formally quantified, and are therefore lost; an assay with Trypan-blue dye exclusion might indicate to what extent cells are killed, and other methods are available to quantify cytotoxic effects, Fotakis & Timbrell, 2005).

- It would be useful to have the dual-luciferase assay work properly, without upregulation of the "constitutive" promoter. It is not unexpected for viral promoters to be stress-responsive (Geelen et al., 1987, Andrews et al., 1997). No other suitable promoter was readily available, but it would be possible to use a promoter-less vector, with the constraint that its activity should be assayed first in the Promega double-assay system (as the quenching of the signal of the first assayed luciferase has been observed to not be quite as efficient as described by the manufacturer).

- It would have been of interest to image the kinetics of induction; IPD imaging was not very well suited to that purpose, because plates are heated from the bottom, leading to heavy evaporation and condensation on the lid, and thus to an increased luciferin concentration in the medium, and an artificially-increased luminescence signal. With Packard imaging,

that problem was alleviated by the fact that both induced and un-induced wells can be imaged at the same time, providing a proper control for variations in luciferin concentration; the problem however is that the machine is designed to maintain a temperature of 25°, and cannot be set to 37°.

3.4.3 Possible improvements to the switch

- It has not been tried to express only PcyA as a biosynthetic enzyme, without exogenous heme oxygenase (omitting heme oxygenase might have beneficial effects on cellular metabolism, and make the use of ALA unnecessary). It could be that endogenous heme oxygenase activity is sufficient to provide biliverdin (especially since ho-1 expression is upregulated by a great variety of stressful conditions, some of which electroporation would possibly provide), but it has been shown that the rate-limiting step of heme degradation is heme oxygenase activity rather than biliverdin reductase (Tenhunen et al., 1969), and one would therefore expect that there would be competition with PcyA for biliverdin, and that it would be helpful to provide that substrate in large quantities.

- An ABC transporter expressed during erythroid maturation has been shown to reduce intra-cellular protoporphyrin levels (Zhou et al., 2005). Another ABC transporter, also induced during erythropoiesis, localizes to the inner mitochondrial membrane, and has been suggested to mediate un-characterized transport functions in heme synthesis (Shirihai et al., 2000; the possibility of the transport of the heme degradation product biliverdin across the mitochondrial membrane does not seem to have been investigated, probably because biliverdin reductase is a cytosolic or nuclear enzyme, Maines et al., 2001, but it could be that a low-specificity transporter helps either its export or import, which could be helpful if rat

ho-1 is misexpressed, see Figure 3.1). Misexpression of these transporters might respectively help alleviate ALA-induced photosensitization, and enhance chromophore synthesis; the cDNA for the latter was obtained, but had not yet been used at the time of writing.

- Since the amount of ferredoxin reductase can be a limiting factor in some biosynthetic processes (Tuckey & Sadleir, 1999), expression vectors for both bovine adrenodoxin and adrenodoxin reductase were obtained; at the time of writing coexpression of these vectors along with the switch vectors had not yet been attempted.

- It remains a possibility that exogenous chromophore uptake might by enhanced by the addition of Tween or dimethylsulfoxide (Kunkel et al., 1995); but it is not clear what the effect on the viability of the Cos cells would be.

- Edaravone could have been a very good anti-oxidant to use, as it has been shown to be a potent inhibitor of photodamage on cells in culture (Tanabe et al., 2005), but it did not seem to be available commercially as of June 2005. It would have also been interesting to try a combination of zeaxanthin and ascorbic acid, as this has been shown to specifically protect cells against photooxidative damage (Wrona et al., 2004).

- Photosensitizers excited by light can directly interact with various molecules, or interact with oxygen; the latter is greatly favoured in most cases (Foote, 1968), and it has been shown that the presence of oxygen is an absolute requirement for photoinactivation of cells incubated with a porphyrin derivative (Moan & Sommer, 1985). The method used here to reduce oxygen did not lead to noticeable results, but according to Moan & Sommer (1985) incubation in a 1% O_2 atmosphere is sufficient for 50% of the photoinactivation effect to occur. It is therefore very possible that

the reduction in oxygen concentration which was achieved was insufficient. Commercial systems used to remove oxygen from vessels used to cultivate anaerobic organisms are available, but carry a high price. Alternatively, it might be worthwhile degasing the medium beforehand, and replacing it with N_2-saturated medium (Camerin et al., 2005).

- The uninduced level of expression of the reporter was very close to the level of expression obtained by electroporating cells with reporter alone (a 1.4-fold difference was measured); the problem with low induction ratios therefore stems from defective activation of the reporter, rather than "leaky" expression of the reporter. To amplify the induction of the reporter, a vector was designed in which the same UAS used for the luciferase reporter drove expression of a GBD-VP16 fusion. This system by itself would not have allowed the switch to be turned off, and a cysteine motif for light-induced degradation (Tour et al., 2003) was thus additionally fused. The switch and UAS-GBD-VP16 vectors, as well as the UAS-luciferase reporter, were coelectroporated. However, the basal expression level of uninduced UAS-GBD-VP16 was sufficient to self-activate the switch, despite the presence of an ARE in the mRNA of the GBD-VP16 fusion. A lentiviral vector containing the UAS driving GBD-VP16 was constructed, and no self-activation observed; it is however not clear whether that construct was functional (as the ARE could have interfered with viral replication).

- While this writing was in progress, the cloning of a heme importer was reported (Shayeghi et al., 2005). Its misexpression in cell-lines increases heme uptake a few fold, and although it has some specificity, it remains a possibility that it might also enhance PCB uptake.

3.5 Conclusion

Shimizu-Sato et al. (2002) report that the level of reporter expression they achieve 3 hours after activation of the light-switch is about 1/6th of the level of expression obtained from the native GAL4 protein. Supposing the response lag due to long mRNA and reporter half-lives is not greater for the adapted light switch than for the original one (which is reasonable because luciferase has a much shorter half-life than betagalactosidase), such a level of expression would translate to an induction ratio of at least $190/(6*1.4) = 20$, where 190 is the induction ratio provided in Cos-cells by the GBD-VP16 fusion, and 1.4 the "leak" of the light-switch proteins in the dark. The induction ratios that were achieved (repeatably around 3) are far below this (this however does not take into account the fact that not all electroporated cells will express the switch vector, which is a reason why it would have been helpful to establish a stable cell-line), and it is doubtful that the system would be useful as such for the applications envisaged.

Even though many variations have been experimented with to improve inducibility, because of the sheer number of combinations, only a very small subset has been tried; it remains a possibility that a specific combination of the variations tried would have given satisfactory results. If this work was to be pursued, it would be essential to determine what proportion of the phytochrome is in the chromophore-bound form.

Chapter 4

Reporting of the clock oscillations

This Chapter describes the development of a real-time reporter for the somitogenesis clock oscillations. This would have been of great interest in its own right, because the oscillations have never been directly visualised, but only inferred from differences in expression patterns across embryos or between embryos halves incubated for different periods of time. In combination with the light-inducible system described in the previous Chapter, it would have allowed to easily visualise perturbations induced in the clock.

4.1 Introduction

To date there has been no real-time reporting of the somitogenesis clock oscillations. This is probably due to the fact that the oscillations occur with a period which is short compared to the time of chromophore formation of the Green Fluorescent Protein (GFP; see Reid & Flynn, 1997, for a kinetic study) and its half-life, even when it is destabilized by addition of a "PEST tag" (the half-life of the destabilized version is 2 hours, Li et al., 1998). Luminescence reporting does not share the time limitations of GFP, as luciferase seems to

be active immediately upon synthesis, and has a short activity half-life when in the presence of its substrate. It also has the great advantage of providing quantitative data.

Various promoters driving luciferase expression were tested to provide reporting of the clock phase after electroporation into chick embryos.

4.2 Materials and methods

Embryo manipulation

Embryos were electroporated dorsally with a DNA solution containing $0.25\mu g/\mu L$ to $1.1\mu g/\mu L$ of luminescent reporter vector, $1\mu g/\mu L$ DsRedExpress-N1 (BD Biosciences), 6% sucrose and 0.04% Fast Green, at stage 5, around the anterior-most primitive streak (where many PSM progenitors seem to be located, Psychoyos & Stern, 1996), with an Intralcel electroporator set to deliver 3 6V, 50ms pulses, New-cultured (New, 1955, Stern & Ireland, 1981) until red fluorescence became visible, transfered to an 1% agar-, 50nM beetle luciferin-supplemented albumin Petri dish, and imaged on the IPD. No integrated atmosphere-control system was available on the IPD, and despite coating the inner face of the lid of the Petri dish with albumin, and sealing the dish with Parafilm, heavy condensation was produced on the lid, altering its optical properties and desiccating the embryo; a custom-made plastic box with a copper base, heated from the bottom, reduced condensation sufficiently.

Construction of a vector for constitutive luciferase expression

The CMV enhancer - beta-actin promoter was inserted into pGL2 (Promega).

Construction of the Lunatic fringe reporter

The mouse Lunatic fringe promoter has been shown to drive cyclic expression of a lacz reporter in PSM (Morales et al., 2002, Cole et al., 2002). The firefly luciferase gene from pGL3 (Promega) was inserted downstream of the mouse Lunatic fringe promoter, provided by Cole et al. (2002), replacing their beta-galactosidase reporter[1].

4.3 Results

IPD imaging of embryos electroporated with a vector driving constitutive luciferase expression showed firefly luciferase to be functional in chicken embryos, and luciferin to be diffusible through the egg white and cell and vitelline membranes. The half-life of luciferase activity, measured after inhibition of protein synthesis with cycloheximide, was 25 minutes.

Promoters tested for oscillatory activity when electroporated into chick PSM were those of the Notch targets Hes1, Hes7, Hey1, and Hey2; these promoters would have been expected to drive oscillatory transcription in mouse embryos, unless there were 3' regulatory regions not included in the constructs, required for oscillating expression in the PSM. Activity could be detected for Hes7 and Hey2, mainly in the PSM, but it proved difficult to observe the expected oscillatory pattern.

The Lunatic fringe luciferase reporter showed on rare occasions oscillatory activity, but never more than two oscillation rounds (see Figure 4.1), and never with the overall pattern that would be expected in the PSM, based on the mRNA in-situ hybridisation data. This is most probably related to the fact

[1]The results of many independent sequencing reactions on the plasmid provided by the authors agreed with the NCBI mouse genome sequence, but differed by one base-pair from the sequence reported by the authors. They did not confirm whether this was due to a sequencing error, but suggested polymorphism as a possible explanation.

that electroporation of the reporter seemed to block segmentation, after the first 6-8 somites (on a set of embryos co-electroporated with the reporter and DsRed, after overnight incubation, 1 had 13 somites but no DsRed expression, 1 had 10 somites and DsRed expression only in the notochord, 1 had 8 somites and PSM expression of DsRed, 2 had 8 somites and PSM and somitic expression of DsRed, 1 had 7 somites and PSM and somitic expression of DsRed, and 1 had 6 somites and somitic expression of DsRed). Concentrations of the reporter as low as $0.25\mu g/\mu L$ were used for electroporation (the vector length is about 10kb); as observed signal intensities decreased with concentration, it is expected that it would be very difficult to get a signal from more diluted reporter.

4.4 Discussion

A possible cause for the segmentation phenotype observed is the introduction of a great number of transcription factor binding sites identical to those in the Lunatic fringe promoter, carried by the reporter. This could disrupt expression of Lunatic fringe, blocking the segmentation clock (it is often the case in mouse and zebrafish that mutations affecting the clock still allow formation of the most anterior somites). In-situ mRNA hybridisation with clock markers would tell whether the clock really is disrupted.

It is plausible that a way to prevent the reporter from interfering with the segmentation clock would be to deliver it as a single copy (or only a few copies) to a large quantity of cells in the PSM. This might be achievable with the same lentivirus as described in the previous chapter. A version of the virus carrying GFP was injected under unincubated embryos, and the embryos antibody-stained for GFP after a 48-hour incubation period. Weak, uniform staining was observed, suggesting that VSV-G-pseudotyped lentiviruses can successfully infect chicken embryos (this has also been shown by McGrew et al., 2004, Chapman et al., 2005). A viral version of the Lunatic fringe-luciferase

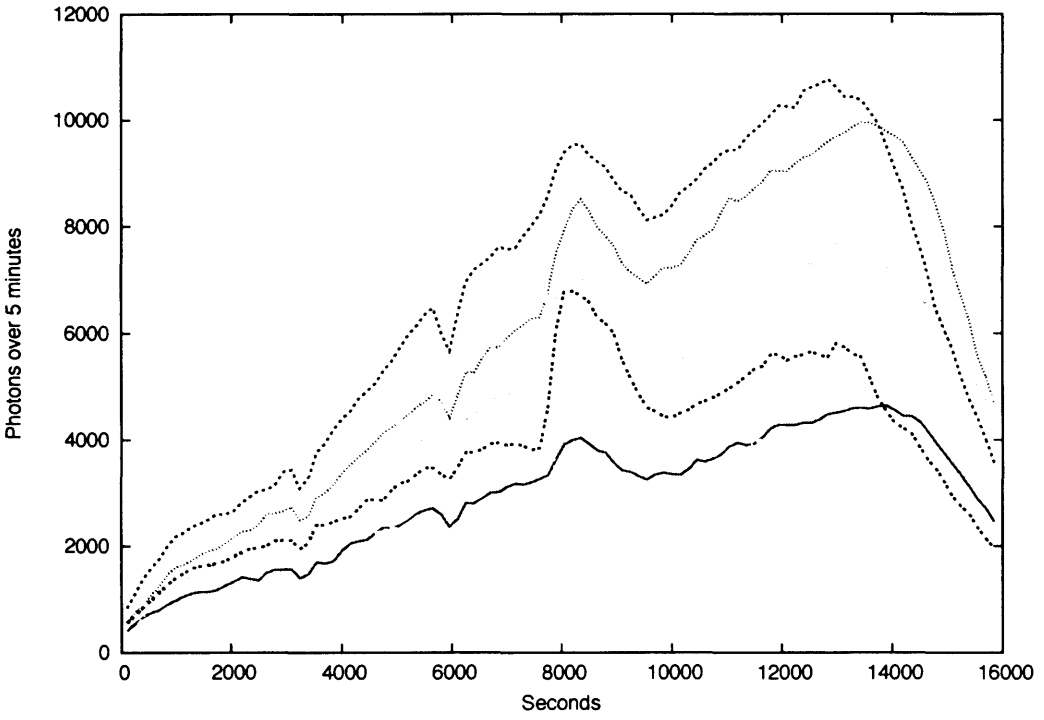

Figure 4.1: Example of the best oscillatory activity which was obtained. Each curve represents the photon-count, integrated over a 5-minute sliding window, registered from a small area of the PSM. The inter-peak distance is roughly 90 minutes, the period of the somitogenesis clock in chicken.

reporter was under construction at the time of writing.

Chapter 5

Fast-tracking morphogen diffusion

This chapter is a reproduction of an article whose reference is Fast-tracking morphogen diffusion, Cinquin O., J. Theor. Biol. (in press)

The previous Chapters address somitogenesis, which is a complex process by which spatial structure is created in embryos. Another way in which spatial structure can be created is by the establishment of positional information within the embryo, and the differentiation of cell behaviour depending on the information they read out at their location. The establishment of positional information and its readout can interfere, and this Chapter proposes a possible solution to that problem, based on recent experimental results. Although positional information is involved in somitogenesis through the FGF8 gradient, it seems to be established by a cell-intrinsic mechanism, rather than by diffusion of a morphogen, which is considered here.

Abstract

The readout of morphogen concentrations has been proposed to be an essential mechanism allowing embryos to specify cell identities (Wolpert Trends Genet

12 (1996) 359), but theoretical and experimental results have led to conflicting ideas as to how useful concentration gradients can be established. In particular, it has been pointed out that some models of passive extracellular diffusion exhibit traveling waves of receptor saturation, inadequate for the establishment of positional information. Two alternative (but not mutually exclusive) models are proposed here, which are based on recent experimental results highlighting the roles of extracellular glycoproteins and morphogen oligomerization. In the first model, inspired from the interactions of Dally and Dally-like with Wingless and Decapentaplegic in the third-instar Drosophila wing disc, two morphogen populations are considered: one in a cell-membrane phase, and another one in an extracellular-matrix phase, which does not interact with receptors; in the second model, inspired from biochemical studies of Sonic Hedgehog, morphogen oligomers are considered to diffuse freely without interacting with receptors. The existence of a dynamic sub-population of freely-diffusing morphogen allows the system to establish a gradient of bound receptor, which is suitable for the specification of positional information. Recent experimental results are discussed within the framework of these models, as well as further possible experiments. The role of Notum in the setup of the Wingless gradient is also shown to be likely not to involve a gradient in Notum distribution, even though Notum is only expressed close to the source of Wingless synthesis.

Abbreviations: Dll: Dally; Dlp: Dally-like; Dpp: Decapentaplegic; Wg: Wingless; Shh: Sonic Hedgehog

5.1 Introduction

The third instar Drosophila wing disc has provided examples of molecules forming morphogen gradients (reviewed by Cadigan, 2002). Whether the transport of morphogens relies on passive extracellular diffusion has been a source of intense debate (see for example Kerszberg & Wolpert, 1998, Lander et al., 2002,

Kruse et al., 2004), but recent experimental data has dealt a new hand by greatly clarifying the role of extracellular proteoglycans in the establishment of morphogen gradients (Baeg et al., 2004, Belenkaya et al., 2004, Han et al., 2004, 2005); mathematical models are yet to be developed to take this role into account.

It was first observed by Kerszberg & Wolpert (1998), and confirmed by Lander et al. (2002), that a simple system of morphogen diffusion and receptor binding will generally create a traveling wave of receptor saturation and not a stable gradient of bound receptor. It has been shown that this problem can be alleviated by hypothesizing a mechanism of ligand-receptor complex degradation and slow association constants (Lander et al., 2002), the possibility of signaling for internalized complexes (Lander et al., 2002), similar to the ligand-triggered, but ligand-free, receptor dimers of Kerszberg & Wolpert (1998), or self-enhanced ligand degradation (Eldar et al., 2003). We propose here two other simple mechanisms for suitably-shaped morphogen gradients to arise, one based on morphogen oligomerization, and one based on the role of extracellular glycoproteins. The latter model illustrates what the role of extracellular glycoproteins could be, and also provides a specific insight into the establishment of the Wingless (Wg) gradient, one of the morphogens identified in the Drosophila wing disc.

5.1.1 Glycoprotein-mediated phase repartition

This model is inspired from the Wg (Zecca et al., 1996) and Decapentaplegic (Dpp; Nellen et al., 1996) morphogen gradients in the Drosophila wing-disc, but could also apply to other gradients, such as the Sonic Hedgehog (Shh) gradient in the developing neural tube (Briscoe et al., 2001). Dally (Tsuda et al., 1999; abbreviated Dll) and Dally-like (Khare & Baumgartner, 2000, Baeg et al., 2001; abbreviated Dlp) are cell-surface heparan sulfate proteoglycans, tethered to the membrane by a GPI anchor (ie, glypicans), which have been shown to influence

both Dpp and Wg signalling. In the Drosophila wing disc, Wg and Dpp cannot diffuse into clones deficient for both Dll and Dlp, or into clones deficient for heparan-sulfate synthesis (Belenkaya et al., 2004, Han et al., 2005); it has been proposed that Dll acts as a Wg co-receptor, while Dlp mediates Wg movement across cells (Baeg et al., 2001), but Dll seems to also have a role in mediating inter-cellular movement (Han et al., 2005). Importantly, Dlp can be released into the extracellular matrix by the secreted protein Notum (Kreuger et al., 2004), and Dll-Notum interactions have been shown to be essential for wing-disc patterning (Han et al., 2005), suggesting that Dll could also be released by Notum. Notum is mainly expressed in the region of high Wg signalling, and can itself be released into the extracellular matrix (Gerlitz & Basler, 2002, Giráldez et al., 2002). Notum would not be taken into account in a model for Dpp gradient establishment (see below for a further discussion of Notum as regards the Wg and Dpp gradients).

In the model proposed here, and illustrated in Figure 5.1 Dll and Dlp are considered as a single entity (noted as d in the equations detailed in Appendix 5.4.4), which binds to the morphogen m. Two populations are considered, one in the extracellular matrix (EM), and one on the cell membrane (mem); cell membrane-attached d molecules are released into the extracellular matrix by Notum (n). The crucial hypothesis of the model is that the morphogen equilibrates between the extracellular matrix and membrane phases, following the repartition of d. Extracellular morphogen is injected at the left boundary, and Notum synthesized (and considered to be immediately secreted) over the first $10\mu m$. Both free and bound receptor populations are taken into account, with a fixed rate of receptor synthesis, and unregulated degradation.

In order for the model to be compatible with the experimental data showing the absence of diffusion of morphogen into clones deficient for Dll and Dlp, only the EM morphogen and Notum are considered to diffuse.

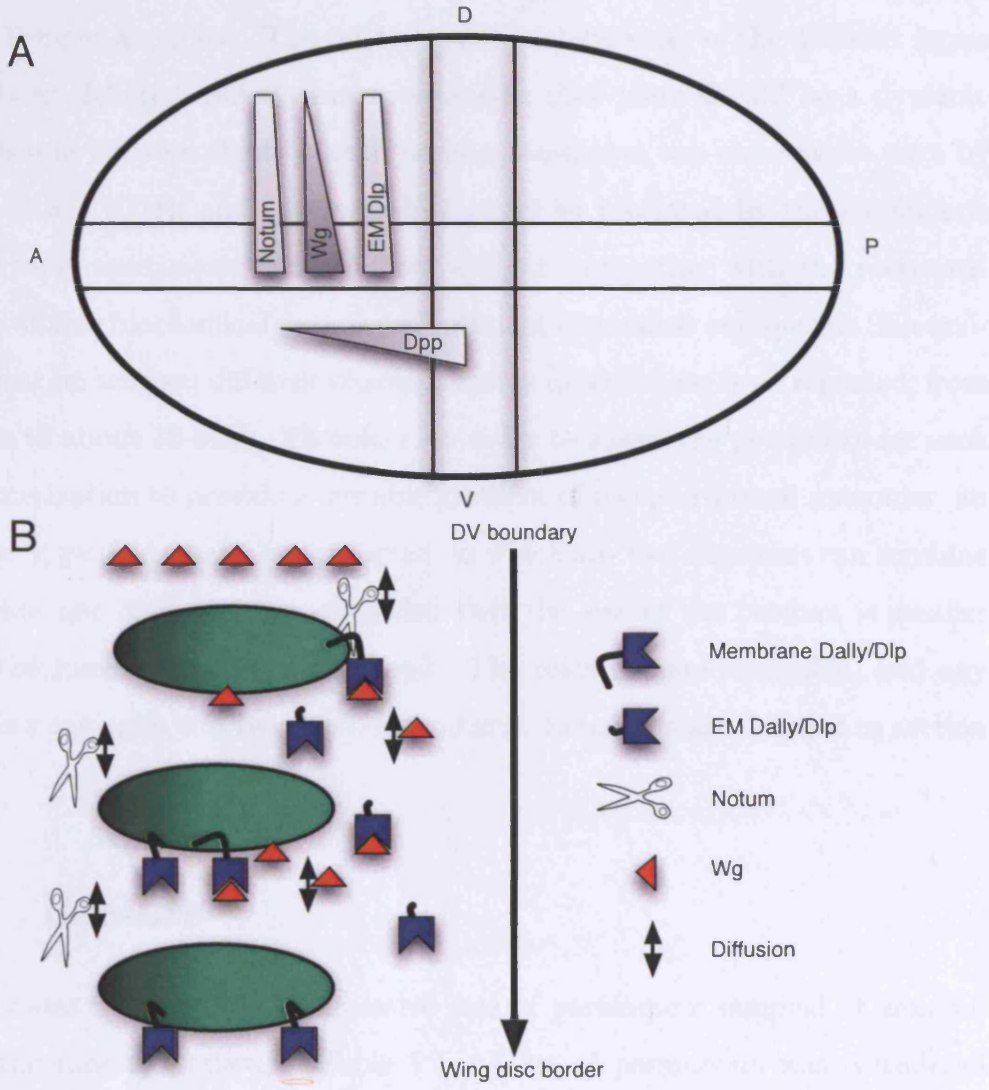

Figure 5.1: (A) Distribution of Wg, Dpp, Dll/Dlp, and Notum in a Drosophila third instar wing disc. (B) Glycoprotein phase-repartition model for Wg signaling.

5.1.2 Shh-like oligomerization

Shh has been shown to oligomerize, and it has been proposed that the higher-order multimers mediate long range signalling (Zeng et al., 2001, Chen et al., 2004, Feng et al., 2004). The relative signaling potencies of the different forms have been debated, but it seems reasonable that there should be a dynamic equilibrium between them (even if no interconversion was observed *in vitro* by Chen et al., 2004), and that signaling could be mediated by the monomeric form, while multimeric forms diffuse without interacting with the receptors. The available biochemical data is not sufficient to propose one specific Shh multimerization scheme; different oligomerization extents have been reported, from 6-mers to about 30-mers. Therefore, in order to assess the possibility for such multimerization to provide a suitable gradient of receptor-bound monomer, an arbitrary, generic scheme was adopted, in which any two oligomers can combine to create one of higher size, provided that the size of the product is smaller than the maximum being considered. The reactions are reversible, and any oligomer can split into two smaller products. Equations are detailed in section 5.4.5.

5.2 Results

Simulations were run with successive sets of parameters sampled at random from the ranges detailed in Table 5.1. A set of parameters was considered to be suitable if the following conditions on the gradient of morphogen-bound receptor were met:

- about 3 hours after the start of the simulation, the concentration of morphogen-bound receptor was sufficiently close to linearity (as per a measure described in the appendix)

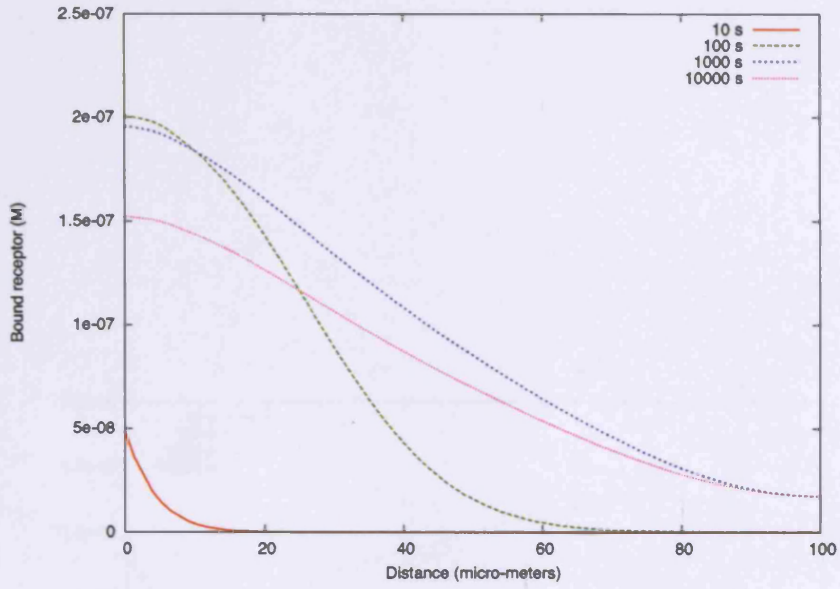

Figure 5.2: Example of a gradient of bound receptor which meets the criteria described in section 5.2.1 10000s after the start of the simulation.

- after a further 3 hours of simulation, the gradient stayed with 30% of its original values
- the range of the gradient was greater than 2-fold
- the concentration of bound-receptor at the high end was greater than 30nM (corresponding to 100 bound receptor molecules, following the calculations in Lander et al., 2002), and more than 2% of the receptors were bound to morphogen 75μm into the field.

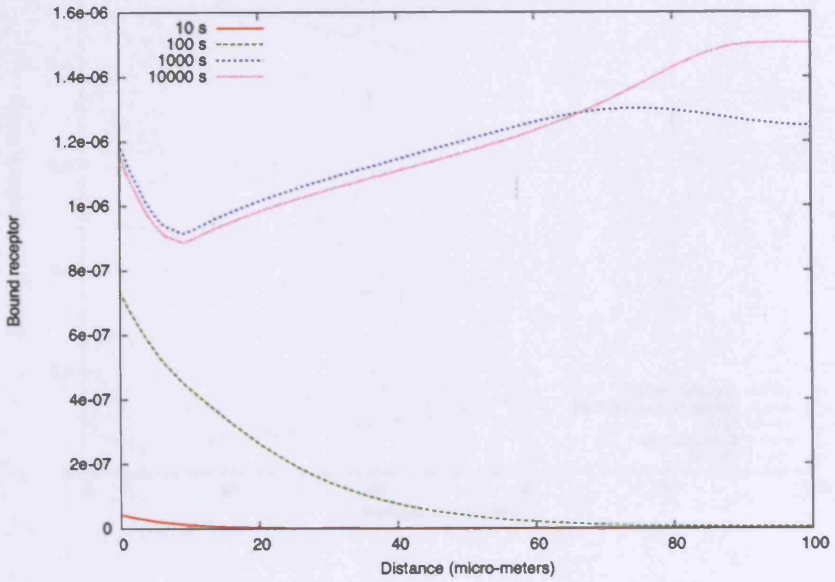

Figure 5.3: Example of a non-monotonous gradient of bound receptor.

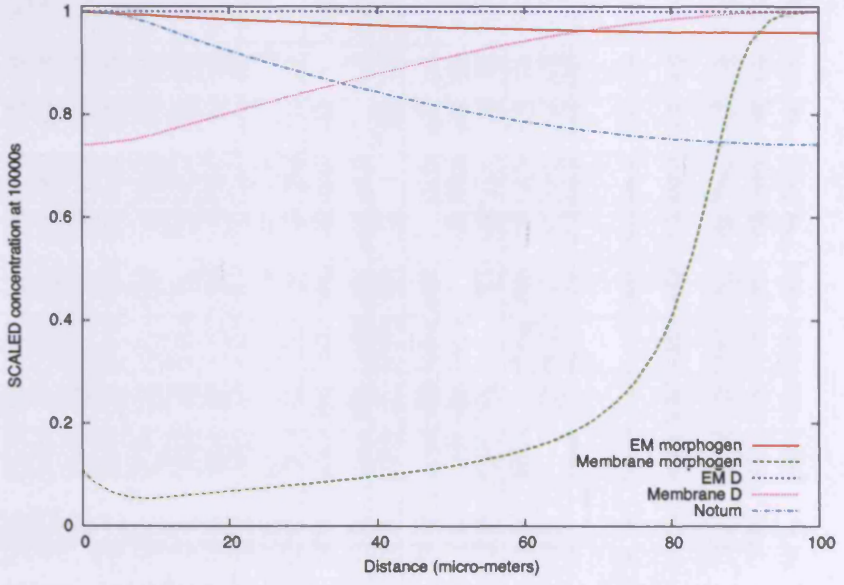

Figure 5.4: Concentrations of other elements of the system, for the same parameter values as in Figure 5.3, at 10000s. The curves were scaled with their highest value so their variations would be visible on the same graph.

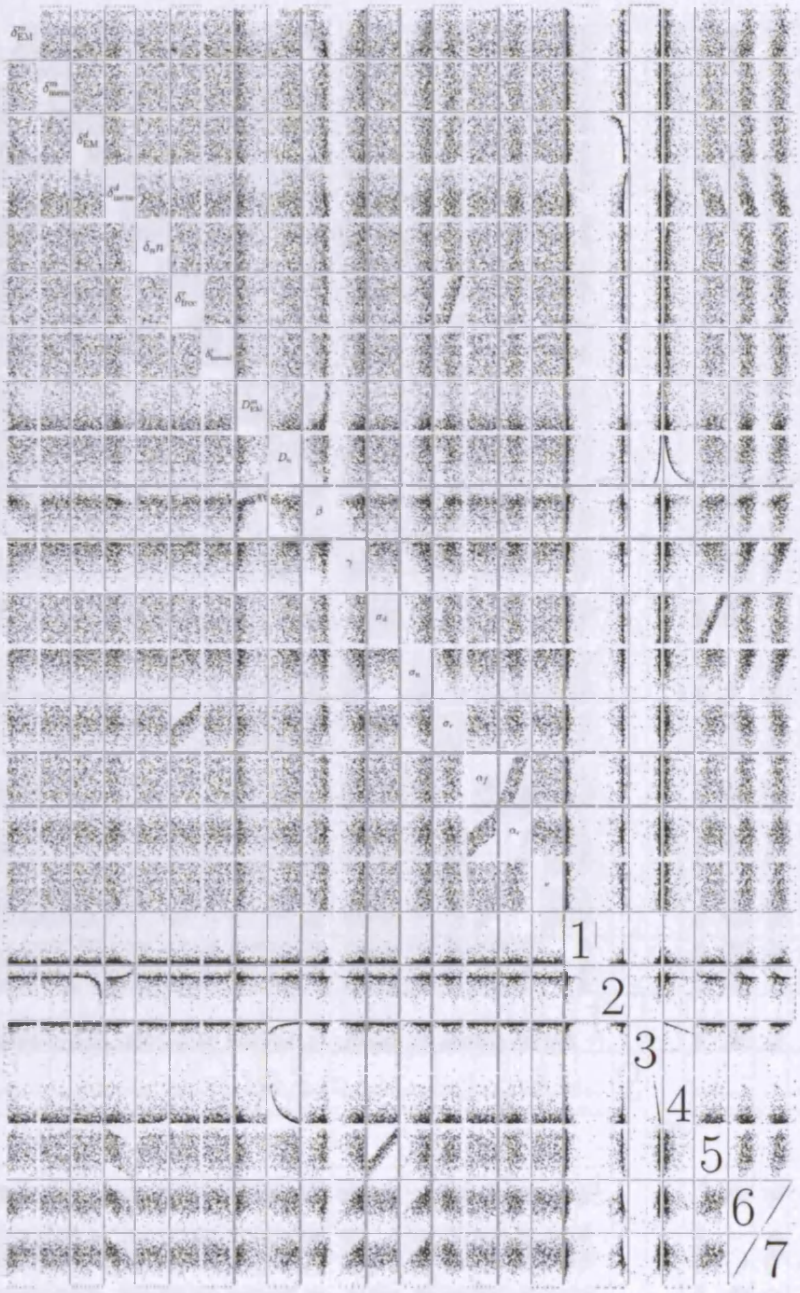

Figure 5.5: Pairwise plot of parameters for which the model with localized Notum synthesis gives rise to a gradient of bound receptor meeting the conditions set out in section 5.2.1. 1: $\frac{r_{\text{bound}}(0)}{r_{\text{bound}}(100)}$, 2: $\frac{d_{\text{EM}}(0)}{d_{\text{EM}}(100)}$, 3: $\frac{d_{\text{mem}}(0)}{d_{\text{mem}}(100)}$, 4: $\frac{n(0)}{n(100)}$, 5: $d_{\text{EM}}(0)$, 6: $\frac{d_{\text{EM}}(0)}{d_{\text{mem}}(0)}$, 7: $\frac{d_{\text{EM}}(100)}{d_{\text{mem}}(100)}$. Ranges are given in section 5.4.6. Scales are logarithmic except for D^m_{EM}, D_n, and $\frac{r_{\text{bound}}(0)}{r_{\text{bound}}(100)}$.

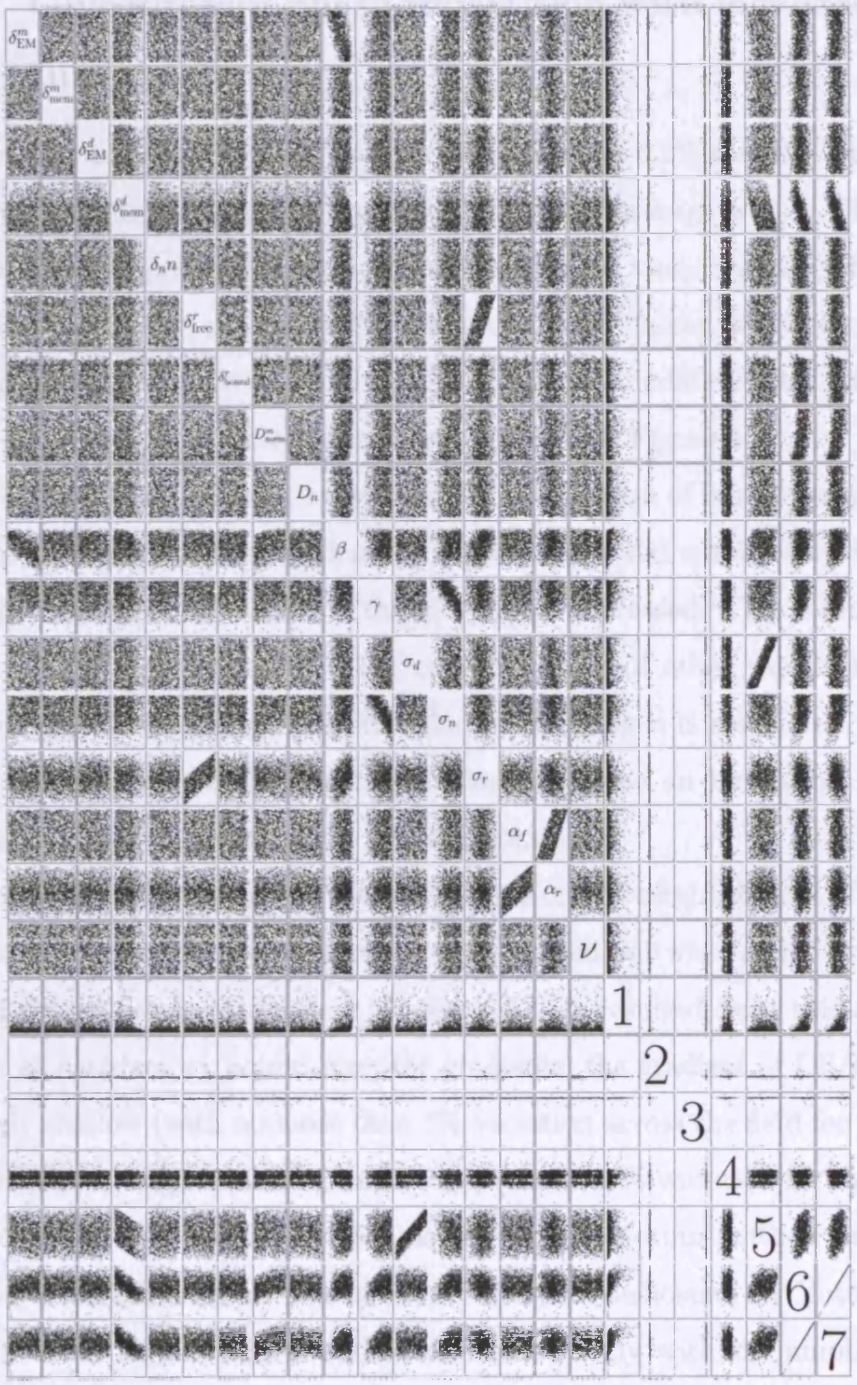

Figure 5.6: Pairwise plot of parameters for which the model with global Notum synthesis gives rise to a gradient of bound receptor meeting the conditions set out in section 5.2.1. Number correspondences are the same as in Figure 5.5.

5.2.1 Glycoprotein phase-repartition with localized Notum synthesis

Out of more than 100,000 parameter sets tested, about 0.5% met the conditions above, with gradient ranges of up to 34-fold (range average was 4). Remarkably, satisfactory parameter sets spanned the entire sampling range for each individual parameter, even though the ranges were chosen to be very wide, showing that the structure of the system can accommodate a wide variety of kinetic parameters. An example gradient is shown in Figure 5.2.

For 4.4% of the parameters tested, the concentration of bound receptor did not form a proper gradient, in that the concentration did not steadily decrease as the distance from the source of the morphogen increased. This is illustrated in Figure 5.3. Figure 5.4 shows the concentrations of other variables of the same system; the increasing concentration of morphogen is associated with an increasing membrane Dll/Dlp concentration (and also an increasing ratio of membrane to EM Dll/Dlp, as the latter is constant).

To examine the influence of the parameters on the establishment of the desired gradient, satisfactory parameters were plotted pairwise, along with measures of the gradients established (Figure 5.5). It resulted from this analysis that for all satisfactory bound-receptor gradients, the gradient of Dll/Dlp was extremely shallow (with no more than 3% variation across the field for the EM form, with an average of 0.16%, and no more than 29% variation for the membrane form, with an average of 3%), as was that of Notum (with a maximum variation of 10% and an average of 3%). Diffusion coefficients for Notum were biased towards higher values, and correlated strongly with the amplitude of both Notum and Dll/Dlp gradients.

This suggested that localized production of Notum was not favorable to the establishment of bound receptor gradient.

5.2.2 Glycoprotein phase-repartition with global Notum

In order to test this, the same simulation was run, but with Notum synthesis over the whole field, rather than over the first 10 μm. Pairwise plots of satisfactory parameters are shown in Figure 5.6. About 1.7% of the parameter tested (out of about 90,000 tested) met the conditions, *i.e.* 3-fold more than with localized Notum synthesis, with ranges of up to 30-fold (range average was 4.6). Only in 0.9% of the cases was the gradient reversed as in Figure 5.3.

Comparison of Figures 5.5 and 5.6 shows that global Notum synthesis relaxes restriction on the relative values of the morphogen diffusion rate D^m and β, the rate of exchange of the morphogen between the membrane and EM phases (the former must be sufficiently high compared to the latter, if Notum is synthesized locally), as well as the restriction on the relative values of D^m and the activity of Notum γ (again, the former tends to be high compared to the latter, if Notum is synthesized locally).

Notable restrictions on parameter sets common to the models with localized or global Notum synthesis are that the product of δ^m_{EM}, the degradation rate of the morphogen in the extracellular matrix and β, as well as that of the activity of Notum γ and its synthesis rate σ_n, must be sufficiently high.

Interestingly, the rate of association of receptor and morphogen is not skewed in the $10^5 - 10^8$ range; the proposed model thus does not share the restriction of that of Lander et al. (2002). Also, to investigate the role of bound-receptor downregulation, the corresponding parameter δ^r_{bound} was set to 0, and the same analysis as previously carried out. The results were roughly identical (data not shown), showing that receptor downregulation is not an important feature of this model.

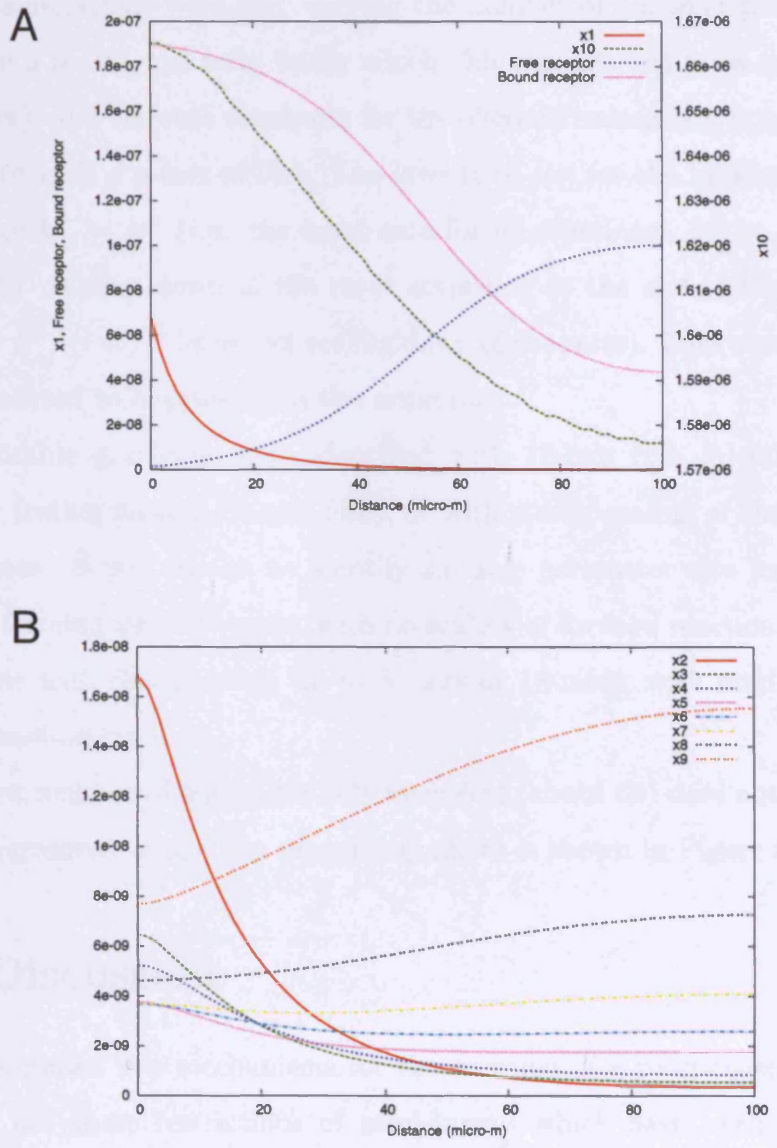

Figure 5.7: Example of a suitable gradient of bound receptor for the Shh-like oligomerization model, with formation of up to 10-mers and no scaling of forward reaction rates, after 15625s of simulation. (A) Concentrations of the monomer x_1, the maximal-size multimer x_{10}, and free and bound receptors; note the different scale for x_{10} (B) Concentrations of intermediary multimer forms.

5.2.3 Shh-like oligomerization

Different simulations were run, varying the number of oligomer forms considered (from 3 to 38), the form under which Shh was injected (as a monomer or a multimer), and the rate constants for the oligomerization reaction $x_i + x_j \leftrightarrow x_{i+j}$, where x_p is a p-mer of Shh. The laws tried out for the forward rate constants were $k^+_{i,j} = k^+$ (*i.e.* the same rate for all reactions), $k^+_{i,j} = k^+/(i+j)$ (*i.e.* "mild" scaling down of the rates according to the size of the product), and $k^+_{i,j} = k^+/(i+j)^2$ (stronger scaling down of the rates). Backward reactions were considered to happen all at the same rate.

No suitable gradients were identified with 18-mer Shh injection at the boundary (rather than monomer Shh), or with strong scaling of the oligomerization rates. It was easiest to identify suitable parameter sets for a system with Shh forming up to 10-mers, with no scaling of forward reaction rates, and for systems with Shh forming up to 8-mers or 18-mers, with mild scaling of forward reaction rates.

The low number of parameter sets identified (about 60) does not warrant a detailed parameter study. An example gradient is shown in Figure 5.7.

5.3 Discussion

We have detailed two mechanisms for the creation of a morphogen gradient, which do not share restrictions of mechanisms which have been previously studied:

- Separation of the morphogen into an extracellular phase, from which it cannot directly interact with receptors, and a cell-membrane phase; the corresponding mathematical model does not require any degradation scheme of receptor-morphogen complexes, and can accommodate biochemical parameters over a very wide range of values. Values which show correlation when interesting gradients are formed are the relative

rates of morphogen degradation and phase equilibration, as well as rates related to the relative levels of extracellular matrix and cell-membrane concentrations. These are good candidates for experimental observation and manipulation.

- Oligomerization of the morphogen into a compound which does not interact with receptors, as could be the case for Sonic Hedgehog.

Both these mechanisms create in effect a dynamic sub-population of morphogen that travels unhindered by receptor interaction, allowing the morphogen gradient not to die off too quickly or saturate receptors. Tracking of the membrane diffusion of single molecules is feasible (as shown for example by Murakoshi et al., 2004); extending these experiments to extracellular diffusion would allow one to assess whether sets of individual paths indeed reflect the sort of diffusion which underlies these new models.

The phase repartition model is compatible with both observations that proteoglycans are indispensable for Dpp and Wg diffusion, and that cell membrane-tethered diffusion would be too slow to account for the observed speed of gradient establishment (Lander et al., 2002). Its absence of requirement for receptor-mediated morphogen degradation is also in line with the lack of requirement of the receptors Fz and Fz2 to establish a Wg gradient (Han et al., 2005).

It has only recently been discovered that Dlp's GPI anchor can be cleaved, releasing it into the extracellular matrix. Since Notum is synthesized only in a region of high Wg signaling, it has been proposed that this localized expression has a role in promoting morphogen diffusion to regions of less intense signaling. However, our model makes the counter-intuitive suggestion that this may not be the case. This is in line with experiments showing that misexpression of Notum in the dorsal compartment of a Drosophila wing disc has symmetrical effects on the dorsal and ventral compartments (Giráldez et al., 2002), and with

the fact that Dpp has been show to also require Dll and Dlp for its diffusion (Belenkaya et al., 2004). If Notum (and the EM and membrane fractions of Dll and Dlp) had a strongly non-homogenous distribution along the dorso-ventral axis, one would expect interference with Dpp signalling, which takes place in a gradient orthogonal to that of Wg (Figure 5.1).

Semi-quantitative imaging of the membrane-associated and free, extracellular sub-populations would provide crucial data to test models with. In particular, to accomodate experimental data showing that morphogen diffusion does not occur over clones deficient in Dll and Dlp (Belenkaya et al., 2004, Han et al., 2005), the phase repartition model makes the important assumption that extracellular Dlp has a negligible diffusion rate.

Even though parameter sets were identified which allow Shh-like oligomerization to give rise to suitable gradients, this did not happen as readily as for the phase repartition model. This could very well have to do with the fact that glycoproteins also seem to be essential to the establishment of a Shh gradient (Han et al., 2004), and that the two phenomena need to be taken into account together.

Acknowledgements

This work was funded by an AstraZeneca scholarship awarded to OC by CoMPLEX. I am grateful to Amanda Albazerchi and Christian Bottomley for discussions, and to Daniel Brewer for computational resources.

5.4 Appendix

5.4.1 Parameter values

The concentrations of morphogens and receptors, as well as their kinetic reaction coefficients, have been precisely evaluated only in a restricted number of

Parameters	Range	Distribution
$\delta^m_{\text{EM}}, \delta^m_{\text{mem}}, \delta^d_{\text{EM}}, \delta^d_{\text{mem}}$	$10^{-7} - 10^{-4} s^{-1}$	Log-uniform
$\delta_n, \delta^r_{\text{free}}, \delta^r_{\text{bound}}, \delta_i$	$10^{-7} - 10^{-4} s^{-1}$	Log-uniform
$D^m_{\text{EM}}, D^n, D_i$	5-30$\mu m^2.s^{-1}$	Uniform
β	$10^{-8} - 1 s^{-1}$	Log-uniform
γ	$1 - 10^6 s^{-1} M^{-1}$	Log-uniform
σ_d, σ_n	$10^{-8} - 10^{-13} M s^{-1}$	Log-uniform
σ_r	$10^{-14} - 10^{-8} M s^{-1}$	$\frac{\sigma_r}{\delta^r_{\text{free}}}$ log-uniform in $10^{-7} - 10^{-4}$
α_f, k^+	$10^5 - 10^8 M^{-1} s^{-1}$	Log-uniform
α_r, k^-	$10^{-7} - 10^{-1} s^{-1}$	$\frac{\alpha_f}{\alpha_r}$, $\frac{k^+}{k^-}$ log-uniform in $10^5 - 10^8$
ν	$10^{-8} - 10^{-13} M \mu m^{-1}$	Log-uniform

Table 5.1: Ranges from which parameters were selected at random for the simulations described in section 5.2.

cases (for example by Dyson & Gurdon, 1998; see Freeman & Gurdon, 2002 for a review). Relevant concentration ranges for morphogens have been proposed to be around 10-100 pM (Freeman & Gurdon, 2002). Dyson & Gurdon (1998) have shown that cells can respond with as few as 2% of their receptors bound to the morphogen (the total of number of receptors per cell being estimated to 5,000); this gives a maximum 50-fold useful variation range of the concentration of bound receptor (also compatible with the data of Gurdon et al., 1999). Cultured S2 cells show responses to Dpp over a 10-fold range, from 100pM to 1000pM (Shimmi & O'Connor, 2003) (but the presence of Dlp could possibly alter those responses). BMP receptor affinity for its ligand is of the order of nanomolars (Koenig et al., 1994, Suzuki et al., 1994), and that of the FGF receptor picomolars (Nugent & Edelman, 1992).

The association rates of two proteins in solution can be as high as 10^8-$10^9 M^{-1} s^{-1}$, close to the rate of random encounter given by Smoluchowski's equation $k_{\text{on}} = 4\Pi DR$, probably thanks to long-range electrostatic interactions

(Northrup & Erickson, 1992, Gabdoulline & Wade, 1997). The order of magnitude of binding rates seems however to normally be around $10^6 M^{-1}s^{-1}$. It has been proposed that, for BMP-like morphogens, it can be as low as $3.10^5 M^{-1}s^{-1}$ (references in Lander et al., 2002). For FGF, the binding rate has been measured at $4.10^6 M^{-1}s^{-1}$ (Nugent & Edelman, 1992); such high values have been used in some simulations (Kruse et al., 2004).

The extracellular diffusion rate of a 50-kDa albumin, *in vivo*, has been reported to be $16\mu m^2 s^{-1}$, and that of a 15-kDa albumin $24\mu m^2 s^{-1}$ (Tao & Nicholson, 1996). The molecular weights of processed Wingless and Decapentaplegic dimers are about 36kDa (value from Pubmed protein) and 30kDa (Doctor et al., 1992), respectively. $10\mu m^2 s^{-1}$ seems therefore to be a good assumption for the order of magnitude of the extracellular diffusion rates (this is the value used by Kerszberg & Wolpert, 1998, and Lander et al., 2002).

5.4.2 Evaluation of gradients

Small dependence of the gradient on the rate of morphogen production has been used as a criterion of biological relevance (Eldar et al., 2003). There are however documented cases of morphogen readouts *not* being buffered against changes in morphogen production rates (Grimm & Pflugfelder, 1996, Staehling-Hampton et al., 1994, Zecca et al., 1996). In this study, gradients were evaluated with the "η" criterion proposed by Lander et al. (2002), which provides a simple measure of how close to linearity they are (as it would be difficult for rapidly-decaying gradients to provide a useful range of concentrations over a high number of cells).

5.4.3 Simulations

Simulations were performed with the Numerical Algorithms Group's Fortran library Mark 20, using the D03PDF function, called from a custom Fortran

77 program (available on request), compiled with the NAGWare compiler, and run on G5 iMacs and PowerMacs. The D03PDF accuracy setting was 10^{-12}, and the degree of the polynomial approximation 2 or 3.

5.4.4 Equations for Wg-like diffusion

$$
\begin{aligned}
\dot{m}_{\mathrm{EM}} &= D^m_{\mathrm{EM}}\Delta m_{\mathrm{EM}} && -\delta^m_{\mathrm{EM}} m_{\mathrm{EM}} + \beta\frac{m_{\mathrm{mem}}d_{\mathrm{EM}} - m_{\mathrm{EM}}d_{\mathrm{mem}}}{d_{\mathrm{EM}} + d_{\mathrm{mem}}} \\
\dot{m}_{\mathrm{mem}} &= && -\delta^m_{\mathrm{mem}} m_{\mathrm{mem}} - \beta\frac{m_{\mathrm{mem}}d_{\mathrm{EM}} - m_{\mathrm{EM}}d_{\mathrm{mem}}}{d_{\mathrm{EM}} + d_{\mathrm{mem}}} \\
& && -\alpha_f r_{\mathrm{free}} m_{\mathrm{mem}} + \alpha_r r_{\mathrm{bound}} \\
\dot{d}_{\mathrm{EM}} &= && -\delta^d_{\mathrm{EM}} d_{\mathrm{EM}} + \gamma n d_{\mathrm{mem}} \\
\dot{d}_{\mathrm{mem}} &= && -\delta^d_{\mathrm{mem}} d_{\mathrm{mem}} - \gamma n d_{\mathrm{mem}} + \sigma_d \\
\dot{n} &= D_n\Delta n && -\delta_n n + \sigma_n \\
\dot{r}_{\mathrm{free}} &= && -\delta^r_{\mathrm{free}} r_{\mathrm{free}} - \alpha_f r_{\mathrm{free}} m_{\mathrm{mem}} + \alpha_r r_{\mathrm{bound}} + \sigma_r \\
\dot{r}_{\mathrm{bound}} &= && -\delta^r_{\mathrm{bound}} r_{\mathrm{bound}} + \alpha_f r_{\mathrm{free}} m_{\mathrm{mem}} - \alpha_r r_{\mathrm{bound}} \\
\frac{\partial m_{\mathrm{EM}}}{\partial x}(x=0) &= && -\nu \\
d_{\mathrm{mem}}(t=0) &= && \sigma_d/\delta^d_{\mathrm{mem}} \\
r_{\mathrm{free}}(t=0) &= && \sigma_r/\delta^r_{\mathrm{free}}
\end{aligned}
$$

Unspecified boundary conditions are zero-flux conditions, and unspecified initial conditions are 0.

5.4.5 Equations for Shh-like oligomerization

$$
\begin{aligned}
\dot{x}_1 = \quad & D_1 \Delta x_1 - \delta_1 x_1 + \Sigma_{j>1} k^-_{1,j-1} x_j + k^-_{1,1} x_2 - \Sigma_{j=1..n-1} k^+_{1,j} x_1 \\
& -\alpha_f r_{\text{free}} x_1 + \alpha_r r_{\text{bound}} \\
\dot{x}_{i,1<i\leq n} = \quad & D_i \Delta x_i - \delta_i x_i + \Sigma_{j+k=i,j>k} \left(k^+_{j,k} x_j x_k - k^-_{j,k} x_i \right) \\
& + \Sigma_{j>i} k^-_{i,j-i} x_j + k^-_{i,i} x_{2i} - \Sigma_{j=1..n-i} k^+_{i,j} x_i x_j - 1_{2i\leq n} k^+_{i,i} x_i^2 \\
\dot{r}_{\text{free}} = \quad & -\delta^r_{\text{free}} r_{\text{free}} - \alpha_f r_{\text{free}} x_1 + \alpha_r r_{\text{bound}} + \sigma_r \\
\dot{r}_{\text{bound}} = \quad & -\delta^r_{\text{bound}} r_{\text{bound}} + \alpha_f r_{\text{free}} x_1 - \alpha_r r_{\text{bound}} \\
\frac{\partial x_1}{\partial x}(x=0) = \quad & -\nu \\
r_{\text{free}}(t=0) = \quad & \sigma_r / \delta^r_{\text{free}}
\end{aligned}
$$

where x_i is an i-mer of Shh, n is the maximum number of Shh proteins which can associate into a single oligomer, $k^+_{i,j}$ and $k^-_{i,j}$ are respectively the association and dissociation rates in the reaction $x_i + x_j \leftrightarrow x_{i+j}$, and the other parameters are the same as previously. Unspecified boundary conditions are zero-flux conditions, and unspecified initial conditions are 0.

The diffusion rates for oligomers were scaled from the rate for the monomer, according to the Stokes-Einstein law for spherical particles: $D_i = D_1 * i^{-1/3}$.

5.4.6 Ranges for the measures plotted in figures 5.5 and 5.6

Number	Measure	Lower bound	Upper bound
1	$\frac{r_{\text{bound}}(0)}{r_{\text{bound}}(100)}$	2	34
2	$\frac{d_{\text{EM}}(0)}{d_{\text{EM}}(100)}$	$-2.9.10^{-2}$	$6.1.10^{-3}$
3	$\frac{d_{\text{mem}}(0)}{d_{\text{mem}}(100)}$	-0.34	-0.015
4	$\frac{n(0)}{n(100)}$	0.015	0.084
5	$d_{\text{EM}}(0)$	-19	-2.9
6	$\frac{d_{\text{EM}}(0)}{d_{\text{mem}}(0)}$	3.0	17.7
7	$\frac{d_{\text{EM}}(100)}{d_{\text{mem}}(100)}$	2.9	17.7

Table 5.2: Ranges for Figure 5.5

Number	Measure	Lower bound	Upper bound
1	$\frac{r_{\text{bound}}(0)}{r_{\text{bound}}(100)}$	2	30
2	$\frac{d_{\text{EM}}(0)}{d_{\text{EM}}(100)}$	$-1.1.10^{-12}$	$3.6.10^{-12}$
3	$\frac{d_{\text{mem}}(0)}{d_{\text{mem}}(100)}$	-4.10^{-11}	3.10^{-12}
4	$\frac{n(0)}{n(100)}$	-8.10^{-15}	$1.9.10^{-14}$
5	$d_{\text{EM}}(0)$	-19	-3.0
6	$\frac{d_{\text{EM}}(0)}{d_{\text{mem}}(0)}$	1.3	17
7	$\frac{d_{\text{EM}}(100)}{d_{\text{mem}}(100)}$	1.3	17

Table 5.3: Ranges for Figure 5.6

Chapter 6

High-dimensional switches and the modelling of cellular differentiation

This chapter is the reproduction of an article whose reference is High-dimensional switches and the modeling of cellular differentiation, Cinquin O. & Demongeot J., J. Theor. Biol. 233(3), pp391-411 (2005)

I am grateful to Jacques Demongeot for contributing the potential in section 6.7.1.

The previous Chapter dealt with the establishment of positional information. In order for the information to be used by differentiating cells, it must be converted into a gene expression pattern, and possibly integrated with other regulatory inputs. The following Chapters deal with mathematical models of the way this can be achieved by networks of transcription factors, at the individual cell level.

6.1 Abstract

Many genes have been identified as driving cellular differentiation, but because of their complex interactions, the understanding of their collective behaviour requires mathematical modelling. Intriguingly, it has been observed in numerous developmental contexts, and particularly hematopoiesis, that genes regulating differentiation are initially co-expressed in progenitors despite their antagonism, before one is upregulated and others downregulated.

We characterise conditions under which 3 classes of generic "master regulatory networks", modelled at the molecular level after experimentally-observed interactions (including bHLH protein dimerisation), and including an arbitrary number of antagonistic components, can behave as a "multi-switch", directing differentiation in an all-or-none fashion to a specific cell-type chosen among more than 2 possible outcomes. bHLH dimerisation networks can readily display coexistence of many antagonistic factors when competition is low (a simple characterisation is derived). Decision-making can be forced by a transient increase in competition, which could correspond to some unexplained experimental observations related to Id proteins; the speed of response varies with the initial conditions the network is subjected to, which could explain some aspects of cell behaviour upon reprogramming.

The coexistence of antagonistic factors at low levels, early in the differentiation process or in pluripotent stem cells, could be an intrinsic property of the interaction between those factors, not requiring a specific regulatory system.

Abbreviations: bHLH, basic Helix-Loop-Helix, Id, Inhibitor of Differentiation

Keywords: multistationarity, cellular differentiation, cellular reprogramming, bHLH dimerization

6.2 Introduction

It has long been recognised that cellular differentiation could result from epigenetic memory, controlled by the dynamical properties of the same system, present with an identical structure in all cells (Delbrück, 1949), rather than from a progressive, irreversible loss of differentiation potential; a fundamental property of such a control system would be the presence of positive feedback circuits (Thomas, 1981, Plahte et al., 1995, Snoussi, 1998, Gouzé, 1998, Cinquin & Demongeot, 2002, Soulé, 2003). Indeed, pioneer experiments showed that the genomes of some differentiated cell types retain the capacity to regenerate a whole organism (Gurdon, 1962, Gurdon et al., 1975), and more recent experiments have strengthened the view that there is extensive plasticity in cell-fate determination (reviewed by Blau & Baltimore, 1991, Blau & Blakely, 1999, and Theise & Krause, 2002).

Bistable switches have been given a thorough theoretical investigation (Cherry & Adler, 2000), and have been constructed *de novo* (Gardner et al., 2000) or modified (Ozbudak et al., 2004). There is evidence, discussed in section 6.2.1, that cells undergoing differentiation sometimes face commitment decisions which involve more than two possible outcomes, but switches involving more than two variables have not been given extensive attention (we are not aware of any generic mathematical model that addresses cellular differentiation, with more than two possible outcomes). In the following, we discuss the relevance of these high-dimensional switches to the modeling of cellular differentiation, and investigate the properties of different molecular models, evaluating them with the current knowledge of the mechanisms of cellular differentiation. In particular, we test whether these models are able to display a coexistence of antagonistic factors at low levels, as decision-making with increased expression levels could be a relevant model of differentiation.

6.2.1 Biological aspects

Some commitments are irreducible to binary steps

Cellular differentiation is often envisioned as a temporal cascade of decisions, by which cells restrict their potential fate further and further, until they reach a unique fate. It has been argued that each of these decisions is binary (Brown et al., 1988, Sternberg & Horvitz, 1989, Kaletta et al., 1997, Lin et al., 1998). However, recent studies of hematopoeisis strongly suggest otherwise (Rothenberg et al., 1999), and point to models in which many cross-antagonising factors compete with each other (see below), receiving activation or inhibition from extracellular signals, leading to the progressive up-regulation of one specific factor, and down-regulation of all others. The hypothesis that decisions are more complex than binary is also supported by the fact that the same cell type can be obtained by different developmental pathways (Rothenberg et al., 1999).

Apart from hematopoiesis, two systems have been described which seem to clearly involve a 3-outcome decision, irreducible to a sequence of 2 binary decisions: cells in the *C. elegans* hermaphrodite germline are directed to mitosis, differentiation as sperm, or differentiation as oocyte (Ellis & Kimble, 1995), and founder cells of Drosophila mesoderm are directed to specific dorsal muscle or pericardial cell phenotypes by 3 mutually-repressive genes (Jagla et al., 2002).

Finally, in at least two instances of neural development, fate choices between a great diversity of possible outcomes have been shown, and are unlikely to be mediated by a series of binary commitments. This is the case of olfactory development (Serizawa et al., 2000, Ebrahimi et al., 2000), which does not involve genetic rearrangements (Eggan et al., 2004), and of the regulation of hundreds of alternatively-spliced transcripts of a single gene in the Drosophila brain (Neves et al., 2004).

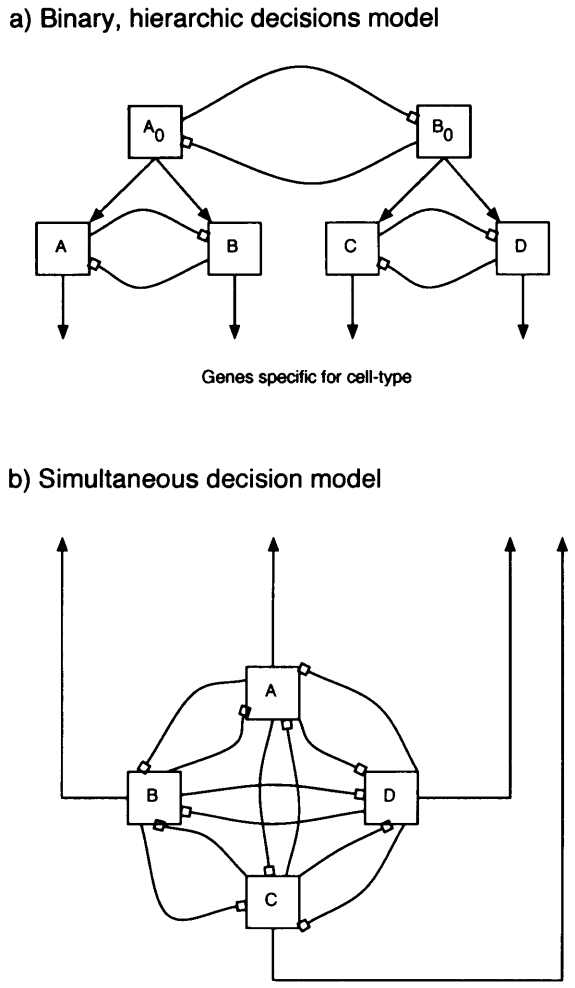

Figure 6.1: Arrows represent activation, and squares inhibition. Adapted from Cinquin & Demongeot (2002).

Thus, it appears that model a, depicted in Figure 6.1, is not the only possibility, and that model b of Figure 6.1 should also be taken into account.

Having shown that high-dimensional switches are necessary for the mathematical modeling of some developmental decisions, we now turn to the way their structure should be modelled: differentiation factors are often antagonistic (section 6.2.1), which does not prevent them from being sometimes coexpressed (section 6.2.1), and modulation of the interaction strength is a way differentiation is regulated (section 6.2.1). The basis for a mathematical formulation of

the models is provided in section 6.2.2.

Antagonism between differentiation factors

Antagonism between genes driving differentiation to different fates has been repeatedly established; often, enforced expression of a differentiated phenotype, whether by specific misexpression of a gene, or fusion of cells with different phenotypes, also leads to repression of the previous phenotype (repression of alternative fates has been proposed to be an essential mechanism of differentiation, reviewed by Cory, 1999). The idea of competition is reinforced by dose-dependency effects, shown for example by comparison of heterozygous and homozygous mutants, heterokaryon studies, or knock-down mutations (Weintraub, 1993, McDevitt et al., 1997, reviewed by Orkin, 2000; Crittenden et al., 2002), by monoallelic expression of a gene such as Pax5 (Nutt et al., 1999), and by dosage effects of interacting bHLH proteins (Zhuang et al., 1996). These effects argue that boolean models, in which a specific master gene would be turned on, initiate transcription of cell-type specific genes, and repress all other fates, are insufficient.

Competition between cell-fate determining factors has also been documented at the molecular level, for example in the case of neurogenesis, where bHLH proteins play a major role in specifying neural subtypes (Chien et al., 1996, Brunet & Ghysen, 1999). Gowan et al. (2001) have identified a network of 3 cross-repressive bHLH proteins (although not all possible cross-repressions have been characterised). Briscoe et al. (2000) have also shown that a cross-repressive gene network reads out the Shh gradient in the neural tube. Two sets of two cross-repressing genes have been identified, with a possibility that there is a larger, totally cross-repressive network (all the possible interactions do not seem to have been assessed yet). The competition can also occur by physical interaction between the factors, rather than by cross-repression of transcription: in hematopoeisis, GATA-1, which drives erythroid and megakaryocytic

differentiation (Kulessa et al., 1995, Visvader et al., 1992, Iwasaki et al., 2003), and PU-1, a transcription factor essential for the expression of myleoid-specific genes (reviewed by Zhang et al., 1996), as well as B-cell specific genes (Chen et al., 1996), suppress each other's activity by physical interaction (Rekhtman et al., 1999, Zhang et al., 1999, Nerlov et al., 2000). This seems to be a general phenomenon in hematopoiesis (Hu et al., 1997, reviewed by Cross & Enver, 1997, Enver & Greaves, 1998).

In addition to repressing other genes, cell-fate determining factors often enhance their own expression; it has been proposed that this is a common property of "master switches" (Rothenberg et al., 1999).

Coexpression of antagonistic factors

Coexpression of antagonistic genes has been shown both for closely-related lineages (for example coexpression of antagonistic hematopoeisis-related genes, Miyamoto et al., 2002, Akashi et al., 2003, Ye et al., 2003, reviewed by Orkin, 2003, transient prespore expression of a prestalk-specific gene in Dictyostelium, Jermyn & Wiliams, 1995, coexpression of lineage-specific genes in pancreas development, Chiang & Melton, 2003, and coexpression of neurogenic genes, Rallu et al., 2002, Pierani et al., 2001, Briscoe et al., 2000, although the latter may be due to a transient effect of the misexpression method), and between more distantly-related lineages (for example expression of neural markers by hematopoietic precursors, Goolsby et al., 2003).

A semi-quantitative analysis of the expression of many hematopoietic genes was performed by Akashi et al. (2000), showing that lineage-specific (and antagonistic) genes were co-expressed at low levels in precursors, before respective upregulation and downregulation (see Rothenberg, 2000, Zhu & Emerson, 2002, for reviews). At an earlier stage of development, markers for different germ layers are also transiently co-expressed (Wardle & Smith, 2004).

Regulation of differentiation

Some proteins have been shown to have regulative effects on differentiation in many different cellular contexts, and would thus prove interesting to incorporate in models of cellular differentiation.

- Id proteins, ubiquitously expressed during development, seem to act as inhibitors of cell differentiation, by sequestering ubiquitously-expressed class A bHLH proteins, preventing class B bHLH to form A-B heterodimers, which are transcriptionally active (Benezra et al., 1990, Garrell & Modolell, 1990, Ellis et al., 1990, reviewed by Norton et al., 1998, Norton, 2000), and by preventing DNA binding (O'Toole et al., 2003); see Massari & Murre (2000) for a precise classification of HLH proteins. Twist can act in the same way (Spicer et al., 1996), or in another, more direct way, by binding to class MyoD (Hamamori et al., 1997).

- Hes1, a bHLH protein, seems in many cases to be essential in the maintenance of an undifferentiated state (Kageyama et al., 2000); its effect can be mediated either by active repression, which involves the recruitment of Groucho, or by passive repression, which involves hetero-dimerisation with other bHLH proteins.

- The PUF family of proteins represses the expression of many genes by regulating their mRNA stability (Wickens et al., 2002), and has been proposed to have the ancestral function of maintaining proliferation of stem cells; in *C. elegans*, sex-determination genes are regulated by PUF members.

- NF-κB has been shown to inhibit differentiation of mesenchymal cells, by destabilisation of the transcripts of Sox9 and MyoD, two transcription factors involved in different differentiation pathways (Sitcheran et al., 2003).

All these differentiation-inhibiting proteins have a negative effect on the strength of transcription of genes which are essential in cell-fate determination. The models presented below suggest that modulation of the transcription strength of proteins involved in cell-fate determination could allow for an initial co-existence of many antagonistic factors, followed by up-regulation of one factor at the expense of others, as the transcription strength is increased.

6.2.2 Mathematical models

The models studied here have an arbitrary number of components. Each variable represents the intracellular concentration of a differentiation factor (called "switch element" in the following), which enhances its own expression and represses that of all others (the system is symmetrical, in that any element has the same relationship with all others, and in that all elements share a common set of parameters). The models can represent different forms of biological interactions. The terminology used below is that of transcriptional control: each factor is supposed to be a protein, which enhances the transcription of its own mRNA, and represses the transcription of the mRNAs for other switch elements, with or without physical interaction with other factors; as a simplification, the translation step is not taken into account in the model, and proteins are thus supposed to act directly on each other's concentrations. There is evidence that translational regulation can play a major role in some cases (Wickens et al., 2000, Okano et al., 2002). In the following models, different forms of post-transcriptional control (by means of regulation of mRNA stability, or translation of the proteins), can be represented in the same way as transcriptional control. Downregulation of cytokine receptors has been observed prior to commitment (Kondo et al., 2000), and downregulation of receptors promoting expression of competing factors could also be accounted for by the following models.

3 kinds of models are studied below:

- Mutual inhibition with autocatalysis: all switch elements repress one another, and enhance their own expression. This is one of the simplest models one can think of that is able to achieve dominant expression of each of its elements, depending on the initial conditions.

- Mutual inhibition with autocatalysis, *and leak*: the same as the previous, with a supplementary term that represents an identical, basal level of expression, which is independent of any element of the network. This could correspond for example to a gene upstream in the differentiation hierarchy, which "primes" the lower level of the differentiation network, as has been proposed within the hematopoietic differentiation network (Ye et al., 2003, reviewed by Orkin, 2003).

- bHLH dimerisation: based on the class A/class B bHLH dimerisation discussed above.

The first two models can be viewed as a generic representation of the interactions between switch elements, while the third is based on an explicit assumption. All are formulated according to standard kinetics.

These models are cell-autonomous, and do not take into account "differentiation cues" that cells receive. The models could be extended to take into account either different initial conditions, leading to various differentiated states, or different biases of the network (for example by providing a higher basal expression level of one of the factors).

6.3 Results

6.3.1 Mutual inhibition with autocatalysis

Each switch element is supposed to undergo non-regulated degradation (modeled as exponential decay, with an arbitrary speed 1), and transcription/translation

with a relative speed σ. Each element positively auto-regulates itself, and represses expression of others, with a cooperativity c. Calling x_i the concentration of each switch element, the corresponding equations are, for n elements:

$$\begin{aligned} \frac{\mathrm{d}x_1}{\mathrm{d}t} &= -x_1 + \frac{\sigma x_1^c}{1 + \Sigma_{i=1}^n x_i^c} \\ &\dots \\ \frac{\mathrm{d}x_n}{\mathrm{d}t} &= -x_n + \frac{\sigma x_n^c}{1 + \Sigma_{i=1}^n x_i^c} \end{aligned} \tag{6.1}$$

The analysis is restricted to $c \geq 1$, as there is only one steady state (0) if $c < 1$. The results presented in appendix 6.6 show that it is possible for one switch element to be on and others off (for $\sigma > 2$), but that if there is some cooperativity in the system (*ie* $c > 1$), it is impossible for more than 1 element to be on at the same time. On the contrary, if there is no cooperativity ($c = 1$), simulations show that a multitude of equilibria exist and are stable (switch elements in the "on" state can even coexist at different concentrations). Thus, the multistability behaviour of this system is tunable only by changes in the strength of the cooperativity, a mechanism which seems to be of unlikely biological relevance.

6.3.2 Mutual inhibition with autocatalysis, and leak

The model is the same as previously, except that each element has a "leaky" expression, modelled as a constant production term α. The equations become:

$$\begin{aligned}
\frac{\mathrm{d}x_1}{\mathrm{d}t} &= -x_1 + \frac{\sigma x_1^c}{1 + \Sigma_{i=1}^n x_i^c} + \alpha \\
&\ldots \\
\frac{\mathrm{d}x_n}{\mathrm{d}t} &= -x_n + \frac{\sigma x_n^c}{1 + \Sigma_{i=1}^n x_i^c} + \alpha
\end{aligned} \tag{6.2}$$

The system is interesting only for $c > 1$ (see appendix 6.7). If the leak is small, it does not have a major effect on the system, except when the cooperativity is close to 1: as shown in appendix 6.7, it is impossible for more than one switch element to be "on", at a much higher level than the leak level α.

Even when the cooperativity is close to 1, it is still the case that only one variable at the same time can dominate all others; in order for that to happen, the transcription strength must be sufficiently high. A simulation was performed for a cooperativity of 1.1, with increasing σ (see Figure 6.2). All switch elements are initially coexpressed, and once σ becomes sufficiently high, one switch element is upregulated, and others downregulated.

The same pattern of coexpression followed by exclusive expression can be achieved with a decreasing leak (see Figure 6.3), with the difference that the level of initial coexpression decreases slightly with time (this level is lower than the relative maximum transcription strength σ, but higher than the leak α). Once the leak has become sufficiently small, exclusive upregulation occurs.

We show in appendix 6.7 that our models with mutual inhibition and autocatalysis, with or without leak, always converge to an equilibrium (and thus never oscillate).

Effect of a perturbation

If two switch elements are given initial values close to the resting value one would have on its own, there is a transient drop in both values, until the higher

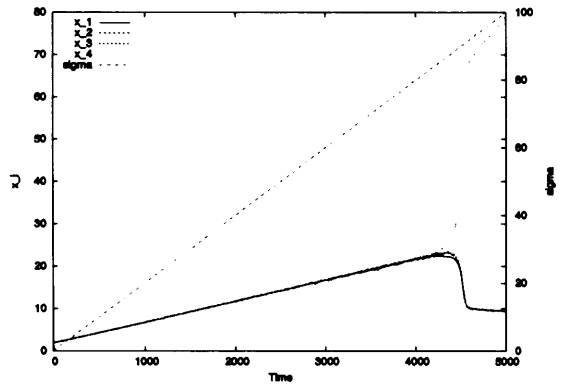

Figure 6.2: Time evolution of the concentrations of 4 switch elements (x_1 to x_4), for the model with mutual inhibition with autocatalysis, and leak, with the transcription strength σ being gradually increased over time. The 4 elements are initially coexpressed at an identical level, which increases with σ; when σ reaches a threshold level, one element is upregulated, and others are downregulated. Parameters in the simulation were $\alpha = 2$ and $c = 1.1$ Low, random noise was added to allow the system to escape the equilibrium as it became unstable.

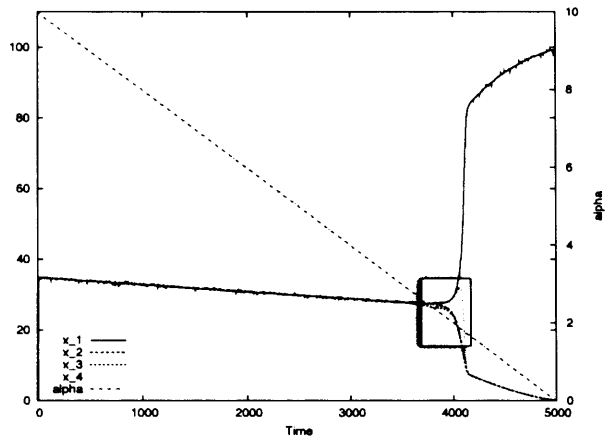

Figure 6.3: Time evolution of the concentrations of 4 switch elements (x_1 to x_4). for the model with mutual inhibition with autocatalysis, and leak, with the leak level α being gradually decreased over time. The 4 elements are initially coexpressed at identical levels (higher than the leak α because of autocatalysis); when the leak reaches a threshold level, one element is upregulated, and others are downregulated. Note that the scales for the x_i and for α are different by a factor of 11, equal to $c/(c-1)$ in this simulation. Thus, it is impossible for the curve of more than one x_i to be above that of α *at equilibrium.* Thus, in the boxed region, the system is in the process of responding to the drop in α, and not at equilibrium. Parameters in the simulation were $\sigma = 100$ and $c = 1.1$ Low, random noise was added to allow the system to escape the equilibrium as it became unstable.

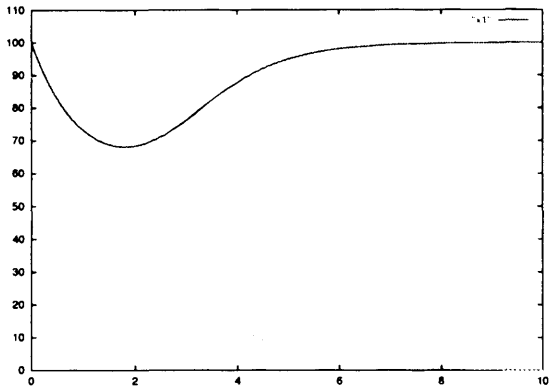

Figure 6.4: Time evolution of the concentrations of two switch elements (x_1 and x_2), for the model with mutual inhibition with autocatalysis, and leak. The resting concentration when one element is on and the other off is roughly 100. Initial concentrations differ by 10. Parameters are $\sigma = 100$, $\alpha = 0.02$, and $c = 2$. The trajectory is essentially the same for all $\alpha < 10$, and very similar for initial concentrations differing by only 1.

one picks up and extinguishes the other (see Figure 6.4). The initial drop is less pronounced than for the bHLH dimerisation model (see below).

6.3.3 A model for bHLH proteins

Each switch bHLH protein is supposed to bind to a common activator according to the law of mass action, with a binding constant K_2, and a total quantity of activator a_t. In turn, the heterodimer activates transcription of the corresponding switch protein only, with Hill kinetics and cooperativity 2 (as with cooperativity 1, no interesting equilibria exist, as shown in appendix 6.8). The equations are:

$$\frac{\mathrm{d}x_1}{\mathrm{d}t} = -x_1 + \sigma \frac{\left(\frac{a_t x_1}{1+\Sigma_{i=1}^n x_i}\right)^2}{K_2 + \left(\frac{a_t x_1}{1+\Sigma_{i=1}^n x_i}\right)^2}$$

$$\ldots \qquad (6.3)$$

$$\frac{\mathrm{d}x_n}{\mathrm{d}t} = -x_n + \sigma \frac{\left(\frac{a_t x_n}{1+\Sigma_{i=1}^n x_i}\right)^2}{K_2 + \left(\frac{a_t x_n}{1+\Sigma_{i=1}^n x_i}\right)^2}$$

These equations simplify to:

$$\frac{\mathrm{d}x_i}{\mathrm{d}t} = -x_i + \sigma \frac{x_i^2}{\alpha D^2 + x_i^2},$$

with $D = 1 + \Sigma_{i=1}^n x_i$, σ, $\alpha = K_2/a_t^2 \in \mathbb{R}_*^+$

Parameter α is a measure of the harshness of the competition between switch elements (it increases if K_2 increases, *ie* if binding to the common activator occurs at higher concentrations, and if a_t diminishes, *ie* if the quantity of common activator goes down). The value of α is essential in determining the behaviour of the system. As shown in appendix 6.8, and summarised in section 6.3.3, switch elements can coexist only if α is sufficiently low, *ie* if the competition is not too harsh (the lower α, the more switch elements can be non-0 at equilibrium). Figure 6.5 shows a simulation with α being increased over time; switch elements are sharply turned off as α reaches threshold values. Figure 6.6 shows how an increase in α leaves only 1 switch element on, which remains exclusively on even if the competition level is relaxed to its original value.

We prove in the appendix that the system always converges to an equilibrium for $\alpha \geq 1/2$; extensive simulations have also shown this to be the case for $\alpha < 1/2$.

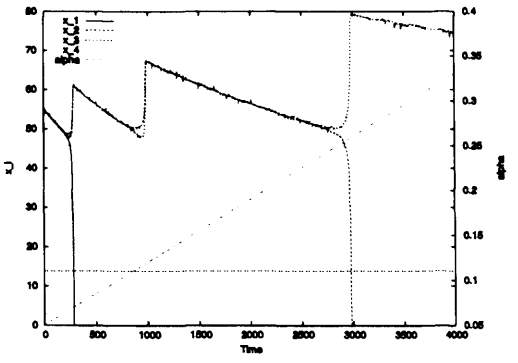

Figure 6.5: Time evolution of the concentrations of 4 switch elements (x_1 to x_4), in the bHLH dimerisation model, with competition parameter α being gradually increased over time. The horizontal lines mark the values $\alpha = 1/4^2$, $\alpha = 1/3^2$, and $\alpha = 1/2^2$. Each time α reaches one of those threshold values, one of the switch elements is repressed. Low, random noise was added to allow the system to escape equilibria as they became unstable. In this simulation $\sigma = 100$.

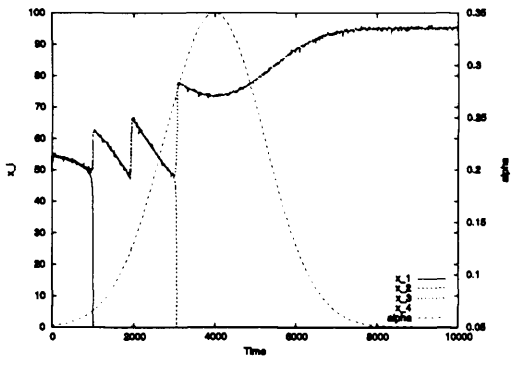

Figure 6.6: Same as Figure 6.5, but with a pulse of the competition parameter α. The initial conditions are such that the switch elements coexist for low α; once α has sufficiently increased, only 1 switch element stays on, and remains on with all others off, even when α is brought back to its initial, low value.

Basins of attraction and times of response

The cell fusion and reprogramming experiments, described below in section 6.4.3, would lead to a situation where a switch element, previously repressed, is brought to a level comparable to that of another switch element which was already expressed. This corresponds to an initial situation in which two elements are not at their resting value, which could also describe the situation in cells in the process of differentiating. For the models studied here, if 2 switch elements are competing, 3 outcomes are possible: the switch element at the higher concentration completely represses the other, both coexist and reach a non-zero equilibrium at the same value (only an element which started at the higher concentration can end up predominating), or both go to 0 (extinction). Figures 6.7 to 6.10 show which equilibrium the system converges to, as a function of the initial state, for different values of the competition parameter α (each domain from which the system converges to the same equilibrium is a "basin of attraction"). If there are 3 switch elements competing, there are more possibilities, as 2 or 3 elements can coexist in the "on" state. Figures 6.11 and 6.12 show the basins of attraction of such a switch (the attraction basins belong to the same system, but were split on two figures to prevent the outer ones from obscuring the inner ones).

The speed at which the competition between the switch elements is carried out could be crucial in determining the dynamical properties of differentiation. We thus computed the time it takes for the system to approach its equilibrium, starting from various initial concentrations of the switch elements (that time is colour-coded in Figures 6.7 to 6.12). This time becomes dramatically higher when the initial conditions come close to the borders of the basins of attraction (*ie* when concentrations are near a threshold around which the system converges to two or more different outcomes). The effect becomes even more pronounced when 3, rather than 2, switch elements are competing (Figures 6.11 and 6.12).

To show the effect in more detail, individual trajectories were plotted for a 2-dimensional switch (Figures 6.13 and 6.14). For cell fusion and reprogramming experiments, the effect on the concentration of switch elements depends on the dynamics of nuclear import and export. Two types of initial conditions were used: two switch elements were given the concentration that one would have at rest, if it was "on" (Figure 6.13), or two switch elements were given half that concentration (as cytoplasmic concentrations of proteins expressed exclusively in 1 of 2 equally-sized cells should be cut by half upon fusion; Figure 6.14). In both cases, the concentrations of the two switch elements, even for that which will eventually prevail, initially go down. The effect is more pronounced for higher values of the initial concentrations, and for close initial values of the two concentrations. This could explain the transient extinction of expression of differentiated markers upon cell fusion (see Discussion): if there is sufficient cooperativity downstream of the switch element, its dip could be sufficient to provoke a temporary extinction of expression of the proteins specific to the differentiated state.

Extinction domain

For $\alpha > \frac{\sigma^2}{4(n\sigma+1)}$, there is an extinction domain around the diagonal $x_1 = .. = x_n$. Simulations show that the domain is very restricted until α becomes very close to its upper threshold value, at which non-0 equilibria cease to exist (see Figures 6.9 and 6.10).

Summary of α threshold values

For the system to be able to sustain k switch elements "on" at the same time, the condition $\alpha < 1/k^2$ must be met (for $\sigma \gg 1$, this condition is also sufficient). Thus, for $\alpha > 1/4$, only 1 switch element can be on at a time. The corresponding equilibrium value is a decreasing function of α. For $\alpha > \frac{\sigma^2}{4(n\sigma+1)}$, there is an "extinction domain" around the diagonal $x_1 = .. = x_n$: match-

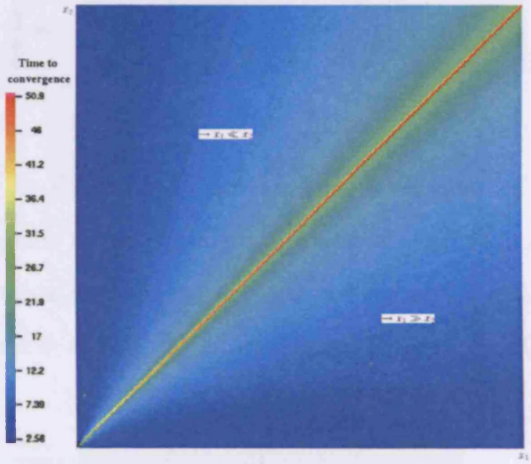

Figure 6.7: Colour-coded time of convergence (as defined in Appendix 6.9.2), as a function of the initial conditions in x_1 and x_2. From the initial conditions to the left of the red region, the system converges to x_2 on and x_1 off, and the opposite for the initial conditions to the right of the red region. Parameters are $\alpha = 0.4$ and $\sigma = 100$. x_1 and x_2 range from 0 to 300.

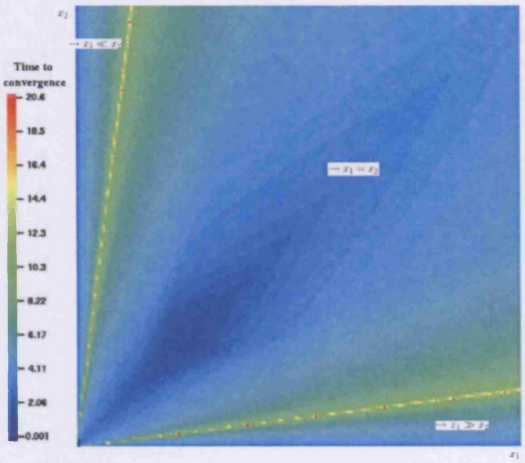

Figure 6.8: Same as Figure 6.7, but with a lower value of α, giving a large domain of convergence to an equilibrium where x_1 and x_2 coexist. Domains of convergence are indicated, and are separated by the two yellow lines. Parameters are $\alpha = 0.1$ and $\sigma = 100$. x_1 and x_2 range from 0 to 300.

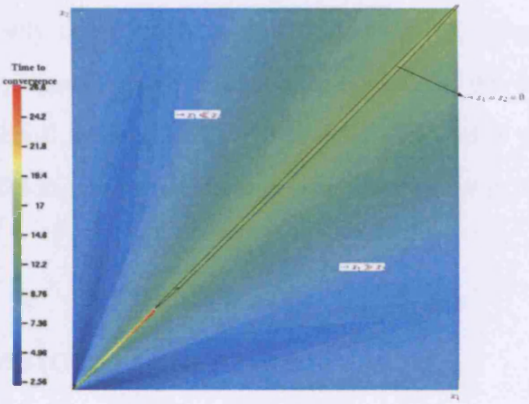

Figure 6.9: Same as Figure 6.7, but with a markedly higher value of α. There are two main domains of convergence (to one switch element on and the other off), and a third domain of convergence to 0 (complete extinction of the switch), in a region very close to the upper part of the diagonal (for clarity reasons, the region is indicated as larger than it actually is). Parameters are $\alpha = 15$ and $\sigma = 100$. x_1 and x_2 range from 0 to 300.

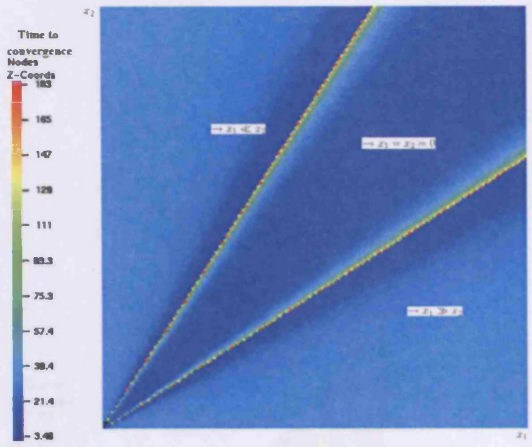

Figure 6.10: Same as Figure 6.7, with α close to the threshold above which 0 is the only equilibrium. The region from which the system converges to 0 has expanded. Parameters are $\alpha = 24.75$ and $\sigma = 100$. x_1 and x_2 range from 0 to 300.

ing sufficiently closely the concentrations of the switch elements, at whatever value, makes the system switch off all switch elements. For large σ, the extent of this domain is small, except in a very narrow range of α values. Finally, for $\alpha > \frac{\sigma^2}{4(\sigma+1)}$, a condition which becomes $\alpha > \sigma/4$ for large σ, there are no non-0 steady states.

6.4 Discussion

6.4.1 Co-expression properties

Of the models proposed here, if the cooperativity of activation is considered to be constant, only the model with bHLH dimerisation is capable both of exclusive expression of an arbitrary number of switch elements, and coexpression at similar levels of all elements. This behaviour is finely tunable with the key competition parameter deriving from the availability of the bHLH

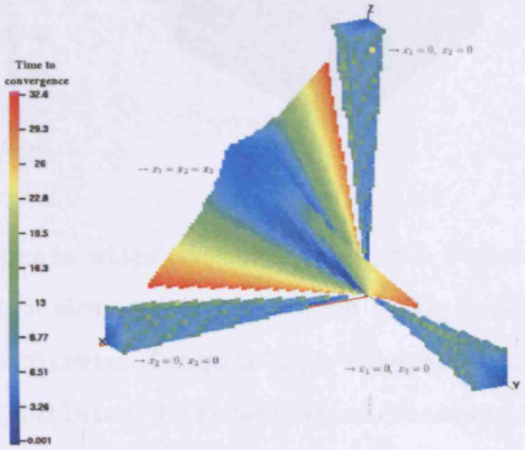

Figure 6.11: Times of convergence as a function of the initial condition, for a 3-dimensional switch. 4 unconnected domains of convergence to the same equilibrium are shown. For visibility, the 3 other domains are shown in Figure 6.12. Parameters are $\alpha = 0.1$ and $\sigma = 25$. A rotation movie is available at `http://www-timc.imag.fr/Olivier.Cinquin/High-dimensional_switches_and_the_modeling_of_cellular_differentiation/rotating_graphs.html`

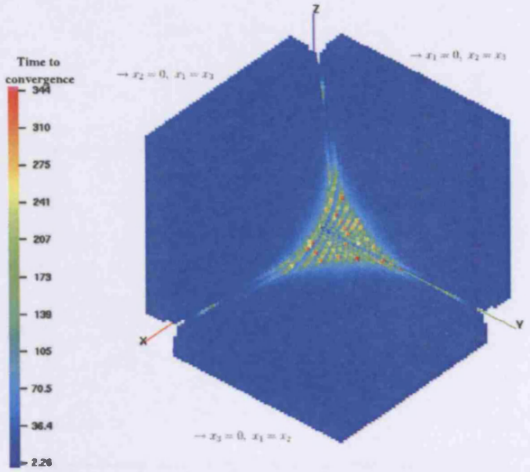

Figure 6.12: Domains in which the same switch as in Figure 6.11 converges to a state with 2 switch elements on. A rotation movie is available at `http://www-timc.imag.fr/Olivier.Cinquin/High-dimensional_switches_and_the_modeling_of_cellular_differentiation/rotating_graphs.html`

hetero-dimerisation partner, with lower availability being unfavourable to co-expression of the antagonistic factors (see below for a further discussion).

The model with mutual inhibition, autocatalysis, and leak can express no more than one switch element at a level higher than the other ones, and is thus less amenable to progressive elimination of unwanted factors in the course of differentiation. In order for coexpression to occur at a significantly-higher level than the leak, the cooperativity of the system must be close to 1. If differentiation was controlled by a network of this kind, initial coexpression could be maintained either by a low transcriptional strength in the system (which is consistent with antagonistic factors being expressed at a lower level in the un-differentiated state), or, as has been suggested, by regulated degradation of mRNAs.

Interestingly, the multistability behaviours of a switch based on bHLH-like dimerisation and that of a switch based on direct cross-repression are quali-

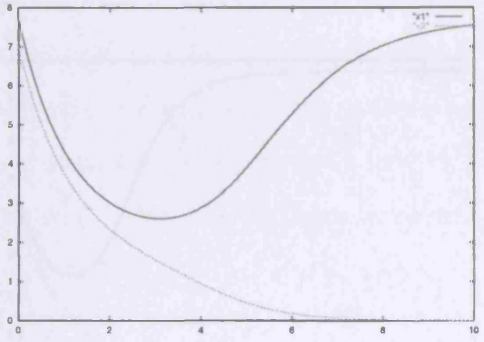

a

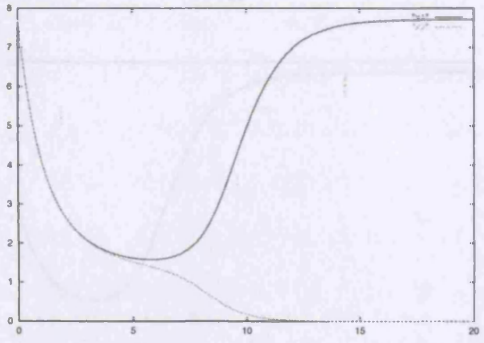

b

Figure 6.13: Time evolution of the concentrations of two switch elements (x_1 and x_2), for the bHLH dimerisation model. The resting concentration when one element is on and the other off is roughly 8. Initial concentrations differ by 0.7 (**a**), or 0.1 (**b**). Notice the differences in scales. Parameters are $\alpha = 50$ and $\sigma = 500$.

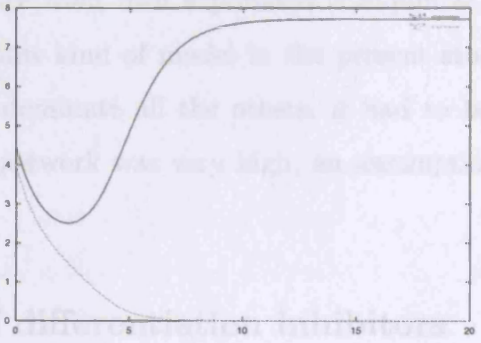

a

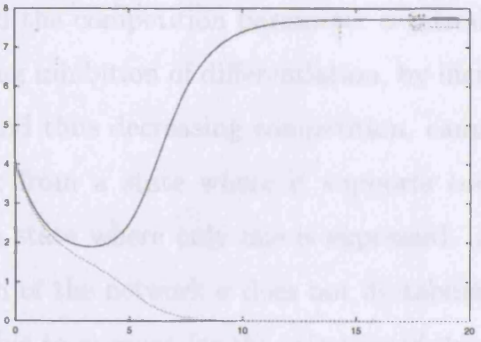

b

Figure 6.14: Same as Figure 6.13, but with initial concentrations at roughly half the equilibrium value when one element is on and all others off. Initial concentrations differ by 0.5 (**a**), or 0.1 (**b**).

tatively different: the former can maintain many variables on at an equilibrium only if those variables are sufficiently high (compared to the transcription strength), while the reverse is true of the latter.

We previously studied networks of cross-repressing factors, in which the factors do not enhance their own expression (Cinquin & Demongeot, 2002). We did not include this kind of model in the present study, because for one factor to be able to dominate all the others, it had to be assumed that the cooperativity of the network was very high, an assumption which is possibly not realistic.

6.4.2 Peaks of differentiation inhibitors

According to the paradigm of inhibition of differentiation by sequestration of class A bHLH proteins, the quantity of binding partner should be low prior to differentiation, and the competition parameter α introduced earlier should thus be high. Relieving inhibition of differentiation, by increasing the quantity of binding partner, and thus decreasing competition, cannot move the bHLH dimerisation network from a state where it supports coexpression of many switch elements, to a state where only one is expressed. Also, increasing the transcription strength of the network σ does not destabilise equilibria.

It is thus impossible to account for the selection of one differentiation outcome by increasing the availability of class A proteins (for example by down-regulation of Id proteins). However, it is still possible that the competition strength, even in the undifferentiated state, is sufficiently low for many switch elements to be co-expressed. A potential mechanism to select 1 element and extinguish all others is then to transiently increase the competition strength, for example by transient up-regulation of Id proteins, just prior to differentiation commitment (a corresponding simulation is shown in Figure 6.6). This is in fact what has been experimentally observed on independent occasions, on a short time scale, during in vitro differentiation of osteoblasts (Ogata et al.,

1993), neurons (Nagata & Todokoro, 1994), myeloid cells (Ishiguro et al., 1996), astrocytes (Andres-Barquin et al., 1997), Schwann cells (Stewart et al., 1997), keratinocytes (Langlands et al., 2000), germ cells (Houldsworth et al., 2001), and fibroblasts (Chambers et al., 2003). No rationale for these transient effects had been proposed so far.

When Id proteins are not up-regulated, other proteins could play the same role of increasing competition in the bHLH network. For example, Hes-1, which also has class A sequestering activity (Sasai et al., 1992), is transiently upregulated upon differentiation of an immortalised hair cell line (Rivolta et al., 2002), an immortalised neural cell line (Ohtsuka et al., 1998), and neuroblastoma (Grynfeld et al., 2000) (although its role in the latter case is complicated by the fact that it also binds Id proteins and interferes with Id2/E2-2 complex formation, Jögi et al., 2002); the transient Hes-1 expression is concomitant with downregulation of the bHLH protein HASH-1. Hes genes are dominant repressors with many targets (Barolo & Levine, 1997), and could also directly repress many elements of the network, which can be modeled by a decrease in the transcription strength σ, and has the same effect of destabilising equilibria where many elements are coexpressed.

Finally, erythroid-specific genes have been observed to be transiently downregulated upon induced, in-vitro differentiation (Lister et al., 1995), which could also be explained by transiently-increased competition in a bHLH dimerisation network.

6.4.3 Dynamical properties

Analysis of the proposed dynamical systems shows that the time to convergence can widely depend on the initial condition. Convergence can be relatively very slow when initial conditions are near a threshold around which the system converges to two or more different outcomes. This is for example the case when 2 or more "switch elements" are at roughly equal concentrations, higher than

that of others (the more elements in competition, the slower the competition becomes). It is interesting to note that slow effects are observed in induced-transdifferentiation experiments, and in cell fusion experiments.

- Fibroblasts reprogrammed to T-cell-like cells need to be incubated for many days before they acquire detectable T-cell characteristics (Håkelien et al., 2002). This may be due to the fact that fibroblast master genes are expressed at a high level, and the counter-acting T-cell master genes, introduced by permeabilisation of the membranes, are also present at a high concentration. An effect of the relative levels of cytoplasmic factor concentrations could be tested by incubation in T-cell and fibroblast cytoplasmic extracts, mixed at different ratios. Further investigation of master networks could involve incubation of cells in cytoplasmic extracts of 3 or more cells-types (or transient misexpression, at controlled levels, of antagonistic master genes).

- In hepatoma-fibroblasts hybrids, extinction of albumin production can take days (Mével-Ninio & Weiss, 1981). Most interestingly, some hybrids show reexpression of albumin after extinction. These two outcomes can be accounted for by the models proposed above: when two antagonistic "switch elements" are coexpressed at a high level (which probably corresponds to the fusion experiments, as upon fusion the protein contents of the cells, which are of different phenotypes, are mixed), it is possible for the system to revert to a state where all switch elements are turned off (total extinction), or for the two switch elements to decrease to a low level, before the trajectory of one of them picks up and goes back to a high state (extinction followed by reexpression).

- Activation of the myogenic phenotype also takes place on the scale of days, when muscle cells are fused to various other cell types, a delay which was suggested not to be linked to DNA duplication (Blau et al.,

1985; see Blau & Blakely, 1999, for an extensive review).

Also, it could be that the progressive upregulation of differentiation-related genes observed during hematopoietic development is a cell-autonomous consequence of the slow dynamics of a switch network.

6.4.4 Stochastic outcomes

It has been observed in the studies cited above that heterokaryons with the same number of nuclei coming from each donor can have different differentiation responses. Blau & Blakely (1999) suggested that the differentiation outcomes are regulated by a network of opposing factors. Within this framework, stochastic responses to cell fusion can readily be explained by slight differences in the quantities of differentiation factors contributed by each cell type, which tip the balance one way or the other. The network determining cell fate would be most sensitive to random noise when the factors are in roughly equal concentrations. The sensitivity to molecular noise of the networks proposed here would be interesting to study, as it has been proposed that some types of differentiation during development could have a stochastic aspect (for example in adipogenesis, Tchkonia et al., 2002, or hematopoiesis, Enver & Greaves, 1998).

6.4.5 Evolvability of switch networks

In addition to having a coexpression behaviour which is easily tunable by one parameter, the generic bHLH network studied here has the advantage of being perhaps more easily evolvable than a network in which every element actively represses all others: the interaction needs only take place between every element and a common activator (which requires n interactions, instead of $n\,(n-1)\,/2$). bHLH networks have been suggested to evolve mainly by single-gene duplication events (Amoutzias et al., 2004), maintaining a topology in which every element of the network interacts with a restricted number of "hubs".

6.5 Conclusion

The models presented here could be useful in understanding development, as well as cell-fate reprogramming (which can be induced artificially, but has also been shown to happen naturally, Weimann et al., 2003). We have derived general results about the dynamics and co-expression properties of switch networks, and shown the flexibility of bHLH dimerisation networks. Of the networks studied here, which were generically formulated with usual kinetic equations, only a subset can co-express antagonistic elements at a similar level, higher than the basal level: those with mutual inhibition, autocatalysis, and leak (but only when the cooperativity is very close to 1, and the transcription strength sufficiently low), and bHLH dimerisation networks (when the competition is sufficiently weak). This restricts the classes of models which can reproduce experimentally-observed co-expression of antagonistic factors, as well as showing how it can occur.

Strikingly, even though bHLH networks are the most apt to coexpression of antagonistic elements, the selection of one element requires a transient increase in competition, which is not what is thought to happen over a long time scale in the course of differentiation. Transient, hitherto-unexplained increases in competition have however been observed in a few cell lines upon differentiation, and could be a general phenomenon.

In order to model specific differentiation events, these networks would probably need to be extended to take into account combinatorial interactions, which could complicate their behaviour. The models would also gain from being extended to take into account non-symmetrical networks, in which some switch elements are stronger than others, and stochastic kinetics.

Acknowledgements

This work was funded by an AstraZeneca studentship awarded to OC by CoMPLEX.

6.6 Analysis of mutual inhibition with autocatalysis

6.6.1 Special case: no cooperativity ($c = 1$)

We assume that $\sigma > 1$. The set of steady states for the system defined by equations 6.1 is 0 and the attracting hyperplane $\{x \mid 1 + \Sigma_{i=1}^{n} x_i = \sigma\}$. Let $s = \Sigma_{i=1}^{n} x_i$. Then s never crosses the value $\sigma - 1$, and since $\dot{x_i} = x_i \left(\frac{(\sigma-1)-s}{1+s}\right)$, $\dot{x_i}$ is of constant sign, and each x_i convergent.

Simulations show that there is a great number of stable steady states.

For $c > 1$, the convergence of the dynamical system (defined by equations 6.1) to an equilibrium, from any initial condition, will be derived in a more general context, in section 6.7.1. In the rest of the appendix we assume $c > 1$.

6.6.2 One on, all others off

Equilibrium existence

The steady-state equations are

$$\forall j, \bar{x}_j \left(1 + \Sigma_{i=1}^{n} \bar{x}_i^c\right) = \sigma \bar{x}_j^c,$$

ie

$$\bar{x}_j^{c-1} = \frac{1}{\sigma}\left(1 + \Sigma_{i=1}^{n} \bar{x}_i^c\right) \text{ or } \bar{x}_j = 0$$

Re-arranging the first equation,

$$\frac{1}{\sigma}\bar{x}_j^c - \bar{x}_j^{c-1} = -\frac{1}{\sigma}\left(1 + \Sigma_{i\neq j}\bar{x}_i^c\right)$$

Let $f(x) = \frac{1}{\sigma}x^c - x^{c-1}$. Then $f'(x) = \frac{c}{\sigma}x^{c-1} - (c-1)x^{c-2}$. $f'(x) < 0$ iff $\frac{c}{\sigma}x < c-1$. The minimal value of f over the positive real set is $f(\frac{c-1}{c}\sigma) = \frac{1}{\sigma}\left(\frac{c-1}{c}\sigma\right)^c - \left(\frac{c-1}{c}\sigma\right)^{c-1} = \sigma^{c-1}\left(\frac{c-1}{c}\right)^{c-1}\left(\frac{c-1}{c} - 1\right) = \sigma^{c-1}\left(\frac{c-1}{c}\right)^{c-1}\frac{-1}{c}$.

The equilibria studied here are such that only $\bar{x}_j$ is non-0, for some j. There are either 0 or 2 solutions, 2 iff

$$\sigma^{c-1}\left(\frac{c-1}{c}\right)^{c-1}\frac{1}{c} > \frac{1}{\sigma}$$

$$\sigma^c > c\left(\frac{c}{c-1}\right)^{c-1}$$

$$\ln\sigma > \frac{\ln c + \ln\left(\frac{c}{c-1}\right)^{c-1}}{c} \tag{6.4}$$

$\ln\left(\frac{c}{c-1}\right)^{c-1}$ is an increasing function of c, and $\lim_{c\to\infty}\ln\left(\frac{c}{c-1}\right)^{c-1} = 1$. $\frac{lnc}{c}$ is decreasing for $c > e \simeq 2.7$. The right-hand side of equation 6.4 has a maximum for $c = 2$, of about 0.7, matched by $\sigma = 2$. Thus, for $\sigma \geq 2$, there are two equilibria. Both large c and large σ are favourable to the existence of an equilibrium with one variable dominating all others.

Local stability analysis

It is useful, for the Jacobian term computations to follow in the rest of the appendix, to note that if $g(x) = \frac{x^m}{\alpha+x^m}$, $g'(x) = \frac{\alpha m x^{m-1}}{(\alpha+x^m)^2}$.

If x_j is at a non-zero steady-state and $\forall i \neq j, x_i = 0$, and if $c > 1$, the stability at that steady state depends only on the sign of the (j,j) coefficient of the Jacobian matrix (this coefficient will be called $J_{j,j}$ in the remainder of the appendix).

$$J_{j,j} = -1 + \sigma c\left(1 + \Sigma_{i\neq j}x_i^c\right)\frac{x_j^{c-1}}{\left(1 + \Sigma_{i=1}^n x_i^c\right)^2} \tag{6.5}$$

$$J_{j,j} = -1 + \sigma c \frac{x_j^{c-1}}{\left(1 + x_j^c\right)^2},$$

with

$$\sigma \bar{x}_j^{c-1} = 1 + \bar{x}_j^c, \tag{6.6}$$

at equilibrium

$$J_{j,j} = -1 + c \frac{1}{\sigma \bar{x}_j^{c-1}},$$

the equilibrium is stable iff

$$\bar{x}_j^{c-1} > \frac{c}{\sigma}, \text{ ie } 1 + \bar{x}_j^c > c$$

It is possible to give a sufficient condition for the equilibrium with the greatest solution to equation 6.6 to be stable. Let $f(x) = x^c - \sigma x^{c-1}$. If $f\left(\left(\frac{c}{\sigma}\right)^{\frac{1}{c-1}}\right) < -1$, then the greatest root of equation 6.6 will be greater than $\left(\frac{c}{\sigma}\right)^{\frac{1}{c-1}}$, and the corresponding equilibrium will be stable. A sufficient stability condition is thus

$$\left(\frac{c}{\sigma}\right)^{\frac{c}{c-1}} < c - 1$$

Numerical investigation shows that this condition is met for $\sigma \geq 2$.

6.6.3 k variables on, others off

With identical parameters, there can be no equilibrium with 2 variables having different, non-zero values.

At any equilibrium, variables can be renumbered so that, in the Jacobian matrix, variables at 0 form an independent block. This block is stable, and the stability of the whole system depends only on the block formed by non-0 variables. Thus, in the following we suppose that no steady-state variable has 0 for a value.

For $i \neq j$,

$$J_{i,j}(\bar{x}) = -\sigma c \frac{\bar{x}^{2c-1}}{(1+k\bar{x}^c)^2}$$

With the same kind of analysis as in Cinquin & Demongeot (2002), the equilibrium is stable only if

$$\sigma c \frac{\bar{x}^{2c-1}}{(1+k\bar{x}^c)^2} < 1 - \sigma c \left(1 + (k-1)\,\bar{x}^c\right) \frac{\bar{x}^{c-1}}{(1+k\bar{x}^c)^2} \tag{6.7}$$

With the definition of the equilibrium,

$$\sigma c \bar{x}^{2c-1} < \sigma^2 \bar{x}^{2c-2} - \sigma c \left(1 + (k-1)\,\bar{x}^c\right) \bar{x}^{c-1}$$

$$x^c < \frac{\sigma}{c} x^{c-1} - \left(1 + (k-1)\,x^c\right)$$

$$\frac{\sigma}{c} x^{c-1} > kx^c + 1$$

Again with the definition of the equilibrium,

$$\frac{1}{c} x^{c-1} > x^{c-1},$$

ie $c < 1$, in which case no interesting equilibria exist.

6.7 Analysis of mutual inhibition with autocatalysis, and leak

If $\alpha \geq 0$, $c \geq 1$, and one of these inequalities is strict, the function $f(x) = x^{1-c} - \alpha x^{-c}$ can take the same value for at most 2 positive values of x. Thus, there are only two values a variable can take at a given steady state (0 cannot

be a steady state value). If two different equilibrium values are taken by some variables, one of these values is higher than $\alpha\frac{c}{c-1}$, and the other lower.

If $\alpha > 0$ and $c = 1$, the system only has one equilibrium, with all variables equal.

6.7.1 Convergence

Let $y_i = \sqrt{x_i}$, and

$$P = \frac{1}{4}\Sigma_{i=1}^{n} y_i^2 - \frac{\sigma}{4c}\log\left(1 + \Sigma_{i=1}^{n} y_i^{2c}\right) - \frac{1}{2}\log\Pi_{i=1}^{n} y_i^{\alpha}$$

$$\dot{y_i} = \frac{\dot{x_i}}{2\sqrt{x_i}}$$

$$2\dot{y_i} = -y_i + \sigma\frac{y_i^{2c-1}}{1 + \Sigma_{i=1}^{n} y_i^{2c}} + \frac{\alpha}{y_i} = 2\frac{\partial P}{\partial y_i}$$

Thus, P is a potential for the system.

If its equilibria are isolated, a gradient system converges to a steady-state regardless of the initial conditions. It is shown below that the number of solutions of the system is finite when the cooperativity c is an integer, and the system thus always converges to a steady state (we expect this result to also hold for non-integer values of c). The model without leak corresponds to $\alpha = 0$, and this convergence result thus also applies to it, for $c > 1$.

6.7.2 Steady-state analysis: all at the same value

Equilibrium existence

$$\forall\ j,\ (x_j - \alpha)\left(1 + \Sigma_{i=1}^{n} x_i^c\right) = \sigma x_j^c$$

If $\forall\ j,\ x_j = \bar{x}$,

$$n\bar{x}^{c+1} - (\sigma + n\alpha)\,\bar{x}^c + \bar{x} - \alpha = 0 \tag{6.8}$$

There is at least one solution, maybe 3 (or 2 in degenerate cases) depending on the parameters. The solutions are noted $\bar{x}_l$, $\bar{x}_u$, and $\bar{x}_h$, with $\bar{x}_l < \bar{x}_i < \bar{x}_h$.

If $f(x) = nx^{c+1} - (\sigma + n\alpha)\, x^c + x$, $f'(x) = (c+1)nx^c - c(\sigma + n\alpha)x^{c-1} + 1$, $f''(x) = c(c+1)nx^{c-1} - c(c-1)(\sigma+n\alpha)x^{c-2}$. $f''\left(\frac{c-1}{n(c+1)}\,(\sigma + n\alpha)\right) = 0$. f' takes negative values iff $f'\left(\frac{c-1}{n(c+1)}\,(\sigma + n\alpha)\right) < 0$, which is a necessary condition for the existence of 3 equilibria with all variables on.

The dynamics of the system constrained to $\forall\ i,\ x_i = x$ are defined by

$$\dot{x} = -x + \frac{\sigma x^c}{1 + nx^c} + \alpha$$

The sign of $\dot{x}(t)$ is the opposite of that of $f(x(t))$. Because $\bar{x}_u$ is such that $f'(\bar{x}_i) < 0$, it is easy to see that the steady state $\bar{x}_u$ is unstable for the constrained system, and thus for the full system.

Local stability analysis

With a leak α, equation 6.7 becomes

$$\bar{x}^c < \frac{\sigma}{c}\frac{\bar{x}^{c+1}}{(\bar{x} - \alpha)^2} - 1 - (k-1)\,\bar{x}^c$$

$$1 + k\bar{x}^c < \frac{\sigma}{c}\frac{\bar{x}^{c+1}}{(\bar{x} - \alpha)^2}$$

$$\frac{\sigma \bar{x}^c}{\bar{x} - \alpha} < \frac{\sigma}{c}\frac{\bar{x}^{c+1}}{(\bar{x} - \alpha)^2}$$

$$\bar{x} - \alpha < \frac{1}{c}\bar{x}$$

Thus the stability condition 6.7 is met iff $\bar{x} < \alpha\frac{c}{c-1}$ (in that case, since non-diagonal terms of the Jacobian are obviously negative, diagonal terms are also negative, and the equilibrium is stable). Since solutions to equation 6.8 can be made arbitrarily high by increasing σ, increasing σ past a threshold value (other

parameters being equal) will prevent the existence of a stable equilibrium with all variables equal.

6.7.3 k on, $k < n$

Let $p = n - k$.

$$(\bar{x}_l - \alpha)\left(1 + p\bar{x}_l^c + k\bar{x}_h^c\right) = \sigma\bar{x}_l^c$$

$$\begin{aligned} p\bar{x}_l^{c+1} - (p\alpha + \sigma)\,\bar{x}_l^c + (1 + k\bar{x}_h^c)\,\bar{x}_l - \alpha\,(1 + k\bar{x}_h^c) &= 0 \\ k\bar{x}_h^{c+1} - (k\alpha + \sigma)\,\bar{x}_h^c + (1 + p\bar{x}_l^c)\,\bar{x}_h - \alpha\,(1 + p\bar{x}_l^c) &= 0 \end{aligned}$$

Choosing for example the graded lexicographic order over $\mathbb{C}[x_l, x_h]$, theorem 5.3.6 from Cox et al. (1996) shows that the system has a finite number of solutions, when c is an integer.

We have

$$J_{i,i} = -1 + c\sigma x_i^{c-1}\frac{D - x_i^c}{D^2}$$

$$J_{i,j} = -c\sigma x_j^{c-1}\frac{x_i^c}{D^2}$$

If $x_i = x_j$,

$$J_{i,i} - J_{i,j} = -1 + cx_i^{c-1}\frac{\sigma}{D} = -1 + c\frac{x_i - \alpha}{x_i}$$

Consider the reordered Jacobian matrix, with k variables "on" with a value $\bar{x_h}$, and p "off" with a value $\bar{x}_l$ $(k + p = n)$.

It follows from the analysis in section 6.8.3 that the equilibrium can be stable only if $J_{i,i} - J_{i,j} < 0$ (ie $x_i < \alpha\frac{c}{c-1}$), if the number of variables having value x_i is strictly greater than 1.

Thus there are only two possible kinds of stable equilibria: all variables equal, in which case the equilibrium value is lower than $\alpha\frac{c}{c-1}$, or one higher than all the other ones (in which case the lower ones are lower than, and the higher one greather than $\alpha\frac{c}{c-1}$).

6.8 Analysis of the bHLH model

Without cooperativity in transcriptional activation by the bHLH dimer, there is only one stable steady-state:

$$\dot{x_i} = x_i \left(-1 + \frac{\sigma}{\alpha \left(1 + \Sigma_{j=1}^{n} x_j\right) + x_i} \right)$$

If at some steady state k variables are on and share a common value $\bar{x}$ (variables at a steady state, if not 0, share a common value),

$$1 = \frac{\sigma}{k\alpha\bar{x} + \bar{x} + \alpha}$$

$$\bar{x} = \frac{\sigma - \alpha}{k\alpha + 1},$$

and if $x_p(t_0) = 0$,

$$J_{p,p} = \left(-1 + \frac{\sigma}{k\alpha\bar{x} + \alpha} \right)$$

$$J_{p,p} = \frac{\sigma - \alpha}{\alpha\left(k\sigma + 1\right)} > 0,$$

and $J_{p,l} = 0$ for $p \neq l$, proving the unstability of the steady state.

In the following, it is assumed that transcriptional activation occurs with cooperativity 2, and the steady-state equations become

$$\bar{x_i} = \sigma \frac{\bar{x_i}^2}{\left(\frac{D}{a_t}\right)^2 K_2 + \bar{x_i}^2}$$

$$\forall\ i,\ \alpha D^2 + \bar{x_i}^2 = \sigma \bar{x_i} \tag{6.9}$$

6.8.1 Dynamical analysis

0 is a stable steady state. If $x_i(0) = 0$, then $\forall\ t > 0,\ x_i(t) = 0$. If $x_i(0) > 0$, then $\forall\ t > 0,\ x_i(t) > 0$. One can thus suppose that $\forall\ i, \forall\ t \geq 0,\ x_i(t) > 0$. Consider a state in which there is one variable strictly superior to all others (ie, a state not belonging to the line $x_1 = x_2 = .. = x_n$). Suppose without loss of generality that the variable in question is x_1. Consider the function

$$f_1(x) = \frac{x_1^2}{\alpha D^2 + x_1^2}$$

$$\dot{f_1}(x) = 2\alpha D x_1 \frac{\dot{x_1}\left(D - x_1\right) - x_1 \Sigma_{i=2}^n \dot{x_i}}{\left(\alpha D^2 + x_1^2\right)^2}$$

$$\frac{\left(\alpha D^2 + x_1^2\right)^2}{2\alpha D x_1} \dot{f_1}(x) = \dot{x_1} + \sigma \Sigma_{i=2}^n \frac{x_1 x_i \left(x_1 - x_i\right)\left(\alpha D^2 - x_1 x_i\right)}{\left(\alpha D^2 + x_1^2\right)\left(\alpha D^2 + x_i^2\right)}$$

For $\alpha \geq 1/2$, the second term is positive.

We have

$$\frac{\mathrm{d}x_1(t)}{\mathrm{d}t} = \sigma f_1(x) - x_1$$

We first consider the case in which $\forall\ t \geq 0, \forall\ n \geq j > 1,\ x_1 > x_j$.

Suppose that $\sigma f_1(0) \geq x(0)$. In this case, $\dot{f_1}\left(0\right) > 0$, and x_1 and f are strictly increasing functions of time. If $\sigma f_1(0) < x_1(0)$, then $\dot{f_1}\left(0\right)$ can be negative or positive. In the first case, x_1 is decreasing as long as f_1 is. If at some time t_0 $\sigma f_1(t_0) \geq x(t_0)$, then for $t > t_0$, x_1 and f_1 are increasing functions of time. Thus there can be at most one change in the monotony of x_1. Thus $\lim_{t\to\infty} x_1(t)$ exists. Since $\ddot{x_1}$ exists and is bounded on any trajectory,

$\lim_{t\to\infty} \dot{x_1}(t) = 0$. All trajectories thus converge to a steady state where $\forall j > 1$, $x_j = x_1$ or $x_j = 0$.

If $\exists\ t$ st $\forall\ n > j > 1$, $x_1(t) = x_j(t)$, the system is brought back to one dimension. Note that it is impossible for any variable to outgrow x_1.

6.8.2 Steady-state analysis: variables on at the same value

Equilibrium existence

Variables zero at the steady state can be discarded from the analysis. If k variables are non-0, and are all equal, to $\bar{x} \neq 0$,

$$\bar{x}^2\left(1 + k^2\alpha\right) + \bar{x}\left(2k\alpha - \sigma\right) + \alpha = 0 \tag{6.10}$$

Solutions are

$$\frac{\sigma - 2k\alpha \pm \sqrt{\sigma^2 - 4\alpha\left(1 + k\sigma\right)}}{2\left(1 + k^2\alpha\right)}$$

A sufficient and necessary condition for the existence is

$$4\alpha\frac{k\sigma + 1}{\sigma^2} < 1$$

It will be shown below that, at a stable steady-state, there is at most 1 non-0 variable which can be different from other non-0 variables. If there is such a variable, equal to y, the equation for the value of other variables becomes

$$\bar{x}^2\left(1 + k^2\alpha\right) + \bar{x}\left(2k\alpha\left(1 + y\right) - \sigma\right) + \alpha\left(1 + y\right)^2 = 0 \tag{6.11}$$

Solutions are

$$\frac{\sigma - 2k\alpha\left(1 + y\right) \pm \sqrt{\sigma^2 - 4\alpha\left(1 + k\sigma + y\right)\left(1 + y\right)}}{2\left(1 + k^2\alpha\right)}$$

and the condition for a solution to exist

$$4\alpha\left(1+y\right)\frac{k\sigma+1+y}{\sigma^2}<1$$

The solutions for y are

$$\frac{\sigma-2\alpha\left(1+k\bar{x}\right)\pm\sqrt{\sigma^2-4\alpha\left(1+\sigma+k\bar{x}\right)\left(1+k\bar{x}\right)}}{2\left(1+\alpha\right)}$$

Local stability analysis

Variables zero at the steady state can be discarded from the analysis.

Using

$$\frac{\dot{x^2}}{ax^2+bx+c}=\frac{bx^2+2cx}{\left(ax^2+bx+c\right)^2},$$

one derives the diagonal term of the Jacobian (with $b=2\alpha\left(D-x_i\right)$ and $c=\alpha\left(D-x_i\right)^2$):

$$J_{i,i}=-1+2\sigma\alpha x_i\frac{D\left(D-x_i\right)}{\left(\alpha D^2+x_i^2\right)^2}$$

Using the steady state equation 6.9,

$$J_{i,i}=-1+\frac{2\alpha}{\sigma x_i}\left(D\left(D-x_i\right)\right)=-1+\frac{2}{\sigma}\left(\sigma-x_i-\alpha D\right)$$

$$J_{i,i}=1-\frac{2}{\sigma}\left(x_i+\alpha D\right)=1-\frac{2}{\sigma}\left(\alpha+x_i\left(1+k\alpha\right)\right)$$

The diagonal terms are negative for

$$x_i>\frac{\sigma/2-\alpha}{1+k\alpha}$$

The off-diagonal terms are given by

$$J_{i,j}=-\sigma x_i^2\frac{2\alpha x_j+2\alpha\left(D-x_j\right)}{\left(\alpha D^2+x_i^2\right)^2}$$

$$J_{i,j} = -2\sigma\alpha x_i^2 \frac{D}{(\alpha D^2 + x_i^2)^2}$$

$$J_{i,j} = -\frac{2\alpha}{\sigma} D$$

$$J_{i,j} - J_{i,i} = -1 + 2\frac{x_i}{\sigma}$$

Thus, a necessary condition for the equilibrium to be stable is

$$\forall\ \bar{x}_i \text{ st } \bar{x}_i \neq 0,\ \bar{x}_i > \sigma/2 \tag{6.12}$$

This is possible if and only if $\alpha < 1/k^2$ and $\sigma > 2\frac{k\alpha+\sqrt{\alpha}}{1-k^2\alpha}$.

Condition 6.12 is stronger than the requirement for the diagonal element to be negative (and is thus also a sufficient condition), and can never be met by variables equal to the lower solution of equations 6.10 or 6.11 .

Thus, for any value of the transcription strength σ and for any number of coexistant variables k, sufficiently low values of α make the equilibrium stable. If there is a stable equilibrium with k variables on, there is also a stable equilibrium with p variables on, for $1 < p < k$. For sufficiently large σ, the necessary condition $\alpha < 1/k^2$ becomes sufficient for stability (see Figure 6.5 for an illustration of the validity of this condition).

6.8.3 On at different values

If at steady state, $x_i \neq x_j$ and both are non-0, then

$$x_i^2 - \sigma x_i = x_j^2 - \sigma x_j \left(= -\alpha D^2\right)$$

There are thus only two possible non-0 steady-state values, noted $\bar{x}_a$ and $\bar{x}_b$, with $\bar{x}_a < \bar{x}_b$. Noting $P(x) = x^2 - \sigma x$, and supposing that $\bar{x}_a$ and $\bar{x}_b$ exist, $P'(\bar{x}_a) < 0$, *ie* $\frac{2\bar{x}_a}{\sigma} < 1$.

Consider the Jacobian matrix of the system, reordered so that variables having $\bar{x}_a$ as a value come before those having $\bar{x}_b$ as a value:

$$\begin{pmatrix} \overbrace{\begin{matrix} a & c & \cdots & c \\ c & \ddots & \cdots & \vdots \\ \vdots & \vdots & \ddots & \vdots \\ c & \cdots & c & a \end{matrix}}^{k} & \overbrace{\begin{matrix} f_1 & \cdots & \cdots & f_1 \\ \vdots & \vdots & \vdots & \vdots \\ \vdots & \vdots & \vdots & \vdots \\ f_1 & \cdots & \cdots & f_1 \end{matrix}}^{p} \\ \begin{matrix} f_2 & \cdots & \cdots & f_2 \\ \vdots & \vdots & \vdots & \vdots \\ \vdots & \vdots & \vdots & \vdots \\ f_2 & \cdots & \cdots & f_2 \end{matrix} & \begin{matrix} b & e & \cdots & e \\ e & \ddots & \cdots & \vdots \\ \vdots & \vdots & \ddots & \vdots \\ e & \cdots & e & b \end{matrix} \end{pmatrix}$$

With the appropriate eigenvectors, it is easy to show that $b - e$ and $a - c$ are eigenvalues for this matrix, of order $k - 1$ and $p - 1$. Thus, if $k > 1$ and $p > 1$, a necessary condition for stability of an equilibrium is $e > b$ and $c > a$. In particular, there can be at most 1 variable having $\bar{x}_a$ as a value.

More precisely, the characteristic polynomial of the matrix is

$$\begin{aligned} P(x) = (a - c - x)^{k-1} (b - e - x)^{p-1} \left[x^2 - x(a + b + (k-1)c + (p-1)e)\right. \\ \left. + (p-1)ea + (k-1)cb + (k-1)(p-1)ec + ab - kpf_1f_2\right] \end{aligned} \tag{6.13}$$

Suppose thus that the number of variables having values $\bar{x}_a$ is 1. Then, a sufficient condition for instability of the equilibrium is

$$(p-1)ea + ab - pf_1f_2 < 0$$

Notice that in this case $f_1 = f_2 = e$. The sufficient condition for instability can thus be written

$$e(pe - (p-1)a) - ab > 0$$

Replacing with the equilibrium values,

$$\frac{-2\alpha D}{\sigma}\left(p\frac{-2\alpha D}{\sigma}-(p-1)\left(1-\frac{2}{\sigma}\left(\bar{x}_a+\alpha D\right)\right)\right)- \left(1-\frac{2}{\sigma}\left(\bar{x}_a+\alpha D\right)\right)\left(1-\frac{2}{\sigma}\left(\bar{x}_b+\alpha D\right)\right)>0$$

$$\left(1-\frac{2}{\sigma}\left(\bar{x}_a+\alpha D\right)\right)\left((p-1)\frac{2\alpha D}{\sigma}-1+\frac{2}{\sigma}\left(\bar{x}_b+\alpha D\right)\right)+p\left(\frac{2\alpha D}{\sigma}\right)^2>0$$

$$\left(1-\frac{2}{\sigma}\left(\bar{x}_a+\alpha D\right)\right)\left(p\frac{2\alpha D}{\sigma}-1+\frac{2\bar{x}_b}{\sigma}\right)+p\left(\frac{2\alpha D}{\sigma}\right)^2>0$$

$$p\frac{2\alpha D}{\sigma}\left(1-\frac{2\bar{x}_a}{\sigma}\right)+\left(\frac{2\bar{x}_b}{\sigma}-1\right)\left(1-\frac{2}{\sigma}\left(\bar{x}_a+\alpha D\right)\right)>0$$

$$\left(1-\frac{2\bar{x}_a}{\sigma}\right)\left(p\frac{2\alpha D}{\sigma}+\frac{2\bar{x}_b}{\sigma}-1\right)-\frac{2\alpha D}{\sigma}\left(\frac{2\bar{x}_b}{\sigma}-1\right)>0$$

$$\frac{2\alpha D}{\sigma}\left(p+1-\frac{2}{\sigma}\left(p\bar{x}_a+\bar{x}_b\right)\right)+\left(1-\frac{2\bar{x}_a}{\sigma}\right)\left(\frac{2\bar{x}_b}{\sigma}-1\right)>0$$

The first term is positive because the values of $\bar{x}_a$ and $\bar{x}_b$ are symmetrical with respect to $\sigma/2$. The second term is also positive, and the sufficient condition for the instability of the equilibrium is thus met.

Thus, there is no stable equilibrium with non-0 variables having different values.

6.9 Methods

6.9.1 Numerical integration

All integration was performed with a custom-written implementation of the 4th-order adaptative stepsize Runge-Kutta algorithm (Press, 1992), with 10^{-3} relative accuracy. Source code is available at `http://www-timc.imag.fr/Olivier.Cinquin/ada/ada_blas_runge_kutta.html`. The data was plotted using GMV or gnuplot.

6.9.2 Computation of convergence times

A custom program was written to do the following, starting from a regular 200*200 grid of initial conditions (for 2D systems), or a 50*50*50 grid (for 3D systems), with $\forall i \neq j,\ x_i \neq x_j$, to avoid reaching unstable steady-states: (1) integrate the system until a steady-state is reached (as defined by the sum of the absolute values of the derivative vector elements begin lower than 10^{-4}) (2) start the integration again, with the same initial conditions, stopping when the system gets close enough to the previous steady-state (each variable with 10% of its steady-state value if it's not 0, lower than 0.15 if it is 0; moderate changes in these arbitrary values do not significantly affect the results). The stepsize of the Runge-Kutta algorithm was kept lower than 0.3.

6.9.3 Simulations with time-dependent parameters

In order for the system to leave steady states which had become unstable because of changed parameters, small random perturbations were applied (each variable was multiplied by a random number uniformly chosen in [0.99 .. 1.01] every 30 time units).

Chapter 7

Addendum to "High-dimensional switches and the modelling of cellular differentiation"

An essential approximation was ommitted by Cinquin & Demongeot (2005), in the section on bHLH competitive heterodimerisation. Let x_i^f denote the concentration of free class B protein i, x_i^T its total concentration, a_t the total quantity of common class A dimerization partners, and D_i the dissociation constant for the $A - B_i$ complex. Then

$$x_i^f \left(1 + \frac{a_t/D_i}{1 + \Sigma_{j=1}^n x_j^f/D_j} \right) = x_i^T$$

x_i^f can be approximated by x_i^T only if $a_t \ll D_i + \Sigma_{j=1}^n x_i^f D_i/D_j$, which is the case in particular if the total quantity of class A dimerization partners is small compared to the dissociation constants of the $A - B_i$ complex. If this is true of all $A - B_i$ complexes, one derives equations numbered (3) by Cinquin & Demongeot (2005).

It is shown in the Appendix that the proof, given by Cinquin & Page, that to have expression of k switch elements, the competition level α needs to verify $\alpha \leq 1/k^2$, still holds without this simplification, as long as all D_is are identical. Numerical simulations suggest that this result extends to arbitrary D_is, but this remains to be proven.

7.1 Appendix

7.2 Study of the full system

The dynamics of the full system are defined by

$$\frac{\mathrm{d}x_i^T}{\mathrm{d}t} = -d_i x_i^T + \sigma_i \frac{\left(\frac{a_t x_i^f/D_i}{1+\Sigma_j x_j^f/D_j}\right)^2}{K_2^2 + \left(\frac{a_t x_i^f/D_i}{1+\Sigma_j x_j^f/D_j}\right)^2} \tag{7.1}$$

$$\frac{\mathrm{d}x_i^T}{\mathrm{d}t} = -d_i x_i^T + \sigma_i \frac{{x_i^f}^2}{\frac{K_2^2 D_i^2}{a_i^2}\left(1+\Sigma x_j^f/D_j\right)^2 + {x_i^f}^2}$$

With $D = 1 + \Sigma x_i^f/D_i$,

$$\frac{\mathrm{d}x_i^T}{\mathrm{d}t} = -d_i x_i^T + \sigma_i \frac{{x_i^T}^2}{{x_i^T}^2 + \alpha\left(D_i D + a_t\right)^2}$$

D is such that

$$D - 1 = \Sigma_i \frac{x_i^T}{D_i + a_t/D}$$

If $\forall\ i,\ D_i = D_0$, then

$$D_0\left(1+\Sigma x_i^f/D_i\right) = \frac{D_0 + \Sigma x_i^T - a_t + \sqrt{\left(D_0 - a_t + \Sigma x_i^T\right)^2 + 4a_t D_0}}{2}$$

and

$$\frac{\mathrm{d}x_i^T}{\mathrm{d}t} = -d_i x_i^T + \frac{\sigma_i {x_i^T}^2}{{x_i^T}^2 + \alpha\left(D_0 + \Sigma x_i^T + a_t + \sqrt{\left(D_0 - a_t + \Sigma x_i^T\right)^2 + 4a_t D_0}\right)^2/4}$$

In the following, x_i^T is replaced by x_i for clarity. As noted by Cinquin & Demongeot (2005), one can suppose without loss of generality that all x_is are

non-zero at the steady state being studied. Using the same notation for the Jacobian as Cinquin & Page, the Jacobian matrix at a steady state is given by

$$J_{i,j}(x) = -P_i + \delta_{i,j} Q_i, \; i,j = 1..n$$

where, noting $s = \sqrt{(D_0 - a_t + \Sigma_{k=1}^n x_k)^2 + 4a_t D_0}$,

$$P_i = -\sigma_i x_i^2 \alpha \frac{\left(1 + \frac{D_0 - a_t + \Sigma_{k=1}^n x_k}{s}\right)(D_0 + \Sigma_{k=1}^n x_k + a_t + s)}{2\left({x_i}^2 + \alpha\left(D_0 + \Sigma_{k=1}^n x_k + a_t + \sqrt{(D_0 - a_t + \Sigma_{k=1}^n x_k)^2 + 4a_t D_0}\right)^2/4\right)}$$

$$P_i = d_i \beta_i \alpha \left(D_0 + \Sigma_{k=1}^n x_k + s/2 + \frac{(D_0 - a_t + \Sigma_{k=1}^n x_k)(D_0 + a_t + \Sigma_{k=1}^n x_k)}{2s}\right)$$

$$Q_i = -d_i + \frac{\alpha \sigma_i}{2 r_i^2 x_i^2} x_i (D_0 + \Sigma_{k=1}^n x_k + a_t + s)^2$$

$$Q_i = -d_i + \alpha \frac{d_i \beta_i}{2 x_i} (D_0 + \Sigma_{k=1}^n x_k + a_t + s)^2$$

Let $W = (D_0 + \Sigma_{k=1}^n x_k + a_t + s)^2$. Then at steady state

$$W = \frac{4}{\alpha}(r_i x_i - x_i^2) \tag{7.2}$$

$$\frac{\beta_i \alpha W}{2 x_i} = 1 \pm \sqrt{1 - \alpha W \beta_i}$$

Therefore,

$$Q_i = \pm d_i \sqrt{1 - \alpha W \beta_i},$$

where the sign is the opposite of that defining x_i at the steady state, in equation 7.2. Following Cinquin & Page, at most one of the x_i can be at the lower solution of equation 7.2; without loss of generality, let x_n be at the lower

solution of equation 7.2. With $r_{\kappa'} = \max_i r_i$, it follows as in Cinquin & Page that $n \neq \kappa'$ at a stable steady state, because if $n = \kappa'$ then

$$\frac{Q_n}{P_n}\frac{P_{n-1}}{Q_{n-1}} = \frac{d_n}{d_{n-1}}\frac{\sqrt{1-\alpha W\beta_n}}{-\sqrt{1-\alpha W\beta_{n-1}}}\frac{d_{n-1}\beta_{n-1}}{d_n\beta_n}$$

$$\frac{Q_n}{P_n}\frac{P_{n-1}}{Q_{n-1}} = -\frac{\beta_{n-1}}{\beta_n}\frac{\sqrt{1-\alpha W\beta_n}}{\sqrt{1-\alpha W\beta_{n-1}}}$$

$$Q_n/P_n \geq |Q_{n-1}/P_{n-1}|$$

Let $\kappa = n$; then one derives as in Cinquin & Page

$$\Sigma_{i=1}^n r_i = 2\Sigma_{k=1}^n x_k - \Sigma_{i\neq\kappa}\sqrt{r_i^2 - \alpha W} + \sqrt{r_\kappa^2 - \alpha W}$$

$$\Sigma_{i=1}^n r_i \leq 2\Sigma_{k=1}^n x_k - \Sigma_{i\neq\kappa,\ \kappa'}\sqrt{r_i^2 - \alpha W} \tag{7.3}$$

Noting $r_s = \min_i r_i$, this inequality holds for

$$D_0 + \Sigma_{k=1}^n x_k + a_t + \sqrt{\left(D_0 - a_t + \Sigma_{k=1}^n x_k\right)^2 + 4a_t D_0} \leq r_s/\sqrt{\alpha}$$

which is equivalent to $r_s\sqrt{\alpha} - a_t - D_0 - \Sigma_{k=1}^n x_k \geq 0$ and

$$\Sigma_{k=1}^n x_k \left(r_s/\sqrt{\alpha} - 2a_t\right) \leq r_s/2\sqrt{\alpha}\left(r_s/\sqrt{\alpha} - 2\left(D_0 + a_t\right)\right) \tag{7.4}$$

It is straightforward to show that the second factor of the left-hand side of this equation is positive, and inequality 7.3 therefore holds for

$$\Sigma_{k=1}^n x_k \geq \frac{r_s}{2\sqrt{\alpha}} - \frac{D_0}{1 - 2a_t\sqrt{\alpha}/r_s}$$

Now let $P(x) = 2x - \Sigma_{i=1}^n\sqrt{r_i^2 - \alpha\left(D_0 + x + a_t + s\right)^2}$. Then
$P'(x) = 2 - \Sigma_{i=1}^n \frac{-\alpha(D_0+x+a_t+s)\left(1+\frac{D_0-a_t+x}{s}\right)}{\sqrt{r_i^2-\alpha(D_0+x+a_t+s)^2}}$
A sufficient condition for $\forall\ x,\ P'(x) > 0$ is

$$D_0 - a_t + x < \sqrt{(D_0 - a_t + x)^2 + 4a_t D_0}$$

which is always the case. Therefore, replacing $\Sigma_{k=1}^{n} x_k$ by $\frac{r_s}{2\sqrt{\alpha}} - \frac{D_0}{1-2a_t\sqrt{\alpha}/r_s}$ in equation 7.3 (as in Cinquin & Page),

$$\Sigma_{i=1}^{n} r_i \leq r_s/\sqrt{\alpha} - \frac{2D_0}{1-2a_r\sqrt{\alpha}/r_s} -$$
$$\Sigma_{i\neq\kappa,\ \kappa'} \sqrt{r_i^2 - \alpha\left(D_0 + r_s/2\sqrt{\alpha} - \frac{D_0}{1-2a_r\sqrt{\alpha}/r_s} + a_t + \sqrt{\left(D_0 - a_t + r_s/2\sqrt{\alpha} - \frac{D_0}{1-2a_r\sqrt{\alpha}/r_s}\right)}\right.}$$

which implies $\alpha \leq 1/k^2$, where k is the number of non-zero x_is.

If all x_is are at the upper solution of equation 7.2, one derives

$$\Sigma_{i=1}^{n} r_i = 2\Sigma_{k=1}^{n} x_k - \Sigma_{i=1}^{n} \sqrt{r_i^2 - \alpha W} \tag{7.5}$$

$$\Sigma_{i=1}^{n} r_i \leq r_s/\sqrt{\alpha} - \frac{2D_0}{1-2a_r\sqrt{\alpha}/r_s} -$$
$$\Sigma_{i=1}^{n} \sqrt{r_i^2 - \alpha\left(D_0 + r_s/2\sqrt{\alpha} - \frac{D_0}{1-2a_r\sqrt{\alpha}/r_s} + a_t + \sqrt{\left(D_0 - a_t + r_s/2\sqrt{\alpha} - \frac{D_0}{1-2a_r\sqrt{\alpha}/r_s}\right)^2} + \right.}$$

which also implies $\alpha \leq 1/k^2$.

7.3 Comparison: with and without approximation

The system defined by equations 7.1 cannot be normalized as the approximated one. Using $\forall\ i,\ D_i = 0.02$, $K_2 = 1$, and α varying from 0.02 to 0.2, $a_t = K_2/\sqrt{\alpha}$ varies from 2.2 to 7. Figure 7.1 shows a numerical simulation for 2 4-way switches with these same parameters, one defined by equations 7.1, and

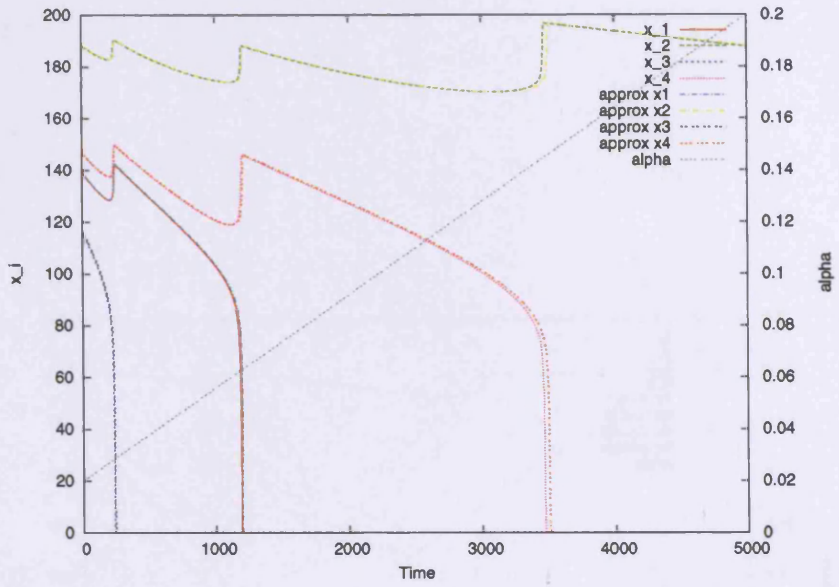

Figure 7.1: Comparison of a 4-switch simulated with equations 7.1 (x_1 to x_4), or with the approximating equations used by Cinquin & Demongeot (2005) (approx x_1 to approx x_4). See main text for values of system-wide parameters; switch-element specific parameters are $d_i = 1$ for all i, $\sigma_1 = 190$, $\sigma_2 = 226$, $\sigma_3 = 177$, and $\sigma_4 = 195$.

one defined by the approximating equations used by Cinquin & Demongeot (2005). The results are virtually identical. However, for lower values of D_i, the difference becomes noticeable (Figure 7.2 shows a comparison for $\forall\ i,\ D_i = 0.011$).

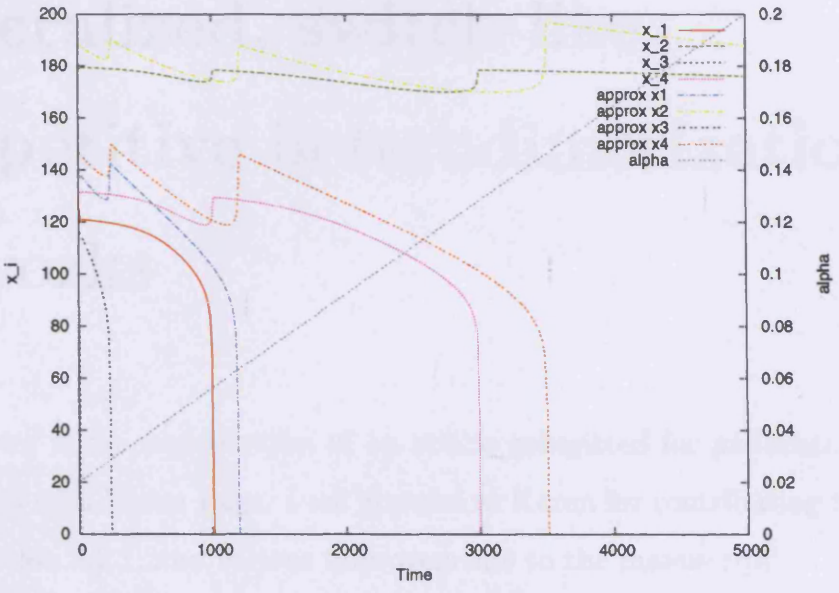

Figure 7.2: Comparison of a 4-switch simulated with equations 7.1 (x_1 to x_4), with $\forall\ i,\ D_i = 0.011$, or with the approximating equations used by Cinquin & Demongeot (2005) (approx x_1 to approx x_4). Other parameters are the same as in Figure 7.1.

Chapter 8

Generalized, switch-like competitive heterodimerization networks

This chapter is the reproduction of an article submitted for publication, and co-authored with Karen Page. I am grateful to Karen for contributing the first part of section 8.3.1, and various improvements to the manuscript.

8.1 Abstract

High-dimensional switches have been proposed as a way to model cellular differentiation, particularly in the context of basic Helix-Loop-Helix (bHLH) competitive heterodimerization networks. The previous study derived a simple rule showing how many elements can be co-expressed, depending on the rate of competition within the network. A limitation to that rule, however, is that many biochemical parameters were considered to be identical. Here we derive a generalized rule, which treats the case of an arbitrary bHLH network. This in turn allows one to study more ways in which these networks could be regulated, linking intrinsic cellular differentiation determinants to extracellular cues.

8.2 Introduction

Switch-like responses are an essential aspect of the dynamics of signaling networks, and are expected to be crucial in mediating cellular differentiation, a process during which one cell-type is chosen and all others excluded, in an all-or-none fashion. Such responses have been documented experimentally (Xiong & Ferrell, 2003), and bistable switches have been thoroughly characterized from a mathematical point of view (Cherry & Adler, 2000). A first study has derived a rule for the behavior of a subset of bHLH heterodimerization networks of arbitrary dimension, which were shown to have the required flexibility to account for many experimental observations related to switches with more than 2 outcomes (Cinquin & Demongeot, 2005). Here we generalize that rule to a wider set of networks.

bHLH networks

bHLH proteins form a large family, which has been shown to have a crucial role in numerous instances of commitment to specific lineages and differentiation (Massari & Murre, 2000). Three important classes in that family, which are the basis for the mathematical model presented below, are the class A, ubiquitously-expressed transcriptional activators capable of forming homodimers and heterodimers, the class B, capable of providing promoter-specific transcriptional activation only when heterodimerized with a class A element, and Id proteins, which have been most often reported to form transcriptionally-unproductive heterodimers with the class A. Since different class B proteins bind the same class A partners, there can be some competition between them for access to those partners. In networks in which class B proteins auto-activate their own transcription (a common feature of determinants of cellular differentiation), class B proteins can therefore inhibit one another's expression, by titrating out the class A. Id proteins have the same effect of titrating out the

class A, but are not explicitly taken into account in the model below because they have not been shown to regulate their own expression.

Mathematical model

A simple kind of model trying to account for switch-like behavior is where a set of class B proteins activate their own transcription. If class A proteins are considered to be expressed in a constitutive way, and not subjected to regulated degradation, they are present at a constant level. Only the time-evolution of each of the class B species is thus of interest. Calling x_i, $i = 1..n$, the concentrations of B_i (class B species), the equations are

$$\frac{\mathrm{d}x_i}{\mathrm{d}t} = -d_i x_i + \sigma_i \frac{x_i^2}{\alpha D^2 + x_i^2}, \tag{8.1}$$

with $D = 1 + \Sigma_{i=1}^{n} x_i$, $\alpha = K_2^2/a_t^2 \in \mathbb{R}_*^+$, where K_2 is the concentration of $A - B_i$ complex at which B_i transcription is half-maximal, a_t is the total quantity of class A proteins, σ_i and d_i are respectively the maximal synthesis rate and the degradation rate of B_i, and where each x_i is normalized with respect to the dissociation constant for the $A - B_i$ complex (this normalization leads to each maximal synthesis rate σ_i being divided by the dissociation constant of the $A - B_i$ complex, see Appendix 8.5).

This set of equations is the same as derived by Cinquin & Demongeot (2005), without the restriction $\forall\ i,\ d_i = 1,\ \sigma_i = \sigma$.

Previous result

It was shown by Cinquin & Demongeot (2005) that, in the case where $\forall\ i,\ d_i = 1,\ \sigma_i = \sigma$ and $\sigma >> 1$, there are stable steady states with k elements "on" (*i.e.* non-0) if and only if

$$\alpha < 1/k^2$$

(when the condition $\sigma >> 1$ is not met, the above condition is necessary but not sufficient).

Since α is a measure of the harshness of the competition in the system (as it depends on the quantity of the common class A activators, and the heterodimer concentration giving half-maximal transcription), this shows that the harsher the competition in the system, the lower the number of elements which can co-exist.

8.3 Results

Let $r_i = \sigma_i/d_i$. Then at any stationary state,

$$\forall\ i \text{ st } x_i \neq 0,\ x_i^2 - r_i x_i + \alpha D^2 = 0,$$

and

$$\forall\ i \text{ st } x_i \neq 0,\ x_i = \frac{r_i \pm \sqrt{r_i^2 - 4\alpha D^2}}{2} \tag{8.2}$$

x_is at 0 can be discarded from the rest of the analysis. It will be shown below that if the stationary state is stable, at most one x_i can be at the lower solution of equation 8.2 (inequality 8.5). Suppose that there is such an x_κ (if there is not, a stronger inequality is derived, see Appendix 8.6), and let κ' be such that $r_{\kappa'} = \max_i r_i$. It will be shown below that any steady state where $\kappa = \kappa'$ is unstable, and we can therefore suppose $\kappa \neq \kappa'$. Then

$$2\,(D-1) = \Sigma_{i\neq\kappa}\left(r_i + \sqrt{r_i^2 - 4\alpha D^2}\right) + r_\kappa - \sqrt{r_\kappa^2 - 4\alpha D^2}$$

$$\Sigma_i r_i + 2 = 2D - \Sigma_{i\neq\kappa}\sqrt{r_i^2 - 4\alpha D^2} + \sqrt{r_\kappa^2 - 4\alpha D^2}$$

$$\Sigma_i r_i + 2 \leq 2D - \Sigma_{i\neq\kappa,\ i\neq\kappa'}\sqrt{r_i^2 - 4\alpha D^2}$$

Consider the right-hand side of the above inequality as a function of D. It is an increasing function, and for the above inequality to hold, it must also hold for the maximum of that function (which is for $D = r_s/2\sqrt{\alpha}$), where $r_s = \min_i r_i$, ie

$$\frac{r_s}{\sqrt{\alpha}} \geq 2 + \Sigma_i r_i + \Sigma_{i \neq \kappa,\ i \neq \kappa'} \sqrt{r_i^2 - r_s^2} \tag{8.3}$$

This implies in particular $\alpha \leq 1/k^2$, where k is the number of non-zero x_is, generalizing the result obtained by Cinquin & Demongeot (2005).

8.3.1 Study of the characteristic polynomial

In a stable steady state at most one x_i takes the "lower" solution

For convenience, let $\beta_i = 1/r_i$. The Jacobian matrix of the system defined by equation 8.1, at a stationary point x in which none of the species has $x_i = 0$, is given by

$$J_{i,j}(x) = -P_i + \delta_{i,j} Q_i,\ i, j = 1..n$$

where $P_i = 2d_i \alpha D \beta_i$, and $Q_i = d_i (1 - 2\beta_i x_i)$. We assume that $\alpha > 0$ and note that $P_i > 0$. Eigenvalues λ of J are solutions to the equation $\det(J - \lambda I_n) = 0$.

$$\det(J - \lambda I_n) = \begin{vmatrix} Q_1 - P_1 - \lambda & -P_1 & -P_1 & \cdots & -P_1 \\ -P_2 & Q_2 - P_2 - \lambda & -P_2 & \cdots & -P_2 \\ \vdots & & & & \\ \vdots & & & & \\ -P_n & \cdots & \cdots & -P_n & Q_n - P_n - \lambda \end{vmatrix}$$

$$\det(J-\lambda I_n)=(\Pi_{i=1}^n P_i)\begin{vmatrix} \frac{Q_1}{P_1}-1-\frac{\lambda}{P_1} & -1 & -1 & \cdots & -1 \\ -1 & \frac{Q_2}{P_2}-1-\frac{\lambda}{P_2} & -1 & \cdots & -1 \\ \vdots & \ddots & \ddots & \ddots & \vdots \\ \vdots & \ddots & \ddots & \ddots & -1 \\ -1 & \cdots & \cdots & -1 & \frac{Q_n}{P_n}-1-\frac{\lambda}{P_n} \end{vmatrix}$$

$$\det(J-\lambda I_n)=(\Pi_{i=1}^n P_i)\begin{vmatrix} \frac{Q_1}{P_1}-1-\frac{\lambda}{P_1} & -1 & -1 & \cdots & -1 \\ -\frac{Q_1}{P_1}+\frac{\lambda}{P_1} & \frac{Q_2}{P_2}-\frac{\lambda}{P_2} & 0 & \cdots & 0 \\ \vdots & 0 & \ddots & \ddots & \vdots \\ \vdots & \vdots & \ddots & \ddots & 0 \\ -\frac{Q_1}{P_1}+\frac{\lambda}{P_1} & 0 & \cdots & 0 & \frac{Q_n}{P_n}-\frac{\lambda}{P_n} \end{vmatrix}$$

With $A=1-\frac{1}{\frac{Q_1}{P_1}-\frac{\lambda}{P_1}}$,

$$\det(J-\lambda I_n)=(\Pi_{i=1}^n P_i)\left(\frac{Q_1}{P_1}-\frac{\lambda}{P_1}\right)\begin{vmatrix} A & -1 & -1 & \cdots & -1 \\ -1 & \frac{Q_2}{P_2}-\frac{\lambda}{P_2} & 0 & \cdots & 0 \\ \vdots & 0 & \ddots & \ddots & \vdots \\ \vdots & \vdots & \ddots & \ddots & 0 \\ -1 & 0 & \cdots & 0 & \frac{Q_n}{P_n}-\frac{\lambda}{P_n} \end{vmatrix}$$

With $B_i=\frac{Q_i}{P_i}-\frac{\lambda}{P_i}$,

$$\det(J-\lambda I_n)=(\Pi_{i=1}^n P_i)\,B_1\begin{vmatrix} A & -1 & -1 & \cdots & -1 \\ -1 & B_2 & 0 & \cdots & 0 \\ \vdots & 0 & \ddots & \ddots & \vdots \\ \vdots & \vdots & \ddots & \ddots & 0 \\ -1 & 0 & \cdots & 0 & B_n \end{vmatrix}$$

For $n\geq 2$, let

$$L_n = \begin{vmatrix} A & -1 & \cdots & \cdots & -1 \\ -1 & B_2 & 0 & \cdots & 0 \\ -1 & 0 & B_3 & \cdots & 0 \\ \vdots & 0 & \cdots & \ddots & 0 \\ -1 & 0 & \cdots & 0 & B_n \end{vmatrix}$$

By developing with respect to the last column, $L_n = B_n L_{n-1} - (-1)^{n-1} C_{n-1}$, where

$$C_{n-1} = \begin{vmatrix} -1 & \cdots & \cdots & \cdots & -1 \\ B_2 & 0 & \cdots & \cdots & 0 \\ 0 & B_3 & 0 & \cdots & 0 \\ \vdots & \ddots & \ddots & \ddots & 0 \\ 0 & \cdots & 0 & B_{n-1} & 0 \end{vmatrix}$$

By developing with respect to the last row, $C_{n-1} = -B_{n-1} C_{n-2}$ for $n \geq 4$. Since $C_2 = \begin{vmatrix} -1 & -1 \\ B_2 & 0 \end{vmatrix} = B_2$, by induction $C_n = (-1)^n \Pi_{i=2}^n B_i$.

Therefore, $L_n = B_n L_{n-1} - \Pi_{i=2}^{n-1} B_i$ for $n \geq 3$. Since $L_2 = \begin{vmatrix} A & -1 \\ -1 & B_2 \end{vmatrix} = AB_2 - 1$, it can be shown by induction that

$$L_n = A\Pi_{i=2}^n B_i - \Sigma_{i=2}^n \Pi_{j=2, j\neq i}^n B_j, \text{ for } n \geq 2$$

Since $AB_1 = B_1 - 1$,

$$B_1 L_n = (B_1 - 1)\,\Pi_{i=2}^n B_i - B_1 \Sigma_{i=2}^n \Pi_{j=2, j\neq i}^n B_j = \Pi_{j=1}^n B_j - \Sigma_{i=1}^n \Pi_{j=1, j\neq i}^n B_j,$$

for $n \geq 2$.

Thus, $\det(J - \lambda I_n) = (\Pi_{i=1}^n P_i)\left(\Pi_{j=1}^n B_j - \Sigma_{i=1}^n \Pi_{j=1, j\neq i}^n B_j\right)$, and any eigenvalue λ of J satisfies

$$P(\lambda) = \Sigma_{i=1}^{n} \Pi_{j=1, j\neq i}^{n} B_j - \Pi_{j=1}^{n} B_j = 0, \tag{8.4}$$

with $B_i = \frac{Q_i}{P_i} - \frac{\lambda}{P_i}$. Suppose without loss of generality that Q_n and Q_{n-1} are respectively the largest and second-largest Q_i. Suppose in addition that these largest values are unique (the case where they are not will be dealt with below). Then $P(Q_n)$ has the same sign as $(-1)^{n-1}$, and $P(Q_{n-1})$ has the same sign as $(-1)^n$. Thus, $\exists\ t \in]Q_{n-1}, Q_n[$ s.t. $P(t) = 0$. Therefore, at any stable steady-state, $Q_{n-1} < 0$, and therefore $\forall\ i \neq n,\ Q_i < 0$, meaning

$$d_i \left(1 - 2\beta_i x_i\right) < 0$$

$$\forall\ i < n,\ x_i > \frac{1}{2\beta_i} = \frac{r_i}{2} \tag{8.5}$$

Therefore, at any stable steady-state, any x_i with $i < n$ is at the higher solution of equation 8.2, and

$$\forall\ i < n,\ x_i = \frac{r_i + \sqrt{r_i^2 - 4\alpha D^2}}{2}$$

If Q_n or Q_{n-1} are not unique in the re-numbering scheme discussed above, then the nonunique value is a root of P and hence cannot be positive. Therefore at most one Q_i can be positive and it is possible to renumber for a non-strict version of inequality 8.5 to hold. Strictness follows follows since $\alpha \neq 0$.

In a stable steady state, "$\kappa \neq \kappa'$"

We now show that there is no stable steady state with $r_n = \max_i r_i$. Suppose that $Q_n > 0$, $Q_{n-1} < 0$, and $r_n = \max_i r_i$. Then

$$P(0) = \Pi_{j\neq n} Q_j/P_j + Q_n/P_n \Sigma_{i=1}^{n-1} \Pi_{j=1, j\neq i}^{n-1} Q_j/P_j - \Pi_{j=1}^{n} Q_j/P_j$$

$$P(0) = \left(\Pi_{j\neq n} Q_j/P_j + Q_n/P_n \Pi_{j=1}^{n-2} Q_j/P_j\right) + Q_n/P_n \Sigma_{i=1}^{n-2} \Pi_{j=1, j\neq i}^{n-1} Q_j/P_j - \Pi_{j=1}^{n} Q_j/P_j$$

$$P(0) = (Q_{n-1}/P_{n-1} + Q_n/P_n)\,\Pi_{j=1}^{n-2} Q_j/P_j + Q_n/P_n \Sigma_{i=1}^{n-2} \Pi_{j=1, j\neq i}^{n-1} Q_j/P_j - \Pi_{j=1}^{n} Q_j/P_j$$

The last two terms in the sum both have the same sign as $(-1)^n$.

Now consider

$$\frac{Q_n}{P_n}\frac{P_{n-1}}{Q_{n-1}} = \frac{1 - 2\beta_n x_n}{1 - 2\beta_{n-1} x_{n-1}}\frac{\beta_{n-1}}{\beta_n}$$

$$\frac{Q_n}{P_n}\frac{P_{n-1}}{Q_{n-1}} = -\frac{\sqrt{1 - 4\alpha D^2 \beta_n^2}}{\sqrt{1 - 4\alpha D^2 \beta_{n-1}^2}}\frac{\beta_{n-1}}{\beta_n}$$

By hypothesis, $\frac{\beta_{n-1}}{\beta_n} \geq 1$, and thus

$$Q_n/P_n \geq |Q_{n-1}/P_{n-1}|$$

Therefore, $P(0)$ has the same sign as $(-1)^n$. Since $P(Q_n)$ has the same sign as $(-1)^{n-1}$, P has a positive root, and the steady state is unstable.

8.4 Discussion

The results above show that, in the case where degradation and normalized synthesis rates are allowed to be different for each element of the network, it becomes more difficult for the system to sustain the co-expression of many elements. Indeed, equation 8.3 implies that the weakest element (in terms of the ratio of the maximal synthesis rate to the product of the degradation rate and the dissociation constant for heterodimer formation with class A proteins) that is "on" cannot be much weaker than the other ones which are being co-expressed (an intuitive result, since a weak element would be too easily repressed by the other ones, and would not stay "on" in their presence). In addition to that, the competition level α restricts the number of elements which can be co-expressed, in the same way as when degradation and normalized synthesis rates are all equal.

It is particularly noteworthy that in the course of cellular differentiation, antagonistic genes are often co-expressed early-on despite their antagonism, before one gradually takes over (as discussed by Cinquin & Demongeot, 2005). It has been proposed that the differentiation of some cell-types has a stochastic aspect, but in many instances, extra-cellular cues play an essential role in controlling cell-fate, although the details of the pathway from extra-cellular cue to intrinsic differentiation determinants are not always clear. Interestingly, the synthesis and degradation rates of key transcription factors have been shown in different instances to be regulated (see Ebert et al., 2003, Lim & Choi, 2004, zur Lage et al., 2004, for examples of regulated synthesis rates, and Horwitz, 1996, Trott et al., 2001, Sriuranpong et al., 2002, Viñals et al., 2004, for examples of regulated degradation rates). The activity of transcription factors can be directly regulated by post-translational modifications such as phosphorylation (for example phosphorylation of myogenic factors can decrease their activity, Winter et al., 1993, Zhou & Olson, 1994, Suelves et al., 2004, and this can also be the case for class A proteins, Page et al., 2004), by physical interactions with other proteins (Bengal et al., 1992, Perry et al., 2001), or indirectly by affecting cofactors (Simone et al., 2004, Seo et al., 2005). Phosphorylation can also modulate the propensity of bHLH proteins to form heterodimers (this can be the case for class B proteins, Firulli et al., 2003, class A proteins, Sloan et al., 1996, Lluis et al., 2005, and also Id proteins, Hara et al., 1997, Deed et al., 1997). It seems to generally be the case that upon cell differentiation, the activity of transcription factors associated with the cell-fate is enhanced.

Within the framework proposed here, the biasing of complex cell-fate decisions to specific outcomes can be mediated by the up- or down-regulation of synthesis rates or affinity for common class A activators, or down- or up-regulation of degradation rates, for favored and unfavored outcomes, respectively. Different signaling pathways can act on one or many factors and do not need to directly cross-talk, as all the inputs are integrated by the competition

between the switch elements.

The result of the decision can be regulated by the synthesis, class A-affinities, and degradation rates of the switch elements, while its timing is dependent on the level of competition in the system: an increase in the competition level, which can for example be mediated by an increase in Id protein expression (shown in many experimental contexts, see references in Cinquin & Demongeot, 2005) sequestering the common activator away from all the elements of the switch, will force the weakest elements to be turned off. The efficiency with which Id proteins sequester the common activator can also be modulated by phosphorylation, which can also just be modeled by a change in the quantity of common activator available for switch elements. Some Id proteins, despite being paradoxically called "Inhibitors of differentiation", have indeed been shown recently to drive tumor-suppression and differentiation (Russell et al., 2004, Yu et al., 2005), as suggested by Cinquin & Demongeot (2005).

There is a great variety of ways in which a switch network can be led from a state of co-expression of all its elements to a state where only one is expressed, by a change in the competition level and in the synthesis and degradation rates. We show here two numerical simulations, to illustrate equation 8.3. In Figure 8.1, the competition level is increased, in a network in which elements have different normalized synthesis to degradation ratios; the weakest non-zero element is turned off every time the competition reaches a threshold. In Figure 8.2, the competition level is kept constant, but one element is made progressively stronger, and turns off all the other ones. Of course, the alteration of all parameters at the same time would be a plausible biological situation.

The networks studied here have been described in the context of class A and class B bHLH heterodimerization, but they could have a much wider relevance. Hox proteins, crucial determinants of tissue identity, have been shown to depend heavily on common binding partners of the PBC and Meis families (Mann & Affolter, 1998). A subfamily of bHLH-leucine zipper proteins

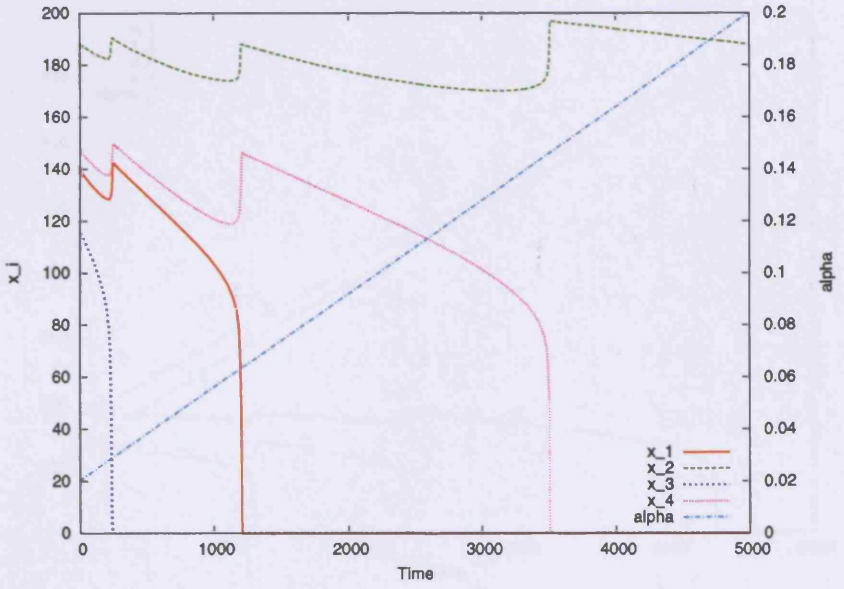

Figure 8.1: Simulation of a 4-dimensional switch defined by equations 8.1; the competition parameter α is progressively increased, causing the weakest non-0 element to be switched off periodically. Specific parameters are $d_i = 1$ for all i, $\sigma_1 = 190$, $\sigma_2 = 226$, $\sigma_3 = 177$, and $\sigma_4 = 195$.

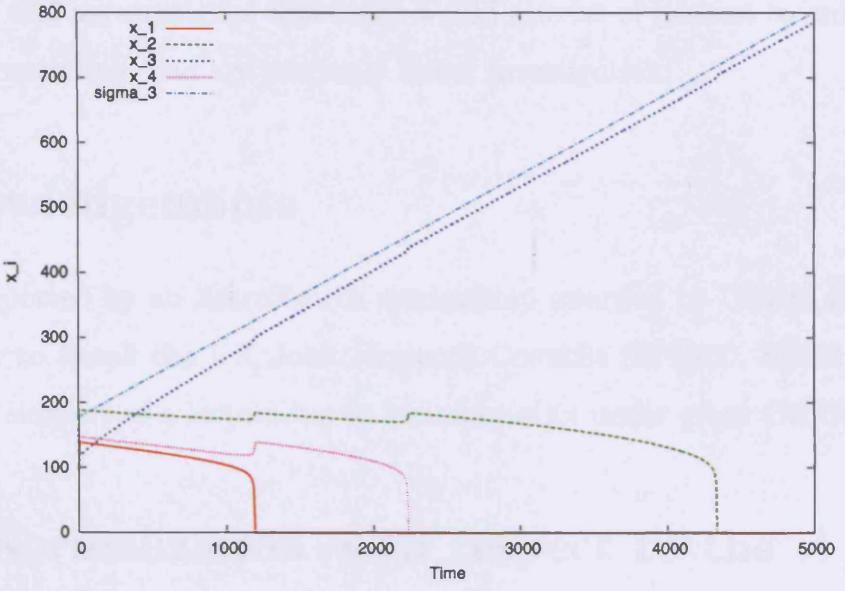

Figure 8.2: Simulation of a 4-dimensional switch defined by equations 8.1; the synthesis rate for x_3 is progressively increased, causing all other elements to be successively switched off. Other synthesis and degradation rates are as in Figure 6.5, and the competition rate $\alpha = 0.02$.

shows tissue-specific expression, homo- and hetero-dimerization, and alternative splicing of dominant-negative forms (Kuiper et al., 2004). Myc and Max, which have opposite roles on cell growth and proliferation, form homodimers and heterodimers with Mad, with different affinities (Grinberg et al., 2004).

Networks in which each element needs to repress all others can easily be created with competition for a common heterodimerization partner, rather than active repression of all other elements. Networks including other forms of cross-repression and asymmetrical topologies would also be of interest to study cellular differentiation, and are currently under investigation.

Acknowledgements

OC is supported by an AstraZeneca studentship awarded by CoMPLEX. KP would like to thank the UK Joint Research Councils (EPSRC, BBSRC, and MRC) for support of a lectureship in bioinformatics under grant GR/R47455.

8.5 Normalization with respect to the $A - B_i$ dissociation constants

Supposing the $A - B_i$ dimerization reactions are at equilibrium, using the law of mass action one gets

$$[AB_i] = \frac{a_t[B_i]/D_i}{1 + \Sigma_j[B_j]/D_j},$$

where D_i is the dissociation constant for each $A - B_i$ complex, and a_t is the total quantity of A. If the synthesis of B_i depends on the concentration of the $A - B_i$ complex, in a non-linear fashion described by a Hill function of degree 2 with maximal value σ_i and half-maximal synthesis for $[AB_i] = K_2$, and B_i has a degradation rate d_i, writing $x_i = [B_i]$ one gets

$$\frac{\mathrm{d}x_i}{\mathrm{d}t} = -d_i x_i + \sigma_i \frac{[AB_i]^2}{K_2^2 + [AB_i]^2}$$

Now let $y_i = x_i/D_i$. Then

$$\frac{\mathrm{d}y_i}{\mathrm{d}t} = \frac{1}{D_i}\frac{\mathrm{d}x_i}{\mathrm{d}t} = -d_i y_i + \frac{\sigma_i}{D_i}\frac{y_i^2}{\alpha D^2 + y_i^2},$$

with $D = 1 + \Sigma_{i=1}^n y_i$, $\alpha = K_2^2/a_t^2 \in \mathbb{R}_*^+$.

The normalization with respect to the dissociation constants D_i has thus led to the replacement of each maximal synthesis rate σ_i by σ_i/D_i.

8.6 Stronger inequality when no x_i is at the "lower solution"

If all x_is are given by the higher root of equation 8.2, one gets

$$2(D-1) = \Sigma_i r_i + \sqrt{r_i^2 - 4\alpha D^2}$$

$$\Sigma_i r_i + 2 = 2D - \Sigma_i \sqrt{r_i^2 - 4\alpha D^2}$$

With the same argument as previously,

$$\frac{r_s}{\sqrt{\alpha}} \geq 2 + \Sigma_i r_i + \Sigma_i \sqrt{r_i^2 - r_s^2}, \tag{8.6}$$

with $r_s = \min_i r_i$.

Chapter 9

Conclusion

The model for somitogenesis presented in Chapter 2 proposes a molecular mechanism for the oscillations in the PSM which is different from that which is commonly accepted. The model proposed here is based on positive feedback, but it is also compatible with all the experimental data interpreted as supporting a negative feedback mechanism (some of which was made available after Chapter 2 was published), as well as with experimental data providing direct evidence against a negative-feedback mechanism.

Many experimentally-testable predictions can be made from the model. However, not all necessary experimental tools are presently available, and an attempt was made to develop them over the past three years. The first tool is a light-inducible gene expression system. Such a tool would be of considerable interest for spatially and temporally manipulating biological systems, well beyond the scope of the experiments discussed in this thesis. Preliminary results have shown reporter induction by a factor of about three, which is a proof of principle, but probably would not be sufficient to obtain easily-interpretable results. A limitation of the system seems to be that it induces photosensitisation, probably because of the accumulation of molecules which generate free radicals or reactive oxygen species when illuminated. It might be possible to improve the system by fine-tuning the quantity of these molecules, using anti-oxidants,

or temporarily depriving the cells of oxygen; all of which have been attempted but, due to time limitations, not in exhaustivity.

The second tool is a real-time reporter of the somitogenesis clock. This was created using the lunatic fringe promoter and a luciferase reporter. Unfortunately, this reporter interferes with somitogenesis, possibly because it introduces a great number of exogenous binding sites for the transcription factors involved in the clock (this is a limitation of the technique of electroporation, which is the most readily available one for misexpression in chick). Another way to deliver the reporter, based on a lentivirus, is under development. Other model systems, such as mouse or zebrafish, more readily allow the generation of transgenic animals; the problem with these animals, however, is that manipulation and culture of the embryos is not so straightforward.

While it would have been ideal to have experimental data to test the model for the somitogenesis clock, and invalidate or refine it, the model does show the usefulness of mathematical modeling in biology, because it makes predictions which it would have been all but impossible to reach based on sheer intuition, and which relate to the heart of the biological mechanism.

Similarly, Chapter 5 is based on a set of experimental data, and proposes a new model for the establishment of morphogen gradients, whose molecular base can be experimentally tested. That model deals with molecular interactions between morphogens, receptors, and glycoproteins; it has become clear recently that glycoproteins play an essential role, but that role is only partially understood. The model is limited by the absence of quantitative details about the molecular interactions, but it shows that it would be extremely interesting to acquire such data, which was not previously obvious, and thus suggests an original experimental approach.

The study of networks controling cellular differentiation, presented in Chapters 6 and 8, is a different sort of modeling, in that it is not based on one specific biological system, but tries to extract essential properties from a wide set of

systems, to investigate their generic properties. One such property of particular interest is the coexpression of antagonistic genes at low levels. It is shown that the generic networks which come most readily to mind to model cellular differentiation cannot in fact account for that property easily. However, bHLH networks, in which elements are competing for access to a common co-activator, have a much broader range of behaviours: the level of competition (which depends on the total quantity of co-activator) determines the number of elements which can be coexpressed, through a rule whose simplicity is surprising: for k coexpressed elements, the level of competition α must be such that $\alpha \leq 1/k^2$. The element expressed most strongly can be selected by increasing the competition level. There is a memory effect, because the level of competition can be brought back to its initial level without turning back on the elements which were switched off.

This "top-down" approach is more abstract than those described in the previous two chapters but it still allows one to derive predictions. In particular, it suggests that the role the Inhibitors of Differentiation proteins (Id) is to tune the level of competition, and that they are much more than mere inhibitors of differentiation: if their role is to reduce the number of fates available to cells by increasing competition, they are in fact necessary for differentiation. A few experimental results published after Chapter 6 confirm that prediction, by showing that that the absence of Id proteins can in certain cases block differentiation. Interestingly, the transient increase in the expression level of Id proteins, observed during the differentiation of a number of independent cell-lines, had so far received no explanation.

Finally, it is interesting to note that many of the genes involved in the somitogenesis clock are bHLH proteins, and it has been shown that their products heterodimerise. They are of a different class than that considered for bHLH networks, and the results derived about those networks probably do not apply directly, but it is a strong possibility that there are competitive heterodimeri-

sation phenomena contributing to the somitogenesis oscillations, particularly since it has recently been shown that the mRNA for one of these proteins is expressed in a gradient in the PSM.

Future work

The mathematical models developed throughout this thesis are based on ordinary differential equations, and do not take into account noise which appears when single-molecule reactions are considered; the reasons for this are computational costs involved with simulations, as well as the great difficulty of deriving analytical results from probabilistic equations. It would prove interesting to study how the analytical results derived here hold up to the introduction of noise and delays.

All the theoretical Chapters in this thesis not only explain current experimental data. but also suggest direct experimental tests. It would prove particularly interesting to carry out those tests, to validate and refine the models.

Bibliography

Adam GI, Miller SJ, Ullerås E & Franklin GC (1996) Cell-type-specific modulation of PDGF-B regulatory elements via viral enhancer competition: a caveat for the use of reference plasmids in transient transfection assays. *Gene* **178**(1-2): pp. 25–9.

Akashi K, He X, Chen J, Iwasaki H, Niu C, Steenhard B, Zhang J, Haug J & Li L (2003) Transcriptional accessibility for genes of multiple tissues and hematopoietic lineages is hierarchically controlled during early hematopoiesis. *Blood* **101**(2): pp. 383–9.

Akashi K, Traver D, Miyamoto T & Weissman IL (2000) A clonogenic common myeloid progenitor that gives rise to all myeloid lineages. *Nature* **404**(6774): pp. 193–7.

Amoutzias GD, Robertson DL, Oliver SG & Bornberg-Bauer E (2004) Convergent evolution of gene networks by single-gene duplications in higher eukaryotes. *EMBO Rep* **5**(3): pp. 274–279.

Ando H, Furuta T, Tsien RY & Okamoto H (2001) Photo-mediated gene activation using caged RNA/DNA in zebrafish embryos. *Nat Genet* **28**(4): pp. 317–25.

Andres-Barquin PJ, Hernandez MC, Hayes TE, McKay RD & Israel MA (1997) Id genes encoding inhibitors of transcription are expressed during in vitro

astrocyte differentiation and in cell lines derived from astrocytic tumors. *Cancer Res* **57**(2): pp. 215–20.

Andrews JM, Newbound GC & Lairmore MD (1997) Transcriptional modulation of viral reporter gene constructs following induction of the cellular stress response. *Nucleic Acids Res* **25**(5): pp. 1082–4.

Artavanis-Tsakonas S, Rand MD & Lake RJ (1999) Notch signaling: cell fate control and signal integration in development. *Science* **284**(5415): pp. 770–6.

Aulehla A, Wehrle C, Brand-Saberi B, Kemler R, Gossler A, Kanzler B & Herrmann BG (2003) Wnt3a plays a major role in the segmentation clock controlling somitogenesis. *Dev Cell* **4**(3): pp. 395–406.

Baeg GH, Lin X, Khare N, Baumgartner S & Perrimon N (2001) Heparan sulfate proteoglycans are critical for the organization of the extracellular distribution of Wingless. *Development* **128**(1): pp. 87–94.

Baeg GH, Selva EM, Goodman RM, Dasgupta R & Perrimon N (2004) The Wingless morphogen gradient is established by the cooperative action of Frizzled and Heparan Sulfate Proteoglycan receptors. *Dev Biol* **276**(1): pp. 89–100.

Barolo S & Levine M (1997) hairy mediates dominant repression in the Drosophila embryo. *EMBO J* **16**(10): pp. 2883–91.

Barrantes IB, Elia AJ, Wünsch K, De Angelis MH, Mak TW, Rossant J, Conlon RA, Gossler A & de la Pompa JL (1999) Interaction between Notch signalling and Lunatic fringe during somite boundary formation in the mouse. *Curr Biol* **9**(9): pp. 470–80.

Battiston L, Passamonti S, Macagno A & Sottocasa GL (1998) The bilirubin-binding motif of bilitranslocase and its relation to conserved motifs in ancient biliproteins. *Biochem Biophys Res Commun* **247**(3): pp. 687–92.

Belenkaya TY, Han C, Yan D, Opoka RJ, Khodoun M, Liu H & Lin X (2004) Drosophila dpp morphogen movement is independent of dynamin-mediated endocytosis but regulated by the glypican members of heparan sulfate proteoglycans. *Cell* **119**(2): pp. 231–44.

Benezra R, Davis RL, Lockshon D, Turner DL & Weintraub H (1990) The protein Id: a negative regulator of helix-loop-helix DNA binding proteins. *Cell* **61**(1): pp. 49–59.

Bengal E, Ransone L, Scharfmann R, Dwarki VJ, Tapscott SJ, Weintraub H & Verma IM (1992) Functional antagonism between c-Jun and MyoD proteins: a direct physical association. *Cell* **68**(3): pp. 507–19.

Bessho Y, Hirata H, Masamizu Y & Kageyama R (2003) Periodic repression by the bHLH factor Hes7 is an essential mechanism for the somite segmentation clock. *Genes Dev* **17**(12): pp. 1451–6.

Bessho Y, Miyoshi G, Sakata R & Kageyama R (2001a) Hes7: a bhlh-type repressor gene regulated by notch and expressed in the presomitic mesoderm. *Genes Cells* **6**(2): pp. 175–85.

Bessho Y, Sakata R, Komatsu S, Shiota K, Yamada S & Kageyama R (2001b) Dynamic expression and essential functions of hes7 in somite segmentation. *Genes Dev* **15**(20): pp. 2642–7.

Blackshaw SE & Warner AE (1976) Low resistance junctions between mesoderm cells during development of trunk muscles. *J Physiol* **255**(1): pp. 209–30.

Blair SS (2000) Notch signaling: Fringe really is a glycosyltransferase. *Curr Biol* **10**(16): pp. R608–12.

Blau HM & Baltimore D (1991) Differentiation requires continuous regulation. *J Cell Biol* **112**(5): pp. 781–3.

Blau HM & Blakely BT (1999) Plasticity of cell fate: insights from heterokaryons. *Semin Cell Dev Biol* **10**(3): pp. 267–72.

Blau HM, Pavlath GK, Hardeman EC, Chiu CP, Silberstein L, Webster SG, Miller SC & Webster C (1985) Plasticity of the differentiated state. *Science* **230**(4727): pp. 758–66.

Briscoe J, Chen Y, Jessell TM & Struhl G (2001) A hedgehog-insensitive form of patched provides evidence for direct long-range morphogen activity of sonic hedgehog in the neural tube. *Mol Cell* **7**(6): pp. 1279–91.

Briscoe J, Pierani A, Jessell TM & Ericson J (2000) A homeodomain protein code specifies progenitor cell identity and neuronal fate in the ventral neural tube. *Cell* **101**(4): pp. 435–45.

Brown G, Bunce CM, Lord JM & McConnell FM (1988) The development of cell lineages: a sequential model. *Differentiation* **39**(2): pp. 83–9.

Brunet JF & Ghysen A (1999) Deconstructing cell determination: proneural genes and neuronal identity. *Bioessays* **21**(4): pp. 313–8.

Cadigan KM (2002) Regulating morphogen gradients in the Drosophila wing. *Semin Cell Dev Biol* **13**(2): pp. 83–90.

Camerin M, Rodgers MA, Kenney ME & Jori G (2005) Photothermal sensitisation: evidence for the lack of oxygen effect on the photosensitising activity. *Photochem Photobiol Sci* **4**(3): pp. 251–3.

Caprioli A, Goitsuka R, Pouget C, Dunon D & Jaffredo T (2002) Expression of Notch genes and their ligands during gastrulation in the chicken embryo. *Mech Dev* **116**(1-2): pp. 161–4.

Chambers RC, Leoni P, Kaminski N, Laurent GJ & Heller RA (2003) Global expression profiling of fibroblast responses to transforming growth factor-beta1

reveals the induction of inhibitor of differentiation-1 and provides evidence of smooth muscle cell phenotypic switching. *Am J Pathol* **162**(2): pp. 533–46.

Chapman SC, Lawson A, Macarthur WC, Wiese RJ, Loechel RH, Burgos-Trinidad M, Wakefield JK, Ramabhadran R, Mauch TJ & Schoenwolf GC (2005) Ubiquitous GFP expression in transgenic chickens using a lentiviral vector. *Development* **132**(5): pp. 935–40.

Chen CY & Shyu AB (1995) AU-rich elements: characterization and importance in mRNA degradation. *Trends Biochem Sci* **20**(11): pp. 465–70.

Chen H, Zhang P, Radomska HS, Hetherington CJ, Zhang DE & Tenen DG (1996) Octamer binding factors and their coactivator can activate the murine PU.1 (spi-1) promoter. *J Biol Chem* **271**(26): pp. 15743–52.

Chen MH, Li YJ, Kawakami T, Xu SM & Chuang PT (2004) Palmitoylation is required for the production of a soluble multimeric Hedgehog protein complex and long-range signaling in vertebrates. *Genes Dev* **18**(6): pp. 641–59.

Cherry JL & Adler FR (2000) How to make a biological switch. *J Theor Biol* **203**(2): pp. 117–33.

Chiang MK & Melton DA (2003) Single-cell transcript analysis of pancreas development. *Dev Cell* **4**(3): pp. 383–93.

Chien CT, Hsiao CD, Jan LY & Jan YN (1996) Neuronal type information encoded in the basic-helix-loop-helix domain of proneural genes. *Proc Natl Acad Sci U S A* **93**(23): pp. 13239–44.

Chou TB & Perrimon N (1992) Use of a yeast site-specific recombinase to produce female germline chimeras in drosophila. *Genetics* **131**(3): pp. 643–53.

Cinquin O (2003) Is the somitogenesis clock really cell-autonomous? A coupled-oscillator model of segmentation. *J Theor Biol* **224**(4): pp. 459–68.

Cinquin O & Demongeot J (2002) Positive and negative feedback: striking a balance between necessary antagonists. *J Theor Biol* **216**(2): pp. 229–41.

Cinquin O & Demongeot J (2005) High-dimensional switches and the modelling of cellular differentiation. *J Theor Biol* **233**(3): pp. 391–411.

Cinquin O & Page KM (????) Generalized, switch-like competitive heterodimerization networks *(submitted)* .

Cole SE, Levorse JM, Tilghman SM & Vogt TF (2002) Clock regulatory elements control cyclic expression of Lunatic fringe during somitogenesis. *Dev Cell* **3**(1): pp. 75–84.

Collier JR, Mcinerney D, Schnell S, Maini PK, Gavaghan DJ, Houston P & Stern CD (2000) A cell cycle model for somitogenesis: mathematical formulation and numerical simulation. *J Theor Biol* **207**(3): pp. 305–16.

Collier JR, Monk NA, Maini PK & Lewis JH (1996) Pattern formation by lateral inhibition with feedback: a mathematical model of delta-notch intercellular signalling. *J Theor Biol* **183**(4): pp. 429–46.

Cooke J (1998) A gene that resuscitates a theory–somitogenesis and a molecular oscillator. *Trends Genet* **14**(3): pp. 85–8.

Cooke J & Zeeman EC (1976) A clock and wavefront model for control of the number of repeated structures during animal morphogenesis. *J Theor Biol* **58**(2): pp. 455–76.

Cory S (1999) Immunology. Wavering on commitment. *Nature* **401**(6753): pp. 538–9.

Cox David A., Little John B. & O'Shea Don (1996) *Ideals, Varieties, and Algorithms* NY: Springer-Verlag 2nd edn. 536 pages.

Crittenden SL, Bernstein DS, Bachorik JL, Thompson BE, Gallegos M, Petcherski AG, Moulder G, Barstead R, Wickens M & Kimble J (2002) A conserved RNA-binding protein controls germline stem cells in Caenorhabditis elegans. *Nature* **417**(6889): pp. 660–3.

Cross MA & Enver T (1997) The lineage commitment of haemopoietic progenitor cells. *Curr Opin Genet Dev* **7**(5): pp. 609–13.

Dale JK, Maroto M, Dequeant ML, Malapert P, McGrew M & Pourquié O (2003) Periodic notch inhibition by lunatic fringe underlies the chick segmentation clock. *Nature* **421**(6920): pp. 275–8.

Dale KJ & Pourquie O (2000) A clock-work somite. *Bioessays* **22**(1): pp. 72–83.

Davis SJ, Bhoo SH, Durski AM, Walker JM & Vierstra RD (2001) The heme-oxygenase family required for phytochrome chromophore biosynthesis is necessary for proper photomorphogenesis in higher plants. *Plant Physiol* **126**(2): pp. 656–69.

Deed RW, Hara E, Atherton GT, Peters G & Norton JD (1997) Regulation of Id3 cell cycle function by Cdk-2-dependent phosphorylation. *Mol Cell Biol* **17**(12): pp. 6815–21.

Delbrück M (1949) Unités biologiques douées de continuité génétique *Colloq. Int. C.N.R.S.* **8**: pp. 33–35.

Delfini MC, Dubrulle J, Malapert P, Chal J & Pourquié O (2005) Control of the segmentation process by graded MAPK/ERK activation in the chick embryo. *Proc Natl Acad Sci U S A* **102**(32): pp. 11343–8.

Doctor JS, Jackson PD, Rashka KE, Visalli M & Hoffmann FM (1992) Sequence, biochemical characterization, and developmental expression of a new member of the TGF-beta superfamily in Drosophila melanogaster. *Dev Biol* **151**(2): pp. 491–505.

Dubrulle J, McGrew MJ & Pourquie O (2001) FGF signaling controls somite boundary position and regulates segmentation clock control of spatiotemporal Hox gene activation. *Cell* **106**(2): pp. 219–32.

Dubrulle J & Pourquié O (2004) fgf8 mRNA decay establishes a gradient that couples axial elongation to patterning in the vertebrate embryo. *Nature* **427**(6973): pp. 419–22.

Dunwoodie SL, Clements M, Sparrow DB, Sa X, Conlon RA & Beddington RS (2002) Axial skeletal defects caused by mutation in the spondylocostal dysplasia/pudgy gene Dll3 are associated with disruption of the segmentation clock within the presomitic mesoderm. *Development* **129**(7): pp. 1795–806.

Dyson S & Gurdon JB (1998) The interpretation of position in a morphogen gradient as revealed by occupancy of activin receptors. *Cell* **93**(4): pp. 557–68.

Ebert PJ, Timmer JR, Nakada Y, Helms AW, Parab PB, Liu Y, Hunsaker TL & Johnson JE (2003) Zic1 represses Math1 expression via interactions with the Math1 enhancer and modulation of Math1 autoregulation. *Development* **130**(9): pp. 1949–59.

Ebrahimi FA, Edmondson J, Rothstein R & Chess A (2000) YAC transgene-mediated olfactory receptor gene choice. *Dev Dyn* **217**(2): pp. 225–31.

Eggan K, Baldwin K, Tackett M, Osborne J, Gogos J, Chess A, Axel R & Jaenisch R (2004) Mice cloned from olfactory sensory neurons. *Nature* **428**(6978): pp. 44–9.

Eichenberg K, Kunkel T, Kretsch T, Speth V & Schäfer E (1999) In vivo characterization of chimeric phytochromes in yeast. *J Biol Chem* **274**(1): pp. 354–9.

Eldar A, Rosin D, Shilo BZ & Barkai N (2003) Self-enhanced ligand degradation underlies robustness of morphogen gradients. *Dev Cell* **5**(4): pp. 635–46.

Elich TD & Chory J (1997) Biochemical characterization of Arabidopsis wild-type and mutant phytochrome B holoproteins. *Plant Cell* **9**(12): pp. 2271–80.

Ellis HM, Spann DR & Posakony JW (1990) extramacrochaetae, a negative regulator of sensory organ development in Drosophila, defines a new class of helix-loop-helix proteins. *Cell* **61**(1): pp. 27–38.

Ellis RE & Kimble J (1995) The fog-3 gene and regulation of cell fate in the germ line of Caenorhabditis elegans. *Genetics* **139**(2): pp. 561–77.

Eloy-Trinquet S & Nicolas JF (2002) Cell coherence during production of the presomitic mesoderm and somitogenesis in the mouse embryo. *Development* **129**(15): pp. 3609–19.

Elsdale T, Pearson M & Whitehead M (1976) Abnormalities in somite segmentation following heat shock to Xenopus embryos. *J Embryol Exp Morphol* **35**(3): pp. 625–35.

Enver T & Greaves M (1998) Loops, lineage, and leukemia. *Cell* **94**(1): pp. 9–12.

Fang B, Ji L, Bouvet M & Roth JA (1998) Evaluation of GAL4/TATA in vivo. Induction of transgene expression by adenovirally mediated gene codelivery. *J Biol Chem* **273**(9): pp. 4972–5.

Feng J, White B, Tyurina OV, Guner B, Larson T, Lee HY, Karlstrom RO & Kohtz JD (2004) Synergistic and antagonistic roles of the Sonic hedgehog N- and C-terminal lipids. *Development* **131**(17): pp. 4357–70.

Firulli BA, Howard MJ, McDaid JR, McIlreavey L, Dionne KM, Centonze VE, Cserjesi P, Virshup DM & Firulli AB (2003) PKA, PKC, and the Protein

Phosphatase 2A Influence HAND Factor Function. A Mechanism for Tissue-Specific Transcriptional Regulation. *Mol Cell* **12**(5): pp. 1225–37.

Foote CS (1968) Mechanisms of photosensitized oxidation. There are several different types of photosensitized oxidation which may be important in biological systems. *Science* **162**(857): pp. 963–70.

Forsberg H, Crozet F & Brown NA (1998) Waves of mouse Lunatic fringe expression, in four-hour cycles at two-hour intervals, precede somite boundary formation. *Curr Biol* **8**(18): pp. 1027–30.

Fotakis G & Timbrell JA (2005) In vitro cytotoxicity assays: Comparison of LDH, neutral red, MTT and protein assay in hepatoma cell lines following exposure to cadmium chloride. *Toxicol Lett* .

Frankenberg N, Moser J & Jahn D (2003) Bacterial heme biosynthesis and its biotechnological application. *Appl Microbiol Biotechnol* **63**(2): pp. 115–27.

Freeman M & Gurdon JB (2002) Regulatory principles of developmental signaling. *Annu Rev Cell Dev Biol* **18**: pp. 515–39.

Freitas C, Rodrigues S, Charrier JB, Teillet MA & Palmeirim I (2001) Evidence for medial/lateral specification and positional information within the presomitic mesoderm. *Development* **128**(24): pp. 5139–47.

Gabdoulline RR & Wade RC (1997) Simulation of the diffusional association of barnase and barstar. *Biophys J* **72**(5): pp. 1917–29.

Gajewski M, Sieger D, Alt B, Leve C, Hans S, Wolff C, Rohr KB & Tautz D (2003) Anterior and posterior waves of cyclic her1 gene expression are differentially regulated in the presomitic mesoderm of zebrafish. *Development* **130**(18): pp. 4269–78.

Galbraith R (1999) Heme oxygenase: who needs it? *Proc Soc Exp Biol Med* **222**(3): pp. 299–305.

Gambetta GA & Lagarias JC (2001) Genetic engineering of phytochrome biosynthesis in bacteria. *Proc Natl Acad Sci U S A* **98**(19): pp. 10566–71.

Gardner TS, Cantor CR & Collins JJ (2000) Construction of a genetic toggle switch in Escherichia coli. *Nature* **403**(6767): pp. 339–42.

Garrell J & Modolell J (1990) The Drosophila extramacrochaetae locus, an antagonist of proneural genes that, like these genes, encodes a helix-loop-helix protein. *Cell* **61**(1): pp. 39–48.

Geelen JL, Boom R, Klaver GP, Minnaar RP, Feltkamp MC, van Milligen FJ, Sol CJ & van der Noordaa J (1987) Transcriptional activation of the major immediate early transcription unit of human cytomegalovirus by heat-shock, arsenite and protein synthesis inhibitors. *J Gen Virol* **68 (Pt 11)**: pp. 2925–31.

Gerlitz O & Basler K (2002) Wingful, an extracellular feedback inhibitor of Wingless. *Genes Dev* **16**(9): pp. 1055–9.

Giráldez AJ, Copley RR & Cohen SM (2002) HSPG modification by the secreted enzyme Notum shapes the Wingless morphogen gradient. *Dev Cell* **2**(5): pp. 667–76.

Gluzman Y (1981) SV40-transformed simian cells support the replication of early SV40 mutants. *Cell* **23**(1): pp. 175–82.

Goolsby J, Marty MC, Heletz D, Chiappelli J, Tashko G, Yarnell D, Fishman PS, Dhib-Jalbut S, Bever CT, Pessac B & Trisler D (2003) Hematopoietic progenitors express neural genes. *Proc Natl Acad Sci U S A* **100**(25): pp. 14926–31.

Gossen M & Bujard H (1992) Tight control of gene expression in mammalian cells by tetracycline-responsive promoters. *Proc Natl Acad Sci U S A* **89**(12): pp. 5547–51.

Gouzé JL (1998) Positive and negative circuits in dynamical systems *J. Biol. Syst* **6**: pp. 11–15.

Gowan K, Helms AW, Hunsaker TL, Collisson T, Ebert PJ, Odom R & Johnson JE (2001) Crossinhibitory activities of Ngn1 and Math1 allow specification of distinct dorsal interneurons. *Neuron* **31**(2): pp. 219–32.

Granick S & Urata G (1963) Increase in activity of alpha-aminolevulinic acid synthetase in liver mitochondria induced by feeding of 3,5-dicarbethoxy-1,4-dihydrocollidine. *J Biol Chem* **238**: pp. 821–7.

Grimm S & Pflugfelder GO (1996) Control of the gene optomotor-blind in Drosophila wing development by decapentaplegic and wingless. *Science* **271**(5255): pp. 1601–4.

Grinberg AV, Hannemann F, Schiffler B, Müller J, Heinemann U & Bernhardt R (2000) Adrenodoxin: structure, stability, and electron transfer properties. *Proteins* **40**(4): pp. 590–612.

Grinberg AV, Hu CD & Kerppola TK (2004) Visualization of Myc/Max/Mad family dimers and the competition for dimerization in living cells. *Mol Cell Biol* **24**(10): pp. 4294–308.

Grynfeld A, Påhlman S & Axelson H (2000) Induced neuroblastoma cell differentiation, associated with transient HES-1 activity and reduced HASH-1 expression, is inhibited by Notch1. *Int J Cancer* **88**(3): pp. 401–10.

Gurdon JB (1962) The developmental capacity of nuclei taken from intestinal epithelial cells of feeding tadpoles *J Embryol Exp Morphol* **10**: pp. 622–640.

Gurdon JB, Laskey RA & Reeves OR (1975) The developmental capacity of nuclei transplanted from keratinized cells of adult frogs *J Embryol Exp Morphol* **34**: pp. 93–112.

Gurdon JB, Standley H, Dyson S, Butler K, Langon T, Ryan K, Stennard F, Shimizu K & Zorn A (1999) Single cells can sense their position in a morphogen gradient. *Development* **126**(23): pp. 5309–17.

Håkelien AM, Landsverk HB, Robl JM, Skålhegg BS & Collas P (2002) Reprogramming fibroblasts to express T-cell functions using cell extracts. *Nat Biotechnol* **20**(5): pp. 460–6.

Halfon MS, Kose H, Chiba A, Keshishian H & Keshishian H (1997) Targeted gene expression without a tissue-specific promoter: creating mosaic embryos using laser-induced single-cell heat shock. *Proc Natl Acad Sci U S A* **94**(12): pp. 6255–60.

Hamamori Y, Wu HY, Sartorelli V & Kedes L (1997) The basic domain of myogenic basic helix-loop-helix (bHLH) proteins is the novel target for direct inhibition by another bHLH protein, Twist. *Mol Cell Biol* **17**(11): pp. 6563–73.

Han C, Belenkaya TY, Wang B & Lin X (2004) Drosophila glypicans control the cell-to-cell movement of Hedgehog by a dynamin-independent process. *Development* **131**(3): pp. 601–11.

Han C, Yan D, Belenkaya TY & Lin X (2005) Drosophila glypicans Dally and Dally-like shape the extracellular Wingless morphogen gradient in the wing disc. *Development* **132**(4): pp. 667–79.

Hara E, Hall M & Peters G (1997) Cdk2-dependent phosphorylation of Id2 modulates activity of E2A-related transcription factors. *EMBO J* **16**(2): pp. 332–42.

Hasan T, Moor AC & Ortel B (2003) Photodynamic therapy of cancer in Kufe DW, Pollock RE, Weichselbaum RR, Jr RC Bast, Gansler TS, Holland JF

& III E Frei, editors, *Cancer Medicine* Hamilton (Canada): BC Decker Inc pp. 489–502.

Hennig L & Schäfer E (1998) Protein purification with C-terminal fusion of maltose binding protein. *Protein Expr Purif* **14**(3): pp. 367–70.

Hennig L & Schäfer E (2001) Both subunits of the dimeric plant photoreceptor phytochrome require chromophore for stability of the far-red light-absorbing form. *J Biol Chem* **276**(11): pp. 7913–8.

Henry CA, Hall LA, Burr Hille M, Solnica-Krezel L & Cooper MS (2000) Somites in zebrafish doubly mutant for knypek and trilobite form without internal mesenchymal cells or compaction. *Curr Biol* **10**(17): pp. 1063–6.

Hirata H, Bessho Y, Kokubu H, Masamizu Y, Yamada S, Lewis J & Kageyama R (2004) Instability of Hes7 protein is crucial for the somite segmentation clock. *Nat Genet* **36**(7): pp. 750–4.

Hirata H, Yoshiura S, Ohtsuka T, Bessho Y, Harada T, Yoshikawa K & Kageyama R (2002) Oscillatory expression of the bHLH factor Hes1 regulated by a negative feedback loop. *Science* **298**(5594): pp. 840–3.

Hlavica P, Schulze J & Lewis DF (2003) Functional interaction of cytochrome P450 with its redox partners: a critical assessment and update of the topology of predicted contact regions. *J Inorg Biochem* **96**(2-3): pp. 279–97.

Holley SA, Geisler R & Nüsslein-Volhard C (2000) Control of her1 expression during zebrafish somitogenesis by a delta-dependent oscillator and an independent wave-front activity. *Genes Dev* **14**(13): pp. 1678–90.

Horwitz M (1996) Hypermethylated myoblasts specifically deficient in MyoD autoactivation as a consequence of instability of MyoD. *Exp Cell Res* **226**(1): pp. 170–82.

Houldsworth J, Reuter VE, Bosl GJ & Chaganti RS (2001) ID gene expression varies with lineage during differentiation of pluripotential male germ cell tumor cell lines. *Cell Tissue Res* **303**(3): pp. 371–9.

Hu M, Krause D, Greaves M, Sharkis S, Dexter M, Heyworth C & Enver T (1997) Multilineage gene expression precedes commitment in the hemopoietic system. *Genes Dev* **11**(6): pp. 774–85.

Huppert SS, Ilagan MX, De Strooper B & Kopan R (2005) Analysis of Notch function in presomitic mesoderm suggests a gamma-secretase-independent role for presenilins in somite differentiation. *Dev Cell* **8**(5): pp. 677–88.

Ishibashi M, Ang SL, Shiota K, Nakanishi S, Kageyama R & Guillemot F (1995) Targeted disruption of mammalian hairy and Enhancer of split homolog-1 (HES-1) leads to up-regulation of neural helix-loop-helix factors, premature neurogenesis, and severe neural tube defects. *Genes Dev* **9**(24): pp. 3136–48.

Ishiguro A, Spirin KS, Shiohara M, Tobler A, Gombart AF, Israel MA, Norton JD & Koeffler HP (1996) Id2 expression increases with differentiation of human myeloid cells. *Blood* **87**(12): pp. 5225–31.

Iso T, Kedes L & Hamamori Y (2003) HES and HERP families: multiple effectors of the Notch signaling pathway. *J Cell Physiol* **194**(3): pp. 237–55.

Iwasaki H, Mizuno S, Wells RA, Cantor AB, Watanabe S & Akashi K (2003) GATA-1 converts lymphoid and myelomonocytic progenitors into the megakaryocyte/erythrocyte lineages. *Immunity* **19**(3): pp. 451–62.

Jaeger J & Goodwin BC (2001) A cellular oscillator model for periodic pattern formation. *J Theor Biol* **213**(2): pp. 171–81.

Jaeger J & Goodwin BC (2002) Cellular oscillators in animal segmentation *In Silico Biology* **2**: p. 0010.

Jagla T, Bidet Y, Da Ponte JP, Dastugue B & Jagla K (2002) Cross-repressive interactions of identity genes are essential for proper specification of cardiac and muscular fates in Drosophila. *Development* **129**(4): pp. 1037–47.

Jang SK, Davies MV, Kaufman RJ & Wimmer E (1989) Initiation of protein synthesis by internal entry of ribosomes into the 5' nontranslated region of encephalomyocarditis virus RNA in vivo. *J Virol* **63**(4): pp. 1651–60.

Jermyn K & Wiliams J (1995) Comparison of the Dictyostelium rasD and ecmA genes reveals two distinct mechanisms whereby an mRNA may become enriched in prestalk cells. *Differentiation* **58**(4): pp. 261–7.

Jiang YJ, Aerne BL, Smithers L, Haddon C, Ish-Horowicz D & Lewis J (2000) Notch signalling and the synchronization of the somite segmentation clock. *Nature* **408**(6811): pp. 475–9.

Jögi A, Persson P, Grynfeld A, Påhlman S & Axelson H (2002) Modulation of basic helix-loop-helix transcription complex formation by Id proteins during neuronal differentiation. *J Biol Chem* **277**(11): pp. 9118–26.

Jouve C, Iimura T & Pourquie O (2002) Onset of the segmentation clock in the chick embryo: evidence for oscillations in the somite precursors in the primitive streak. *Development* **129**(5): pp. 1107–17.

Jouve C, Palmeirim I, Henrique D, Beckers J, Gossler A, Ish-Horowicz D & Pourquié O (2000) Notch signalling is required for cyclic expression of the hairy-like gene HES1 in the presomitic mesoderm. *Development* **127**(7): pp. 1421–9.

Kaern M, Menzinger M & Hunding A (2000) Segmentation and somitogenesis derived from phase dynamics in growing oscillatory media. *J Theor Biol* **207**(4): pp. 473–93.

Kageyama R, Ohtsuka T & Tomita K (2000) The bHLH gene Hes1 regulates differentiation of multiple cell types. *Mol Cells* **10**(1): pp. 1–7.

Kaletta T, Schnabel H & Schnabel R (1997) Binary specification of the embryonic lineage in Caenorhabditis elegans. *Nature* **390**(6657): pp. 294–8.

Kamisako T, Gabazza EC, Ishihara T & Adachi Y (1999) Molecular aspects of organic compound transport across the plasma membrane of hepatocytes. *J Gastroenterol Hepatol* **14**(5): pp. 405–12.

Kawakami Y, Raya A, Raya RM, Rodríguez-Esteban C & Belmonte JC (2005) Retinoic acid signalling links left-right asymmetric patterning and bilaterally symmetric somitogenesis in the zebrafish embryo. *Nature* **435**(7039): pp. 165–71.

Kepler TB & Elston TC (2001) Stochasticity in transcriptional regulation: origins, consequences, and mathematical representations. *Biophys J* **81**(6): pp. 3116–36.

Kerszberg M (1996) Accurate reading of morphogen concentrations by nuclear receptors: a formal model of complex transduction pathways. *J Theor Biol* **183**(1): pp. 95–104.

Kerszberg M (1999) Morphogen propagation and action: towards molecular models. *Semin Cell Dev Biol* **10**(3): pp. 297–302.

Kerszberg M & Changeux JP (1994) A model for reading morphogenetic gradients: autocatalysis and competition at the gene level. *Proc Natl Acad Sci U S A* **91**(13): pp. 5823–7.

Kerszberg M & Wolpert L (1998) Mechanisms for positional signalling by morphogen transport: a theoretical study. *J Theor Biol* **191**(1): pp. 103–14.

Kerszberg M & Wolpert L (2000) A clock and trail model for somite formation, specialization and polarization. *J Theor Biol* **205**(3): pp. 505–10.

Keynes RJ & Stern CD (1988) Mechanisms of vertebrate segmentation. *Development* **103**(3): pp. 413–29.

Khanna R, Huq E, Kikis EA, Al-Sady B, Lanzatella C & Quail PH (2004) A novel molecular recognition motif necessary for targeting photoactivated phytochrome signaling to specific basic helix-loop-helix transcription factors. *Plant Cell* **16**(11): pp. 3033–44.

Khare N & Baumgartner S (2000) Dally-like protein, a new Drosophila glypican with expression overlapping with wingless. *Mech Dev* **99**(1-2): pp. 199–202.

Kim HP, Wang X, Galbiati F, Ryter SW & Choi AM (2004) Caveolae compartmentalization of heme oxygenase-1 in endothelial cells. *FASEB J* **18**(10): pp. 1080–9.

Koenig BB, Cook JS, Wolsing DH, Ting J, Tiesman JP, Correa PE, Olson CA, Pecquet AL, Ventura F & Grant RA (1994) Characterization and cloning of a receptor for BMP-2 and BMP-4 from NIH 3T3 cells. *Mol Cell Biol* **14**(9): pp. 5961–74.

Kondo M, Scherer DC, Miyamoto T, King AG, Akashi K, Sugamura K & Weissman IL (2000) Cell-fate conversion of lymphoid-committed progenitors by instructive actions of cytokines. *Nature* **407**(6802): pp. 383–6.

Kreuger J, Perez L, Giraldez AJ & Cohen SM (2004) Opposing Activities of Dally-like Glypican at High and Low Levels of Wingless Morphogen Activity. *Dev Cell* **7**(4): pp. 503–12.

Kruse K, Pantazis P, Bollenbach T, Jülicher F & González-Gaitán M (2004) Dpp gradient formation by dynamin-dependent endocytosis: receptor trafficking and the diffusion model. *Development* **131**(19): pp. 4843–56.

Kuiper RP, Schepens M, Thijssen J, Schoenmakers EF & van Kessel AG (2004) Regulation of the MiTF/TFE bHLH-LZ transcription factors through re-

stricted spatial expression and alternative splicing of functional domains. *Nucleic Acids Res* **32**(8): pp. 2315–22.

Kulesa PM & Fraser SE (2002) Cell dynamics during somite boundary formation revealed by time-lapse analysis. *Science* **298**(5595): pp. 991–5.

Kulessa H, Frampton J & Graf T (1995) GATA-1 reprograms avian myelomonocytic cell lines into eosinophils, thromboblasts, and erythroblasts. *Genes Dev* **9**(10): pp. 1250–62.

Kunkel T, Speth V, Büche C & Schäfer E (1995) In vivo characterization of phytochrome-phycocyanobilin adducts in yeast. *J Biol Chem* **270**(34): pp. 20193–200.

Kuroda H, Fuentealba L, Ikeda A, Reversade B & De Robertis EM (2005) Default neural induction: neuralization of dissociated Xenopus cells is mediated by Ras/MAPK activation. *Genes Dev* **19**(9): pp. 1022–7.

Ladi E, Nichols JT, Ge W, Miyamoto A, Yao C, Yang LT, Boulter J, Sun YE, Kintner C & Weinmaster G (2005) The divergent DSL ligand Dll3 does not activate Notch signaling but cell autonomously attenuates signaling induced by other DSL ligands. *J Cell Biol* .

Lander AD, Nie Q & Wan FY (2002) Do morphogen gradients arise by diffusion? *Dev Cell* **2**(6): pp. 785–96.

Langlands K, Down GA & Kealey T (2000) Id proteins are dynamically expressed in normal epidermis and dysregulated in squamous cell carcinoma. *Cancer Res* **60**(21): pp. 5929–33.

Lash JW & Ostrovsky D (1986) On the formation of somites. *Dev Biol (N Y 1985)* **2**: pp. 547–63.

Lee T, Bradley ME & Walowitz JL (1998) Influence of promoter potency on the transcriptional effects of YY1, SRF and Msx-1 in transient transfection analysis. *Nucleic Acids Res* **26**(13): pp. 3215–20.

Leimeister C, Dale K, Fischer A, Klamt B, Hrabe de Angelis M, Radtke F, McGrew MJ, Pourquié O & Gessler M (2000) Oscillating expression of c-Hey2 in the presomitic mesoderm suggests that the segmentation clock may use combinatorial signaling through multiple interacting bHLH factors. *Dev Biol* **227**(1): pp. 91–103.

Lewis J (2003) Autoinhibition with transcriptional delay: a simple mechanism for the zebrafish somitogenesis oscillator. *Curr Biol* **13**(16): pp. 1398–408.

Li L & Lagarias JC (1992) Phytochrome assembly. Defining chromophore structural requirements for covalent attachment and photoreversibility. *J Biol Chem* **267**(27): pp. 19204–10.

Li X, Zhao X, Fang Y, Jiang X, Duong T, Fan C, Huang CC & Kain SR (1998) Generation of destabilized green fluorescent protein as a transcription reporter. *J Biol Chem* **273**(52): pp. 34970–5.

Li Y, Fenger U, Niehrs C & Pollet N (2003) Cyclic expression of esr9 gene in Xenopus presomitic mesoderm. *Differentiation* **71**(1): pp. 83–9.

Lim J & Choi KW (2004) Induction and autoregulation of the anti-proneural gene Bar during retinal neurogenesis in Drosophila. *Development* **131**(22): pp. 5573–80.

Lin R, Hill RJ & Priess JR (1998) POP-1 and anterior-posterior fate decisions in C. elegans embryos. *Cell* **92**(2): pp. 229–39.

Lister J, Forrester WC & Baron MH (1995) Inhibition of an erythroid differentiation switch by the helix-loop-helix protein Id1. *J Biol Chem* **270**(30): pp. 17939–46.

Lluis F, Ballestar E, Suelves M, Esteller M & Muñoz-Cánoves P (2005) E47 phosphorylation by p38 MAPK promotes MyoD/E47 association and muscle-specific gene transcription. *EMBO J* **24**(5): pp. 974–84.

Maden M, Graham A, Zile M & Gale E (2000) Abnormalities of somite development in the absence of retinoic acid. *Int J Dev Biol* **44**(1): pp. 151–9.

Maines MD (1997) The heme oxygenase system: a regulator of second messenger gases. *Annu Rev Pharmacol Toxicol* **37**: pp. 517–54.

Maines MD, Ewing JF, Huang TJ & Panahian N (2001) Nuclear localization of biliverdin reductase in the rat kidney: response to nephrotoxins that induce heme oxygenase-1. *J Pharmacol Exp Ther* **296**(3): pp. 1091–7.

Mann RS & Affolter M (1998) Hox proteins meet more partners. *Curr Opin Genet Dev* **8**(4): pp. 423–9.

Maroto M, Dale JK, Dequéant ML, Petit AC & Pourquié O (2005) Synchronised cycling gene oscillations in presomitic mesoderm cells require cell-cell contact. *Int J Dev Biol* **49**(2-3): pp. 309–15.

Maruhashi M, Van De Putte T, Huylebroeck D, Kondoh H & Higashi Y (2005) Involvement of SIP1 in positioning of somite boundaries in the mouse embryo. *Dev Dyn* .

Massari ME & Murre C (2000) Helix-loop-helix proteins: regulators of transcription in eucaryotic organisms. *Mol Cell Biol* **20**(2): pp. 429–40.

McCarrey JR & Riggs AD (1986) Determinator-inhibitor pairs as a mechanism for threshold setting in development: a possible function for pseudogenes. *Proc Natl Acad Sci U S A* **83**(3): pp. 679–83.

McCoubrey WK, Huang TJ & Maines MD (1997) Heme oxygenase-2 is a hemoprotein and binds heme through heme regulatory motifs that are not involved in heme catalysis. *J Biol Chem* **272**(19): pp. 12568–74.

McCoubrey WK, Huang TJ & Maines MD (1997) Isolation and characterization of a cdna from the rat brain that encodes hemoprotein heme oxygenase-3. *Eur J Biochem* **247**(2): pp. 725–32.

McDevitt MA, Shivdasani RA, Fujiwara Y, Yang H & Orkin SH (1997) A "knockdown" mutation created by cis-element gene targeting reveals the dependence of erythroid cell maturation on the level of transcription factor GATA-1. *Proc Natl Acad Sci U S A* **94**(13): pp. 6781–5.

McGrew MJ, Dale JK, Fraboulet S & Pourquié O (1998) The lunatic fringe gene is a target of the molecular clock linked to somite segmentation in avian embryos. *Curr Biol* **8**(17): pp. 979–82.

McGrew MJ, Sherman A, Ellard FM, Lillico SG, Gilhooley HJ, Kingsman AJ, Mitrophanous KA & Sang H (2004) Efficient production of germline transgenic chickens using lentiviral vectors. *EMBO Rep* **5**(7): pp. 728–33.

Meinhardt H (1986) *Somites in developing embryos* chap. Models of segmentation New York: Plenum Press pp. 179–191.

Mével-Ninio M & Weiss MC (1981) Immunofluorescence analysis of the time-course of extinction, reexpression, and activation of albumin production in rat hepatoma-mouse fibroblast heterokaryons and hybrids. *J Cell Biol* **90**(2): pp. 339–50.

Miyamoto T, Iwasaki H, Reizis B, Ye M, Graf T, Weissman IL & Akashi K (2002) Myeloid or lymphoid promiscuity as a critical step in hematopoietic lineage commitment. *Dev Cell* **3**(1): pp. 137–47.

Moan J & Sommer S (1985) Oxygen dependence of the photosensitizing effect of hematoporphyrin derivative in NHIK 3025 cells. *Cancer Res* **45**(4): pp. 1608–10.

Morales AV, Yasuda Y & Ish-Horowicz D (2002) Periodic Lunatic fringe Expression Is Controlled during Segmentation by a Cyclic Transcriptional Enhancer Responsive to Notch Signaling. *Dev Cell* **3**(1): pp. 63–74.

Morimoto M, Takahashi Y, Endo M & Saga Y (2005) The Mesp2 transcription factor establishes segmental borders by suppressing Notch activity. *Nature* **435**(7040): pp. 354–9.

Mumm JS & Kopan R (2000) Notch signaling: from the outside in. *Dev Biol* **228**(2): pp. 151–65.

Murakoshi H, Iino R, Kobayashi T, Fujiwara T, Ohshima C, Yoshimura A & Kusumi A (2004) Single-molecule imaging analysis of Ras activation in living cells. *Proc Natl Acad Sci U S A* **101**(19): pp. 7317–22.

Nagata Y & Todokoro K (1994) Activation of helix-loop-helix proteins Id1, Id2 and Id3 during neural differentiation. *Biochem Biophys Res Commun* **199**(3): pp. 1355–62.

Nagy F & Schäfer E (2002) Phytochromes control photomorphogenesis by differentially regulated, interacting signaling pathways in higher plants. *Annu Rev Plant Biol* **53**: pp. 329–55.

Nellen D, Burke R, Struhl G & Basler K (1996) Direct and long-range action of a DPP morphogen gradient. *Cell* **85**(3): pp. 357–68.

Nerlov C, Querfurth E, Kulessa H & Graf T (2000) GATA-1 interacts with the myeloid PU.1 transcription factor and represses PU.1-dependent transcription. *Blood* **95**(8): pp. 2543–51.

Neves G, Zucker J, Daly M & Chess A (2004) Stochastic yet biased expression of multiple Dscam splice variants by individual cells. *Nat Genet* **36**(3): pp. 240–6.

New DAT (1955) A new technique for the cultivation of the chick embryo *J Embryol Exp Morphol* **3**: pp. 326–331.

Nomura-Kitabayashi A, Takahashi Y, Kitajima S, Inoue T, Takeda H & Saga Y (2002) Hypomorphic Mesp allele distinguishes establishment of rostrocaudal polarity and segment border formation in somitogenesis. *Development* **129**(10): pp. 2473–2481.

Northrup SH & Erickson HP (1992) Kinetics of protein-protein association explained by Brownian dynamics computer simulation. *Proc Natl Acad Sci U S A* **89**(8): pp. 3338–42.

Norton JD (2000) ID helix-loop-helix proteins in cell growth, differentiation and tumorigenesis. *J Cell Sci* **113 (Pt 22)**: pp. 3897–905.

Norton JD, Deed RW, Craggs G & Sablitzky F (1998) Id helix-loop-helix proteins in cell growth and differentiation. *Trends Cell Biol* **8**(2): pp. 58–65.

Nugent MA & Edelman ER (1992) Kinetics of basic fibroblast growth factor binding to its receptor and heparan sulfate proteoglycan: a mechanism for cooperactivity. *Biochemistry* **31**(37): pp. 8876–83.

Nutt SL, Vambrie S, Steinlein P, Kozmik Z, Rolink A, Weith A & Busslinger M (1999) Independent regulation of the two Pax5 alleles during B-cell development. *Nat Genet* **21**(4): pp. 390–5.

Oates AC & Ho RK (2002) Hairy/E(spl)-related (Her) genes are central components of the segmentation oscillator and display redundancy with the Delta/Notch signaling pathway in the formation of anterior segmental boundaries in the zebrafish. *Development* **129**(12): pp. 2929–46.

Ogata T, Wozney JM, Benezra R & Noda M (1993) Bone morphogenetic protein 2 transiently enhances expression of a gene, Id (inhibitor of differentia-

tion), encoding a helix-loop-helix molecule in osteoblast-like cells. *Proc Natl Acad Sci U S A* **90**(19): pp. 9219–22.

Ohtsuka T, Asahi M, Matsuura N, Kikuchi H, Hojo M, Kageyama R, Ohkubo H & Hoshimaru M (1998) Regulated expression of neurogenic basic helix-loop-helix transcription factors during differentiation of the immortalized neuronal progenitor cell line HC2S2 into neurons. *Cell Tissue Res* **293**(1): pp. 23–9.

Ohtsuka T, Ishibashi M, Gradwohl G, Nakanishi S, Guillemot F & Kageyama R (1999) Hes1 and Hes5 as notch effectors in mammalian neuronal differentiation. *EMBO J* **18**(8): pp. 2196–207.

Okano H, Imai T & Okabe M (2002) Musashi: a translational regulator of cell fate. *J Cell Sci* **115**(Pt 7): pp. 1355–9.

Orkin SH (2000) Diversification of haematopoietic stem cells to specific lineages. *Nat Rev Genet* **1**(1): pp. 57–64.

Orkin SH (2003) Priming the Hematopoietic Pump. *Immunity* **19**(5): pp. 633–634.

O'Toole PJ, Inoue T, Emerson L, Morrison IE, Mackie AR, Cherry RJ & Norton JD (2003) Id proteins negatively regulate basic helix-loop-helix transcription factor function by disrupting subnuclear compartmentalization. *J Biol Chem* **278**(46): pp. 45770–6.

Ozbudak EM, Thattai M, Kurtser I, Grossman AD & van Oudenaarden A (2002) Regulation of noise in the expression of a single gene. *Nat Genet* **31**(1): pp. 69–73.

Ozbudak EM, Thattai M, Lim HN, Shraiman BI & Van Oudenaarden A (2004) Multistability in the lactose utilization network of Escherichia coli. *Nature* **427**(6976): pp. 737–40.

Paardekooper M, Van Gompel AE, Van Steveninck J & Van den Broek PJ (1995) The effect of photodynamic treatment of yeast with the sensitizer chloroaluminum phthalocyanine on various cellular parameters. *Photochem Photobiol* **62**(3): pp. 561–7.

Packard DS, Zheng RZ & Turner DC (1993) Somite pattern regulation in the avian segmental plate mesoderm. *Development* **117**(2): pp. 779–91.

Page JL, Wang X, Sordillo LM & Johnson SE (2004) MEKK1 signaling through p38 leads to transcriptional inactivation of E47 and repression of skeletal myogenesis. *J Biol Chem* **279**(30): pp. 30966–72.

Palmeirim I, Henrique D, Ish-Horowicz D & Pourquie O (1997) Avian hairy gene expression identifies a molecular clock linked to vertebrate segmentation and somitogenesis. *Cell* **91**(5): pp. 639–48.

Passamonti S & Sottocasa GL (1988) The quinoid structure is the molecular requirement for recognition of phthaleins by the organic anion carrier at the sinusoidal plasma membrane level in the liver. *Biochim Biophys Acta* **943**(2): pp. 119–25.

Perry RL, Parker MH & Rudnicki MA (2001) Activated MEK1 binds the nuclear MyoD transcriptional complex to repress transactivation. *Mol Cell* **8**(2): pp. 291–301.

Pierani A, Moran-Rivard L, Sunshine MJ, Littman DR, Goulding M & Jessell TM (2001) Control of interneuron fate in the developing spinal cord by the progenitor homeodomain protein Dbx1. *Neuron* **29**(2): pp. 367–84.

Plahte E, Mestl T & Omholt WS (1995) Feedback circuits, stability and multistationarity in dynamical systems *J. Biol. Syst.* **3**: pp. 409–413.

Press WH (1992) *Numerical recipes in C : the art of scientific computing* Cambridge: Cambridge University Press.

Primmett DR, Norris WE, Carlson GJ, Keynes RJ & Stern CD (1989) Periodic segmental anomalies induced by heat shock in the chick embryo are associated with the cell cycle. *Development* **105**(1): pp. 119–30.

Primmett DR, Stern CD & Keynes RJ (1988) Heat shock causes repeated segmental anomalies in the chick embryo. *Development* **104**(2): pp. 331–9.

Prince VE, Holley SA, Bally-Cuif L, Prabhakaran B, Oates AC, Ho RK & Vogt TF (2001) Zebrafish lunatic fringe demarcates segmental boundaries. *Mech Dev* **105**(1-2): pp. 175–80.

Psychoyos D & Stern CD (1996) Fates and migratory routes of primitive streak cells in the chick embryo. *Development* **122**(5): pp. 1523–34.

Rallu M, Corbin JG & Fishell G (2002) Parsing the prosencephalon. *Nat Rev Neurosci* **3**(12): pp. 943–51.

Ramezani A, Hawley TS & Hawley RG (2003) Performance- and safety-enhanced lentiviral vectors containing the human interferon-beta scaffold attachment region and the chicken beta-globin insulator. *Blood* **101**(12): pp. 4717–24.

Rees S, Coote J, Stables J, Goodson S, Harris S & Lee MG (1996) Bicistronic vector for the creation of stable mammalian cell lines that predisposes all antibiotic-resistant cells to express recombinant protein. *Biotechniques* **20**(1): pp. 102–4, 106, 108–10.

Reid BG & Flynn GC (1997) Chromophore formation in green fluorescent protein. *Biochemistry* **36**(22): pp. 6786–91.

Rekhtman N, Radparvar F, Evans T & Skoultchi AI (1999) Direct interaction of hematopoietic transcription factors PU.1 and GATA-1: functional antagonism in erythroid cells. *Genes Dev* **13**(11): pp. 1398–411.

Rimington C (1966) Porphyrin and haem biosynthesis and its control. *Acta Med Scand Suppl* **445**: pp. 11–24.

Rivolta MN, Halsall A, Johnson CM, Tones MA & Holley MC (2002) Transcript profiling of functionally related groups of genes during conditional differentiation of a mammalian cochlear hair cell line. *Genome Res* **12**(7): pp. 1091–9.

Rørth P (1996) A modular misexpression screen in Drosophila detecting tissue-specific phenotypes. *Proc Natl Acad Sci U S A* **93**(22): pp. 12418–22.

Rothenberg EV (2000) Stepwise specification of lymphocyte developmental lineages. *Curr Opin Genet Dev* **10**(4): pp. 370–9.

Rothenberg EV, Telfer JC & Anderson MK (1999) Transcriptional regulation of lymphocyte lineage commitment. *Bioessays* **21**(9): pp. 726–42.

Roy MN, Prince VE & Ho RK (1999) Heat shock produces periodic somitic disturbances in the zebrafish embryo. *Mech Dev* **85**(1-2): pp. 27–34.

Russell RG, Lasorella A, Dettin LE & Iavarone A (2004) Id2 drives differentiation and suppresses tumor formation in the intestinal epithelium. *Cancer Res* **64**(20): pp. 7220–5.

Saga Y & Takeda H (2001) The making of the somite: molecular events in vertebrate segmentation. *Nat Rev Genet* **2**(11): pp. 835–45.

Sasai Y, Kageyama R, Tagawa Y, Shigemoto R & Nakanishi S (1992) Two mammalian helix-loop-helix factors structurally related to Drosophila hairy and Enhancer of split. *Genes Dev* **6**(12B): pp. 2620–34.

Sato Y & Takahashi Y (2005) A novel signal induces a segmentation fissure by acting in a ventral-to-dorsal direction in the presomitic mesoderm. *Dev Biol* **282**(1): pp. 183–91.

Sato Y, Yasuda K & Takahashi Y (2002) Morphological boundary forms by a novel inductive event mediated by Lunatic fringe and Notch during somitic segmentation. *Development* **129**(15): pp. 3633–44.

Saúde L, Lourenço R, Gonçalves A & Palmeirim I (2005) terra is a left-right asymmetry gene required for left-right synchronization of the segmentation clock. *Nat Cell Biol* **7**(9): pp. 918–20.

Sawada A, Shinya M, Jiang YJ, Kawakami A, Kuroiwa A & Takeda H (2001) Fgf/MAPK signalling is a crucial positional cue in somite boundary formation. *Development* **128**(23): pp. 4873–80.

Schepens I, Duek P & Fankhauser C (2004) Phytochrome-mediated light signalling in Arabidopsis. *Curr Opin Plant Biol* **7**(5): pp. 564–9.

Schnell S & Maini PK (2000) Clock and induction model for somitogenesis. *Dev Dyn* **217**(4): pp. 415–20.

Selleck MA & Stern CD (1991) Fate mapping and cell lineage analysis of Hensen's node in the chick embryo. *Development* **112**(2): pp. 615–26.

Selleck MAJ & Stern CD (1992) *Formation and Differentiation of Early Embryonic Mesoderm* chap. Evidence for stem cells in the mesoderm of Hensen's node and their role in embryonic pattern formation New York: Plenum Press pp. 23–31.

Seo S, Herr A, Lim JW, Richardson GA, Richardson H & Kroll KL (2005) Geminin regulates neuronal differentiation by antagonizing Brg1 activity. *Genes Dev* **19**(14): pp. 1723–34.

Serizawa S, Ishii T, Nakatani H, Tsuboi A, Nagawa F, Asano M, Sudo K, Sakagami J, Sakano H, Ijiri T, Matsuda Y, Suzuki M, Yamamori T, Iwakura Y & Sakano H (2000) Mutually exclusive expression of odorant receptor transgenes. *Nat Neurosci* **3**(7): pp. 687–93.

Serth K, Schuster-Gossler K, Cordes R & Gossler A (2003) Transcriptional oscillation of Lunatic fringe is essential for somitogenesis. *Genes Dev* **17**(7): pp. 912–25.

Shayeghi M, Latunde-Dada GO, Oakhill JS, Laftah AH, Takeuchi K, Halliday N, Khan Y, Warley A, McCann FE, Hider RC, Frazer DM, Anderson GJ, Vulpe CD, Simpson RJ & McKie AT (2005) Identification of an intestinal heme transporter. *Cell* **122**(5): pp. 789–801.

Shigeri Y, Tatsu Y & Yumoto N (2001) Synthesis and application of caged peptides and proteins. *Pharmacol Ther* **91**(2): pp. 85–92.

Shimizu-Sato S, Huq E, Tepperman JM & Quail PH (2002) A light-switchable gene promoter system. *Nat Biotechnol* **20**(10): pp. 1041–4.

Shimmi O & O'Connor MB (2003) Physical properties of Tld, Sog, Tsg and Dpp protein interactions are predicted to help create a sharp boundary in Bmp signals during dorsoventral patterning of the Drosophila embryo. *Development* **130**(19): pp. 4673–82.

Shirihai OS, Gregory T, Yu C, Orkin SH & Weiss MJ (2000) ABC-me: a novel mitochondrial transporter induced by GATA-1 during erythroid differentiation. *EMBO J* **19**(11): pp. 2492–502.

Simone C, Forcales SV, Hill DA, Imbalzano AN, Latella L & Puri PL (2004) p38 pathway targets SWI-SNF chromatin-remodeling complex to muscle-specific loci. *Nat Genet* **36**(7): pp. 738–43.

Sitcheran R, Cogswell PC & Baldwin AS (2003) NF-kappaB mediates inhibition of mesenchymal cell differentiation through a posttranscriptional gene silencing mechanism. *Genes Dev* **17**(19): pp. 2368–73.

Sloan SR, Shen CP, McCarrick-Walmsley R & Kadesch T (1996) Phosphorylation of E47 as a potential determinant of B-cell-specific activity. *Mol Cell Biol* **16**(12): pp. 6900–8.

Snoussi EH (1998) Necessary conditions for multistationarity and stable periodicity *J. Biol. Syst* **6**: pp. 3–9.

Soulé C (2003) Graphic requirements for multistationarity *Complexus* **1**: pp. 123–33.

Spicer DB, Rhee J, Cheung WL & Lassar AB (1996) Inhibition of myogenic bHLH and MEF2 transcription factors by the bHLH protein Twist. *Science* **272**(5267): pp. 1476–80.

Sriuranpong V, Borges MW, Strock CL, Nakakura EK, Watkins DN, Blaumueller CM, Nelkin BD & Ball DW (2002) Notch signaling induces rapid degradation of achaete-scute homolog 1. *Mol Cell Biol* **22**(9): pp. 3129–39.

Staehling-Hampton K, Jackson PD, Clark MJ, Brand AH & Hoffmann FM (1994) Specificity of bone morphogenetic protein-related factors: cell fate and gene expression changes in Drosophila embryos induced by decapentaplegic but not 60A. *Cell Growth Differ* **5**(6): pp. 585–93.

Stern CD, Fraser SE, Keynes RJ & Primmett DR (1988) A cell lineage analysis of segmentation in the chick embryo. *Development* **104 Suppl**: pp. 231–44.

Stern CD & Ireland GW (1981) An integrated experimental study of endoderm formation in avian embryos. *Anat Embryol (Berl)* **163**(3): pp. 245–63.

Stern CD & Keynes RJ (1987) Interactions between somite cells: the formation and maintenance of segment boundaries in the chick embryo. *Development* **99**(2): pp. 261–72.

Sternberg PW & Horvitz HR (1989) The combined action of two intercellular signaling pathways specifies three cell fates during vulval induction in C. elegans. *Cell* **58**(4): pp. 679–93.

Stewart HJ, Zoidl G, Rossner M, Brennan A, Zoidl C, Nave KA, Mirsky R & Jessen KR (1997) Helix-loop-helix proteins in Schwann cells: a study of regulation and subcellular localization of Ids, REB, and E12/47 during embryonic and postnatal development. *J Neurosci Res* **50**(5): pp. 684–701.

Stickney HL, Barresi MJ & Devoto SH (2000) Somite development in zebrafish. *Dev Dyn* **219**(3): pp. 287–303.

Suelves M, Lluís F, Ruiz V, Nebreda AR & Muñoz-Cánoves P (2004) Phosphorylation of MRF4 transactivation domain by p38 mediates repression of specific myogenic genes. *EMBO J* **23**(2): pp. 365–75.

Suzuki A, Thies RS, Yamaji N, Song JJ, Wozney JM, Murakami K & Ueno N (1994) A truncated bone morphogenetic protein receptor affects dorsal-ventral patterning in the early Xenopus embryo. *Proc Natl Acad Sci U S A* **91**(22): pp. 10255–9.

Swindle CS, Kim HG & Klug CA (2004) Mutation of CpGs in the murine stem cell virus retroviral vector long terminal repeat represses silencing in embryonic stem cells. *J Biol Chem* **279**(1): pp. 34–41.

Szymczak AL, Workman CJ, Wang Y, Vignali KM, Dilioglou S, Vanin EF & Vignali DA (2004) Correction of multi-gene deficiency in vivo using a single 'self-cleaving' 2A peptide-based retroviral vector. *Nat Biotechnol* **22**(5): pp. 589–94.

Takebayashi K, Sasai Y, Sakai Y, Watanabe T, Nakanishi S & Kageyama R (1994) Structure, chromosomal locus, and promoter analysis of the gene

encoding the mouse helix-loop-helix factor HES-1. Negative autoregulation through the multiple N box elements. *J Biol Chem* **269**(7): pp. 5150–6.

Tanabe T, Oyamada M, Fujita K, Dai P, Tanaka H & Takamatsu T (2005) Multiphoton excitation-evoked chromophore-assisted laser inactivation using green fluorescent protein. *Nat Methods* **2**(7): pp. 503–5.

Tao L & Nicholson C (1996) Diffusion of albumins in rat cortical slices and relevance to volume transmission. *Neuroscience* **75**(3): pp. 839–47.

Tchkonia T, Giorgadze N, Pirtskhalava T, Tchoukalova Y, Karagiannides I, Forse RA, DePonte M, Stevenson M, Guo W, Han J, Waloga G, Lash TL, Jensen MD & Kirkland JL (2002) Fat depot origin affects adipogenesis in primary cultured and cloned human preadipocytes. *Am J Physiol Regul Integr Comp Physiol* **282**(5): pp. R1286–96.

Tenhunen R, Marver HS & Schmid R (1969) Microsomal heme oxygenase. Characterization of the enzyme. *J Biol Chem* **244**(23): pp. 6388–94.

Theise ND & Krause DS (2002) Toward a new paradigm of cell plasticity. *Leukemia* **16**(4): pp. 542–8.

Thomas R (1981) On the relation between the logical structure of systems and their ability to generate multiple steady states or sustained oscillations *Springer Ser. Synergetics* **9**: pp. 180–193.

Tour O, Meijer RM, Zacharias DA, Adams SR & Tsien RY (2003) Genetically targeted chromophore-assisted light inactivation. *Nat Biotechnol* **21**(12): pp. 1505–8.

Trott RL, Kalive M, Paroush Z & Bidwai AP (2001) Drosophila melanogaster casein kinase II interacts with and phosphorylates the basic helix-loop-helix proteins m5, m7, and m8 derived from the Enhancer of split complex. *J Biol Chem* **276**(3): pp. 2159–67.

Tsuda M, Kamimura K, Nakato H, Archer M, Staatz W, Fox B, Humphrey M, Olson S, Futch T, Kaluza V, Siegfried E, Stam L & Selleck SB (1999) The cell-surface proteoglycan Dally regulates Wingless signalling in Drosophila. *Nature* **400**(6741): pp. 276–80.

Tuckey RC & Sadleir J (1999) The concentration of adrenodoxin reductase limits cytochrome p450scc activity in the human placenta. *Eur J Biochem* **263**(2): pp. 319–25.

Vermot J, Llamas JG, Fraulob V, Niederreither K, Chambon P & Dollé P (2005) Retinoic acid controls the bilateral symmetry of somite formation in the mouse embryo. *Science* **308**(5721): pp. 563–6.

Vermot J & Pourquié O (2005) Retinoic acid coordinates somitogenesis and left-right patterning in vertebrate embryos. *Nature* **435**(7039): pp. 215–20.

Viñals F, Reiriz J, Ambrosio S, Bartrons R, Rosa JL & Ventura F (2004) BMP-2 decreases Mash1 stability by increasing Id1 expression. *EMBO J* **23**(17): pp. 3527–37.

Visvader JE, Elefanty AG, Strasser A & Adams JM (1992) GATA-1 but not SCL induces megakaryocytic differentiation in an early myeloid line. *EMBO J* **11**(12): pp. 4557–64.

Wang Y, O'Malley BW, Tsai SY & O'Malley BW (1994) A regulatory system for use in gene transfer. *Proc Natl Acad Sci U S A* **91**(17): pp. 8180–4.

Wardle FC & Smith JC (2004) Refinement of gene expression patterns in the early Xenopus embryo. *Development* **131**(19): pp. 4687–96.

Weimann JM, Johansson CB, Trejo A & Blau HM (2003) Stable reprogrammed heterokaryons form spontaneously in Purkinje neurons after bone marrow transplant. *Nat Cell Biol* **5**(11): pp. 959–66.

Weintraub H (1993) The MyoD family and myogenesis: redundancy, networks, and thresholds. *Cell* **75**(7): pp. 1241–4.

Wickens M, Bernstein DS, Kimble J & Parker R (2002) A PUF family portrait: 3'UTR regulation as a way of life. *Trends Genet* **18**(3): pp. 150–7.

Wickens M, Goodwin EB, Kimble J, Strickland S & Hentze MW (2000) Translational control in developmental decisions in Sonenberg N, editor, *Translational control of gene expression* New York: Cold Spring Harbor Press pp. 295–370.

Winter B, Braun T & Arnold HH (1993) cAMP-dependent protein kinase represses myogenic differentiation and the activity of the muscle-specific helix-loop-helix transcription factors Myf-5 and MyoD. *J Biol Chem* **268**(13): pp. 9869–78.

Wolpert L (1969) Positional information and the spatial pattern of cellular differentiation. *J Theor Biol* **25**(1): pp. 1–47.

Wolpert L (1996) One hundred years of positional information. *Trends Genet* **12**(9): pp. 359–64.

Wrona M, Rózanowska M & Sarna T (2004) Zeaxanthin in combination with ascorbic acid or alpha-tocopherol protects ARPE-19 cells against photosensitized peroxidation of lipids. *Free Radic Biol Med* **36**(9): pp. 1094–101.

Wu JY, Wen L, Zhang WJ & Rao Y (1996) The secreted product of Xenopus gene lunatic Fringe, a vertebrate signaling molecule. *Science* **273**(5273): pp. 355–8.

Xiong W & Ferrell JE (2003) A positive-feedback-based bistable 'memory module' that governs a cell fate decision. *Nature* **426**(6965): pp. 460–5.

Ye M, Iwasaki H, Laiosa CV, Stadtfeld M, Xie H, Heck S, Clausen B, Akashi K & Graf T (2003) Hematopoietic Stem Cells Expressing the Myeloid Lysozyme Gene Retain Long-Term, Multilineage Repopulation Potential. *Immunity* **19**(5): pp. 689–699.

Yu L, Liu C, Vandeusen J, Becknell B, Dai Z, Wu YZ, Raval A, Liu TH, Ding W, Mao C, Liu S, Smith LT, Lee S, Rassenti L, Marcucci G, Byrd J, Caligiuri MA & Plass C (2005) Global assessment of promoter methylation in a mouse model of cancer identifies ID4 as a putative tumor-suppressor gene in human leukemia. *Nat Genet* **37**(3): pp. 265–74.

Yu SF, von Rüden T, Kantoff PW, Garber C, Seiberg M, Rüther U, Anderson WF, Wagner EF & Gilboa E (1986) Self-inactivating retroviral vectors designed for transfer of whole genes into mammalian cells. *Proc Natl Acad Sci U S A* **83**(10): pp. 3194–8.

Yu YA & Szalay AA (2002) A Renilla luciferase-Aequorea GFP (ruc-gfp) fusion gene construct permits real-time detection of promoter activation by exogenously administered mifepristone in vivo. *Mol Genet Genomics* **268**(2): pp. 169–78.

Zecca M, Basler K & Struhl G (1996) Direct and long-range action of a wingless morphogen gradient. *Cell* **87**(5): pp. 833–44.

Zeng X, Goetz JA, Suber LM, Scott WJ, Schreiner CM & Robbins DJ (2001) A freely diffusible form of Sonic hedgehog mediates long-range signalling. *Nature* **411**(6838): pp. 716–20.

Zhang DE, Hohaus S, Voso MT, Chen HM, Smith LT, Hetherington CJ & Tenen DG (1996) Function of PU.1 (Spi-1), C/EBP, and AML1 in early myelopoiesis: regulation of multiple myeloid CSF receptor promoters. *Curr Top Microbiol Immunol* **211**: pp. 137–47.

Zhang P, Behre G, Pan J, Iwama A, Wara-Aswapati N, Radomska HS, Auron PE, Tenen DG & Sun Z (1999) Negative cross-talk between hematopoietic regulators: GATA proteins repress PU.1. *Proc Natl Acad Sci U S A* **96**(15): pp. 8705–10.

Zhou J & Olson EN (1994) Dimerization through the helix-loop-helix motif enhances phosphorylation of the transcription activation domains of myogenin. *Mol Cell Biol* **14**(9): pp. 6232–43.

Zhou S, Zong Y, Ney PA, Nair G, Stewart CF & Sorrentino BP (2005) Increased expression of the Abcg2 transporter during erythroid maturation plays a role in decreasing cellular protoporphyrin IX levels. *Blood* **105**(6): pp. 2571–6.

Zhu J & Emerson SG (2002) Hematopoietic cytokines, transcription factors and lineage commitment. *Oncogene* **21**(21): pp. 3295–313.

Zhuang Y, Cheng P & Weintraub H (1996) B-lymphocyte development is regulated by the combined dosage of three basic helix-loop-helix genes, E2A, E2-2, and HEB. *Mol Cell Biol* **16**(6): pp. 2898–905.

zur Lage PI, Powell LM, Prentice DR, McLaughlin P & Jarman AP (2004) EGF receptor signaling triggers recruitment of Drosophila sense organ precursors by stimulating proneural gene autoregulation. *Dev Cell* **7**(5): pp. 687–96.